

THE UNIVERSITY OF CALGARY

CONTROL OF MULTI-MODES OF OSCILLATION USING A
MULTI-INPUT MULTI-CHANNEL CONTROLLER

by

Solomon Chebib

A THESIS

SUBMITTED TO THE FACULTY OF GRADUATE STUDIES
IN PARTIAL FULFILLMENT OF THE REQUIREMENTS FOR THE
DEGREE OF MASTER OF SCIENCE

DEPARTMENT OF ELECTRICAL ENGINEERING

CALGARY, ALBERTA

JAN, 1988

© Solomon Chebib 1988

Permission has been granted to the National Library of Canada to microfilm this thesis and to lend or sell copies of the film.

The author (copyright owner) has reserved other publication rights, and neither the thesis nor extensive extracts from it may be printed or otherwise reproduced without his/her written permission.

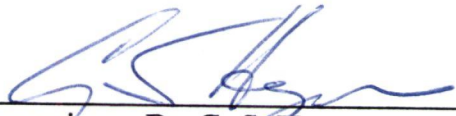
L'autorisation a été accordée à la Bibliothèque nationale du Canada de microfilmer cette thèse et de prêter ou de vendre des exemplaires du film.

L'auteur (titulaire du droit d'auteur) se réserve les autres droits de publication; ni la thèse ni de longs extraits de celle-ci ne doivent être imprimés ou autrement reproduits sans son autorisation écrite.


ISBN 0-315-42487-7

THE UNIVERSITY OF CALGARY
FACULTY OF GRADUATE STUDIES

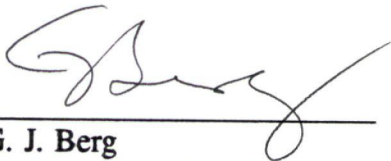
The undersigned certify that they have read, and recommended to the Faculty of Graduate Studies for acceptance, a thesis entitled *Control of Multi-Modes of Oscillation Using a Multi-Input Multi-Channel Controller*, submitted by Solomon Chebib in partial fulfillment of the requirements for the degree of Master of Science.




Supervisor - Dr. G. S. Hope
Department of Electrical Engineering



Dr. O. P. Malik
Department of Electrical Engineering



Prof. G. J. Berg
Department of Electrical Engineering



Dr. N. E. Kalogerakis
Department of Chemical & Petroleum Engineering

Date: January 26, 1988

ABSTRACT

Conventional power system stabilizers (CPSS) are widely used in the power industry to improve the stability of power systems. The CPSS is designed to provide adequate local mode damping under all operating conditions, and simultaneously to provide a high contribution to damping of interarea modes [26] This is a compromise in the design of CPSS to damp multi-modes of oscillation. For power systems in which multi-modes of oscillation exist, CPSSs become less effective.

This thesis introduces the contradiction that exists in controlling multi-modes of oscillation. A multi-input multi-channel (MIMC) controller which eliminates this contradiction is developed. The MIMC has two channels, each channel is assigned to one mode of oscillation.

The effectiveness of the MIMC is demonstrated through both computer simulation and testing on an experimental setup. The simulation model was used as reference for setting up the experimental power system. However it is difficult to simulate large machines with the small machines available. The time constants and inertias of the larger machines could not be achieved.

The studies conducted in simulation and on the experimental setup show that the MIMC controller is capable of effectively damping both local and interarea modes of oscillation.

ACKNOWLEDGEMENTS

The author wishes to express his sincere gratitude to Dr. G.S. Hope for his guidance throughout the course of the project. His advice and corrections in preparing the manuscript are greatly appreciated.

Special appreciation goes to Dr. O.P. Malik and other members in the power system research group for their helpfull criticisms and discussions. Special thanks to Mr. P. Walsh for his assistance and suggestions in constructing the experimental setup. The author would also like to thank Nalin Pahalawaththa for his assistance in debugging some problems associated with the experimental setup.

TABLE OF CONTENTS

TABLE OF CONTENTS	v
LIST OF FIGURES	vii
LIST OF SYMBOLS	x
1. INTRODUCTION	1
1.1 Power system stability	2
1.2 Contradictions and conflict in large systems	2
1.3 Why a multi-channel controller?	5
1.4 Thesis Objective	6
1.5 Organization of thesis	7
2. MULTI-CHANNEL CONTROLLER	9
2.1 Power system stabilizer	9
2.2 Multi-channel controller	14
2.3 Single input multi-channel controller	16
2.4 Multi-input multi-channel controller	18
2.5 Summary	21
3. MULTI-MACHINE POWER SYSTEM MODEL	22
3.1 Multi-machine power system model	22

3.2 System modes of oscillation	23
3.3 Simulation procedure	26
3.4 Summary	32
4. SIMULATION RESULTS FOR MULTI-CHANNEL CONTROLLER	33
4.1 Simulation studies	33
4.2 Simulation results	36
4.3 Some special problems of SIMC	51
4.4 Some special problems of MIMC	61
4.5 Analysis of MIMC results	62
4.6 Summary	66
5. IMPLEMENTATION RESULTS	67
5.1 Experimental setup	67
5.2 Implementation studies	72
5.3 Implementation results	74
5.4 Summary	77
6. CONCLUSIONS	86
6.1 Conclusions and Thesis contributions	86
6.2 Future works	88
REFERENCES	89
APPENDIX A: Filter design for the SIMC structure	93
APPENDIX B: Multi-machine model parameters	98

APPENDIX C: Experimental setup machine parameters	104
---	-----

LIST OF FIGURES

Fig. 2.1 Block diagram of conventional excitation control	12
Fig. 2.2 Block diagram of multi-channel controller	15
Fig. 2.3 Block diagram of a single input multi-channel controller	17
Fig. 2.4 Block diagram of a multi-input multi-channel controller	20
Fig. 3.1 Five machine power system used in simulation	24
Fig. 3.2 Local mode oscillation between G #1 and G #2	27
Fig. 3.3 Local (dominant) and interarea mode oscillation between G #1 and G #3	27
Fig. 3.4 Local and interarea (dominant) mode oscillation between G #2 and G #3	28
Fig. 3.5 Local and interarea (dominant) mode oscillation between G #2 and G #4	28
Fig. 3.6 Interarea mode oscillation between G #3 and G #5	29
Fig. 3.7 Interarea mode oscillation between G #4 and G #5	29
Fig. 3.8 Frame transformation for a multi-machine system	31
Fig. 4.1 SIMC case (1)	37
Fig. 4.2 SIMC case (2)	38

Fig. 4.3 MIMC case (1)	41-43
Fig. 4.4 MIMC case (2)	44-46
Fig. 4.5 MIMC case (3)	48-50
Fig. 4.6 MIMC case (4)	52-54
Fig. 4.7 MIMC case (5)	55-57
Fig. 4.8 Phase characteristics for 6th order bandpass filter	59
Fig. 4.9 Time delay characteristics for 6th order bandpass filter	60
Fig. 4.10 MIMC case (6)	63
Fig. 4.11 MIMC case (7)	64
Fig. 5.1 Multi-machine experimental setup	68
Fig. 5.2 Pi section representations of transmission lines	70
Fig. 5.3 Micro-machine experimental setup	73
Fig. 5.4 Short-circuit test, 0.8 pf lag, ΔP_e output of micro-machine	78-79
Fig. 5.5 Short-circuit test, 0.8 pf lag, ΔP_e output of 50 Hp generator	80-81
Fig. 5.6 Short-circuit test, 0.9 pf lead, ΔP_e output of micro-machine	82-83
Fig. 5.7 Short-circuit test, 0.9 pf lead, ΔP_e output of 50 Hp generator	84-85
Fig. C.1 ΔP_e channel controller op-amp circuit	108
Fig. C.2 $p\delta$ channel controller op-amp circuit	109
Fig. C.3 AVR and exciter op-amp circuit	110

LIST OF SYMBOLS

AVR	Automatic Voltage Regulator
CPSS	Conventional Power System Stabilizer
d	direct axis
e_d''	d-axis subtransient voltage
\dot{e}_d''	Rate of change in d-axis subtransient voltage
e_f	Field voltage
e_q'	q-axis transient voltage
e_q''	q-axis subtransient voltage
\dot{e}_q'	Rate of change in q-axis transient voltage
\dot{e}_q''	Rate of change in q-axis subtransient voltage
g	Governor output
G	Generator
$G_e(s)$	Exciter and AVR transfer function
$G_{p\delta}(s)$	Transfer function of $p\delta$ channel
$G_{\Delta P_e}(s)$	Transfer function of ΔP_e channel
$G_w(s)$	Washout circuit transfer function
H	Machine time constant
$H_{bp}(s)$	Bandpass filter transfer function
$H_{lp}(s)$	Lowpass filter transfer function
i_d, I_d	d-axis current
i_q, I_q	q-axis current
I_T	Terminal current

I_x	x-axis current
I_y	y-axis current
K_A	AVR gain
K_{P_e}	P_e channel gain
K_δ	δ channel gain
L	Load
m/c	Machine
MIMC	Multi-Input Multi-Channel
pf	power factor
PSS	Power System Stabilizer
P_e	Electrical power output
ΔP_e	Rate of change in electrical power
q	quadrature axis
SIMC	Single Input Multi-Channel
Δt	Time interval
TCR	Time Constant Regulator
T_{do}'	d-axis open circuit transient time constant
T_{do}''	d-axis open circuit subtransient time constant
T_e	Electrical torque
T_m	Mechanical torque
T_{qo}''	q-axis open circuit subtransient time constant
T_q	Washout filter time constant
T_1, T_2, T_3	PSS time constants
u, U	Control parameter
V_d	d-axis voltage
V_q	q-axis voltage

V_{ref}	Reference voltage
V_T	Terminal voltage
V_x	x-axis voltage
V_y	y-axis voltage
ω_o	Reference speed
$\Delta\omega, \dot{v}$	Rate of change in speed
x_d	d-axis synchronous reactance
x_d'	d-axis transient reactance
x_d''	d-axis subtransient reactance
x_q	q-axis reactance
x_q''	q-axis subtransient reactance
μ m/c	Micro-machine
v, ω	speed
$p\delta, \dot{\delta}$	rate of change in load angle

CHAPTER 1

INTRODUCTION

Man's demand for and consumption of energy has increased steadily since the invention of the induction motor [1]. Electrical energy comprises the main component in this ever increasing need. To satisfy this need, complex power systems have been designed and built.

Power is generated in the locations that economy and availability dictate, and consumed at other locations determined by population density and industrial influences. The trend in electrical power production is to build interconnected networks of transmission lines linking generators and loads together into large integrated systems. As the demand for electrical power increases, complexity increases. With the increased complexity in power systems comes an increased complexity in operation and control of these systems. Careful planning and design is required by the engineer to ensure that proper power system stability is maintained.

In this chapter the concept of stability is introduced. The concept of conflict and contradictions in the control of large systems, and the contradiction that exists in controlling multi-modal oscillation is also introduced. The multi-channel controller that overcomes this contradiction, and is used to stabilize the multi-modes of oscillation is described, and the thesis objective is outlined.

1.1. Power system stability

Successful operation of a power system depends largely on whether generators can provide reliable and uninterrupted service to the customers [1]. Reliability implies that the voltage and frequency at the loads are kept constant. Practically, this implies that the loads must be provided with voltages and frequencies that remain within certain allowable limits. Therefore the stability problem of power systems is one of the main concerns of an engineer in the power industry.

When dealing with the stability problem, a concern is with the behaviour of the power system after it is perturbed. In the power industry, a power system is said to be stable if the oscillatory response of the system during the transient period following a disturbance is damped and the system settles in a finite period of time to a new steady state operating condition [1]. This is not a strict definition, however it does give an idea of the concept of power system stability.

When a system is subjected to an impact load, the transient that follows this perturbation is oscillatory in nature. These oscillations are undesirable in that they are reflected as fluctuations in the power flow over the transmission line to the consumer [1]. Since these fluctuations are undesirable, some form of automatic control is used to increase the stability of the power system.

1.2. Contradictions and conflict in large systems

Classical control theory does not consider the fact that in systems of object control, contradictions can and do exist [2]. Rather than dealing with these

contradictions, they are simply eliminated from the control strategy used. However, recently this new line of thought has received more attention for several reasons. They are a result of observing very large systems, in which contradictory relations between sub-systems exist [2]. These contradictory goals detract from system performance. Examples of large systems are living organisms observed in the fields of medicine, biology, and sociology. These large systems contain control systems which are characterized by internal contradictions in the operation of their sub-systems [2]. The experiences of Vsevolod I. Astafiev, Yuri M. Gorsky, and Dmitriy A. Pospelov show that "the development and operation of large systems, their interaction, and operation of man-machine systems are full of contradictions" [2]. To illustrate this, the following examples are given :

- (1) It is a well known fact that the human brain consists of two hemispheres, the left and the right hemisphere [3]. When a given situation arises, each hemisphere views and evaluates the situation accordingly, and produces a solution to the situation. The solutions provided by each hemisphere are contradictory in nature due to the fact that each hemisphere tries to achieve its own objectives and goals [2]. The result is two sub-systems that exhibit contradictions. Without coordination of these conflicting or contradictory signals, the response to the situation would be non-sensible.

There are cases where the left and the right hemisphere do become isolated. When this happens the patient exhibits interesting phenomena. The realization of some action induced by one hemisphere involves a negative

response to the action from the other hemisphere [2]. It is assumed that within the brain there is some form of control that takes into account the internal contradiction and coordinates the signals provided by the two hemispheres to provide a sensible solution.

- (2) Pizotifen an antihistamine which is chemically similar to cyproheptadine, also shares its side effects. When used to treat migraines, an increase in weight occurs. When used to improve appetite, sleepiness and dizziness occurs [4]. A contradiction exists in its two different objectives as a drug.

In control problems contradictions also exist as a result of trying to achieve certain goals. For example, in second order systems, increasing the damping ratio results in a reduction in the overshoot, settling time, and the number of oscillations [5]. These are considered desirable objectives or goals. However, an increase in damping ratio also results in increases in peak time, delay time, and rise time [5]. All of these are undesirable objectives or goals. Any attempt to reduce the peak time, delay time or the rise time, would result in increases in the overshoot, settling time, and number of oscillations. The contradiction arises in attempting to achieve two different goals.

This problem of contradiction arises in the control of multi-modes of oscillation with conventional power system stabilizers, and is the main incentive for the development of a controller capable of resolving this contradiction. This is achieved through a multi-channel structure.

1.3. Why a multi-channel controller

Various control strategies have been implemented to increase the stability limits of power systems. One type of control strategy is to use a fixed transfer function controller. The fixed transfer function techniques include methods such as optimal control theory and classical control theory. Optimal control is based on the idea of minimizing a scalar performance index in both the system state variables and the system inputs [6]. This provides excellent damping since it utilizes all the state variables of the system to obtain the control parameter. However, there are disadvantages to this approach. These are :

- (1) the optimal solution is sensitive to the mathematical model of the system [7]
- (2) since power systems are high order systems, implementation of these techniques becomes difficult since all state variables are desirable for this method. Some of the the state variables are unmeasurable or difficult to obtain [6].

Conventional power system stabilizers (CPSS) utilize a fixed transfer function. They are easy to tune and implement and are widely used in power systems and have proven effective in improving the dynamic stability of a power system [8,9,10]. There are some disadvantages to using CPSSs. Since a fixed transfer function is used, it can be tuned to effectively damp one mode of oscillation. However when multi-modes of oscillation exist in a system a CPSS cannot adequately handle both modes. This is due to the conflicting or contradictory requirement on the CPSS to handle the two different frequencies of oscillation.

The increase in damping of one mode of oscillation results in a depreciated improvement in the other mode of oscillation. The best that can be achieved from a CPSS is a compromise in damping of the two modes of oscillation. Since a PSS is best capable of handling one mode of oscillation at a time, a new algorithm or method is required.

Another problem with the CPSS is that it cannot adapt to various operating conditions. A change in the operating condition usually causes a change in the mode of oscillation frequency, and the best damping action is not obtained from the PSS. However, this is not a *major* problem because the operating condition usually doesn't change sufficiently to cause catastrophic deterioration in the performance of the CPSS.

The problem of multi-modal oscillations in power systems is examined from the point of view of contradictions and conflict between the need to damp oscillations of different frequencies. The conflict is resolved by a controller proposed in this thesis having a multi-input multi-channel (MIMC) structure. *It is discussed in chapter 2 in more detail.*

1.4. Thesis Objective

Power systems can and do exhibit contradictions. These contradictory goals tend to deter the system performance and obscure goals. The objective of this thesis is to introduce a multi-channel controller that is designed to eliminate contradiction. The effectiveness of the multi-channel controller in controlling

multi-modes of oscillation is demonstrated. This is achieved by applying various types of disturbances and operating conditions to a multi-machine power system, and obtaining comparison results between the multi-channel controller and a conventional stabilizer.

Simulation studies were performed on a five machine power system model developed to exhibit multi-modes of oscillation. The short circuit test and change in reference voltage were conducted in the simulation studies. Various studies involving these tests were performed.

Experimental studies were performed on a five machine power system. The setup consists of a synchronous micro-machine, a 50 Hp generator, and three 5 Hp generators connected in parallel. Short circuit tests applied at the micro-machine were conducted with the MIMC controller, no controller, and each channel of the MIMC controller applied to the micro-machine.

1.5. Organization of Thesis

The thesis is organized in the following manner.

Chapter 2 introduces the power system stabilizer and explains how it is used to improve the stability of a power system. The contradiction that exists in controlling multi-modes of oscillation using a CPSS is outlined, and two different multi-channel structures are introduced and a detailed analysis of these structures in handling multi-modes of oscillation and eliminating this conflict is discussed.

Chapter 3 introduces the five machine power system model used for simulation. The set up and features of this multi-machine model are discussed. The problem of multi-modes of oscillation is discussed, and the two modes of oscillation observed in the multi-machine power system are described.

Chapter 4 gives the simulation results obtained using the five machine power system. The various disturbances and tests performed using the single-input multi-channel (SIMC) controller and MIMC controller are given. Comparative results between the MIMC controller and a CPSS that show the effectiveness of the MIMC controller are introduced and discussed.

Chapter 5 describes the experimental setup and the results obtained using this setup. A multi-machine power system that exhibits multi-modes of oscillation is introduced. Results obtained from the short circuit tests with no controller, a MIMC controller, and each channel of the MIMC controller applied to the multi-machine power system are introduced and discussed.

Chapter 6 gives concluding remarks and further possible research in this area.

CHAPTER 2

MULTI-CHANNEL CONTROLLER

The following chapter deals with the problem of stability in power systems. The three different types of power system stability are defined, and the problem of stability encountered in complex power systems is discussed. The function of power system stabilizers and the use of a supplementary control signal to improve the stability limits is also discussed. However, the main objective of this chapter is to introduce the multi-channel controller used in the simulations to overcome the problem of contradiction that arises in the control of the special problem of multi-modes of oscillation.

2.1. Power System Stabilizer

When analyzing power system stability, one must take into account the three different types:

- (1) steady state
- (2) transient, and
- (3) dynamic stability.

Steady state stability is simply the observation of the system behaviour around an equilibrium point with no disturbance applied to the system. This basically

means that this type of stability is dependent on the operating condition of the system only.

Transient stability is the study of the system behaviour under sudden impact or large disturbances. This type of stability problem is mainly dependent on the type and location of the disturbance, and not on the operating condition.

Dynamic stability is the study of the behaviour of a power system under the influence of small random disturbances or changes in load. This type of stability problem causes low frequency oscillations to be present on the system [11]. These oscillations usually remain well after the disturbance has been applied. If the system damping is insufficient, the oscillations grow and cause the system to become unstable. Unlike transient stability, dynamic stability is dependent on the state or operating condition of the system.

After the late 1950's the generating units added to power systems were equipped with high gain, fast acting automatic voltage regulators (AVR). When the number of these units became a larger percentage of the generation capacity, it was observed that the AVR action had a negative effect on the dynamic stability [12,13]. This detrimental effect reduces the stability margins of the machines, and hence presents limitations on power transfer capabilities. Emphasis has been given to controls that provide the required compensating effects to offset this problem [14]. Particular attention has been placed on stability of synchronous machine operation [15]. Various methods have been implemented to improve power system stability limits. These methods include generator excitation control [16-20], and

generator input power control [21-23]. The most commonly used is generator excitation control [6] because

- (1) usually the electrical system time constant is much smaller than that of a mechanical system, and
- (2) electrical control systems are more economical and are easier to implement than mechanical systems.

The trend in solving the stability problem is towards the use of supplementary control that is fed back to the excitation system [8,24]. This is achieved by a power system stabilizer (PSS). PSSs are widely used in power systems for the control of oscillations present in the system.

The basic function of a PSS is to extend stability limits by modulating generator excitation to provide damping to the oscillation of synchronous machine rotors relative to one another. To provide damping to these oscillations, the stabilizer must produce a component of electrical torque on the rotor which is in phase with speed variations. For any given input signal the transfer function of the stabilizer must compensate for the gain and phase of the excitation system, the generator, and the power system [12].

A block diagram of conventional excitation control using a PSS is shown in Fig. 2.1. Conventional means of stabilization are obtained by the use of a PSS having some fixed transfer function. An appropriate output is selected which contains information on the modes of oscillation present in the system. The output

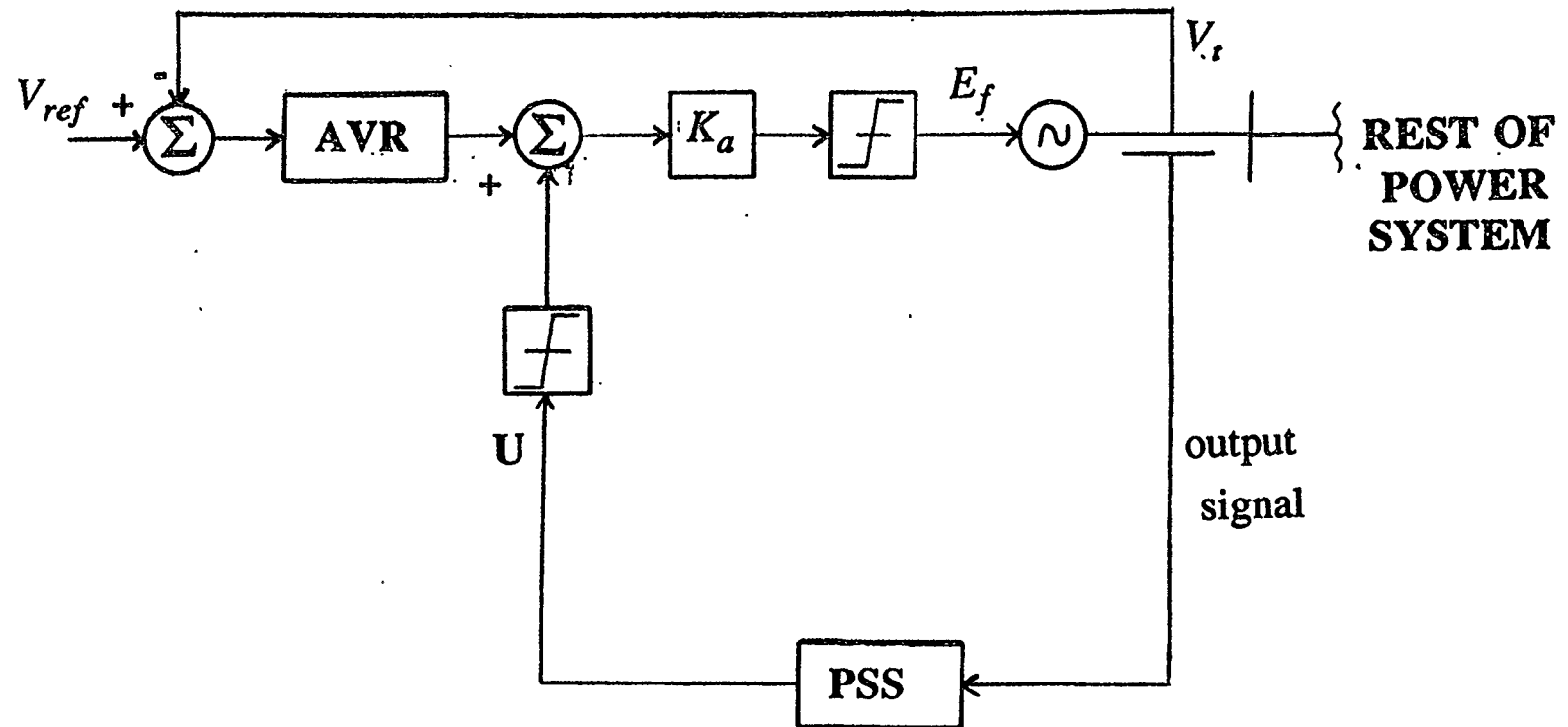


Fig. 2.1 Block diagram of conventional excitation control

signal is passed through a stabilizer, which has been designed for the known modes of oscillation, and a control parameter u is obtained. This control parameter is passed through a limiter which limits the control signal. In the simulation studies the limits were set to ± 0.03 p.u. This signal is then combined with the output of the AVR and is amplified by K_a . K_a is the gain of the exciter. The signal obtained after the amplification stage is passed through another limiter. The signal obtained is E_f , which is fed into the excitation system of the generator. E_f is limited to ± 6 volts in the simulation studies.

The PSS is designed to provide adequate local mode damping under all operating conditions, and simultaneously to provide a high contribution to damping of interarea modes [25] (*modes of oscillation are discussed in more detail in Chapter 3*). This is due to the fact that the PSS has a fixed transfer function. Each mode of oscillation requires some phase and gain compensation to effectively damp the oscillations out. These phase and gain margins cannot be achieved simultaneously from a fixed transfer function PSS.

It is a contradictory requirement of damping out two different frequencies of oscillation. This is because each mode of oscillation requires its own phase and gain margins, which cannot be achieved simultaneously using a CPSS. Therefore the PSS does not provide the optimal or best damping action for either mode of oscillation. The conventional control scheme is limited to power systems in which a single mode of oscillation exists or power systems in which one mode of oscillation dominates over the other mode of oscillation. Therefore another method

of providing the damping to the two modes of oscillation is required. To handle the contradiction that exists in controlling multi-modes of oscillation using a conventional PSS, a multi-channel controller is proposed.

2.2. Multi-channel controller

For multi-machine power systems in which multi-modes of oscillation exist, output signals can be properly selected to contain the modes of oscillation required. Each mode of oscillation can be stabilized independently by using a multi-channel stabilizing system. The proposed structure is shown in Fig. 2.2.

This scheme shows two channels, each dedicated to damping out one mode of oscillation. Each channel is tuned independently, one channel is tuned to provide the best damping action to local modes of oscillation, and the other channel is tuned to provide the best damping action to interarea modes of oscillation. Two control parameters u_1 and u_2 are obtained, which correspond to the controls applied for the local mode and interarea mode of oscillations respectively. These are combined together to obtain the control parameter u which is added to the AVR signal to form the excitation signal. The contradiction is resolved by assigning each mode of oscillation to its own channel, with each channel tuned separately to provide the best phase and gain margins, and hence the best damping.

Two schemes are possible, a single input multi-channel controller and a multi-input multi-channel controller. They are discussed in the following sections.

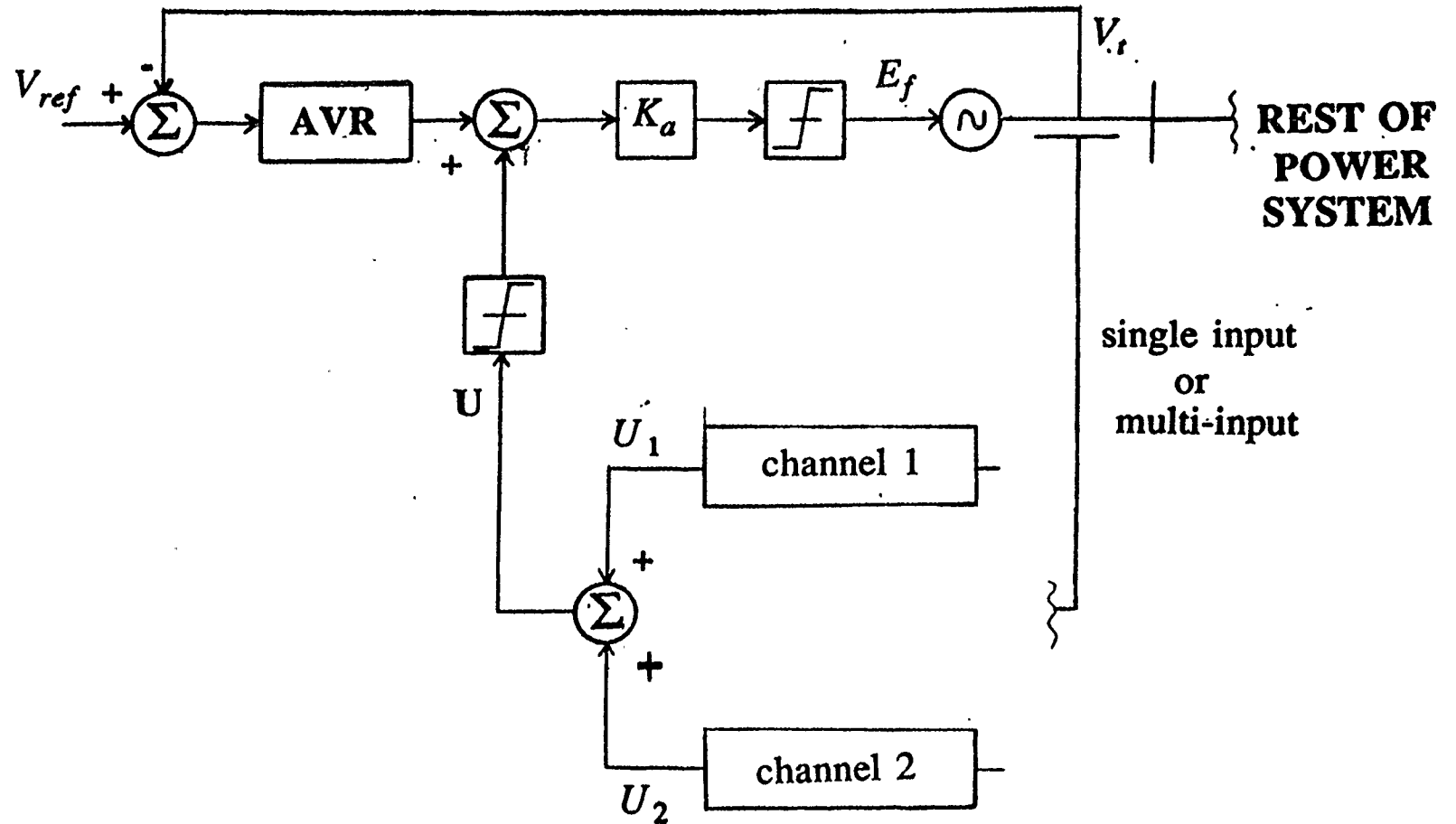


Fig. 2.2 Block diagram of multi-channel controller

2.3. Single input multi-channel controller

A single input multi-channel controller (SIMC) basically has only one input. The input to the multi-channel controller is chosen to be $p\delta$ (the rate of change in load angle). Each channel is comprised of a power system stabilizer and a filter, as shown in Fig. 2.3. In the proposed controller, the two modes of oscillation are first isolated using two filters. Filter #1 is a lowpass filter designed to pass all frequencies below 0.5 Hz, i.e the interarea mode of oscillation. A 4th order lowpass filter is used to ensure the attenuation of the local mode of oscillation. The lowpass filter has the transfer function:

$$H_{lp}(s) = \frac{b_4}{s^4 + a_1s^3 + a_2s^2 + a_3s + a_4} \quad (2.1)$$

Filter #2 is a bandpass filter designed to pass all frequencies between 0.8 and 1.2 Hz. A 6th order bandpass filter is used to ensure the attenuation of the interarea and interplant modes of oscillation. The bandpass filter has the transfer function:

$$H_{bp}(s) = \frac{b_3s^3}{s^6 + a_1s^5 + a_2s^4 + a_3s^3 + a_4s^2 + a_5s + a_6} \quad (2.2)$$

Each stabilizer is designed to provide the best damping action for each mode of oscillation. The filter design and parameters are given in appendix A. A power system stabilizer suggested by Ontario Hydro [26], that is used for PSS1 and PSS2,

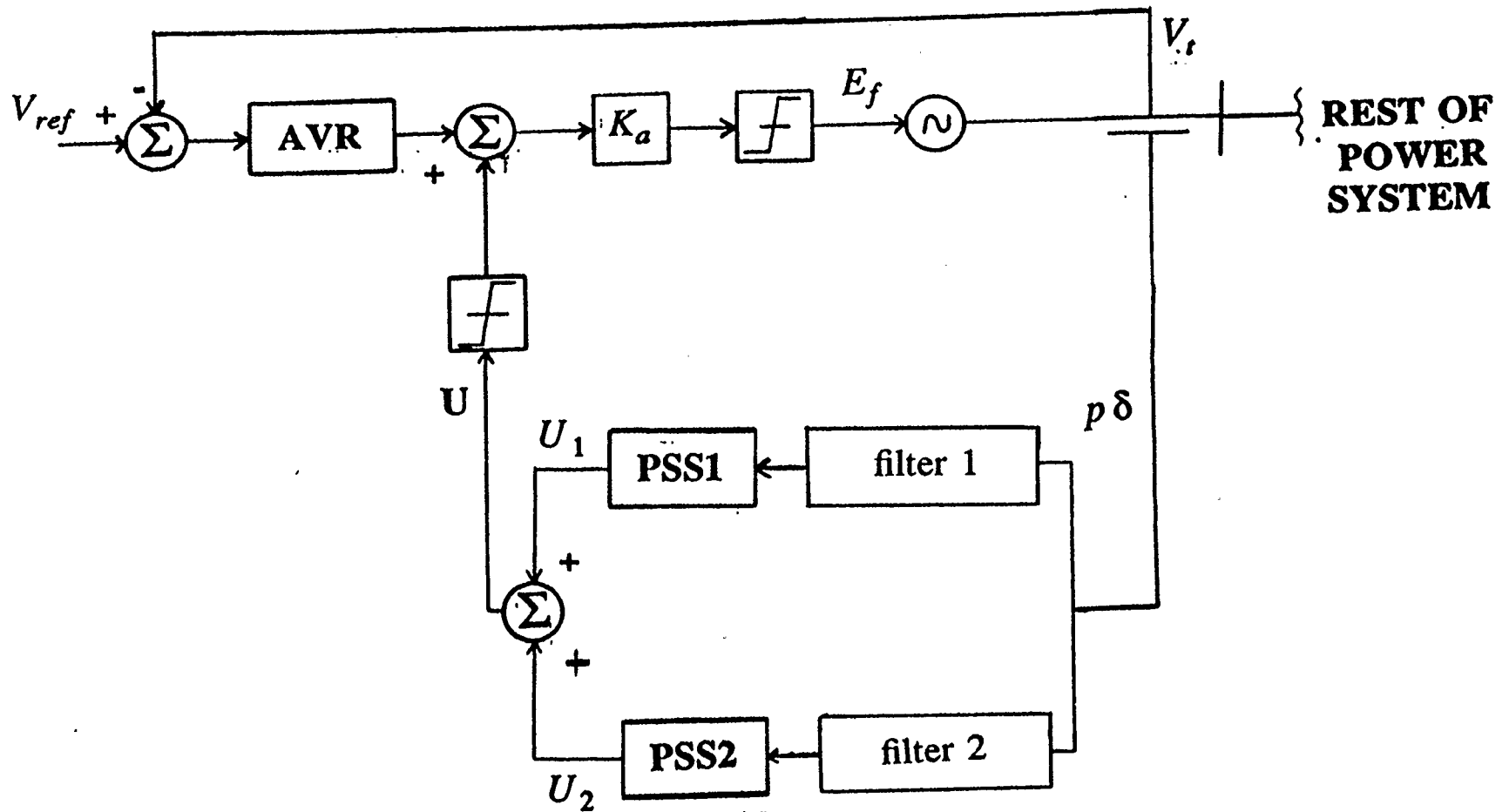


Fig. 2.3 Block diagram of a single input multi-channel controller

has the following transfer function

$$U(s) = K_{\delta} \cdot \frac{sT_q}{1 + sT_q} \cdot \frac{sT_1 + 1}{sT_2 + 1} \cdot p \delta(s) \quad (2.3)$$

where

T_q = time constant of washout filter

T_1, T_2 = time constants of controller

K_{δ} = gain of controller

A washout filter is needed to remove any dc superimposed on the desired signal. T_1 , T_2 , and K_{δ} are selected to provide the best damping action for each mode of oscillation. T_q is selected to provide the required removal of dc, and is also selected to provide minimum effect on the control aspect.

There are two problems associated with this scheme. These problems are due to the filters used. The filters introduce time delay and phase into the system. These problems are discussed in more detail in chapter 4.

2.4. Multi-input multi-channel controller

A multi-input multi-channel controller basically has the configuration of Fig. 2.2. with two inputs. The inputs to the multi-channel controller are speed ($p\delta$) and

electric power (P_e) obtained from the machines, as shown in Fig. 2.4. The same power system stabilizer that was suggested in the previous section is used for PSS1 and has the following transfer function

$$U_1(s) = K_\delta \cdot \frac{sT_q}{1 + sT_q} \cdot \frac{sT_1 + 1}{sT_2 + 1} \cdot p \delta(s) \quad (2.4)$$

For PSS2 a modified power system stabilizer is used from that suggested by Ontario Hydro. PSS2 has the following transfer function

$$U_2(s) = -K_P \cdot \frac{sT_q}{1 + sT_q} \cdot \frac{sT_1 + 1}{sT_2 + 1} \cdot \frac{1}{sT_3 + 1} \cdot P_e(s) \quad (2.5)$$

where

T_q = time constant of washout filter

T_1, T_2, T_3 = time constants of controller

K_P = gain of controller

A modified PSS is required because of the nature of the electrical power signal. It is 90 degrees out of phase with the $p\delta$ signal, and modification to the transfer function must be made to take this into account. Again a washout filter is needed

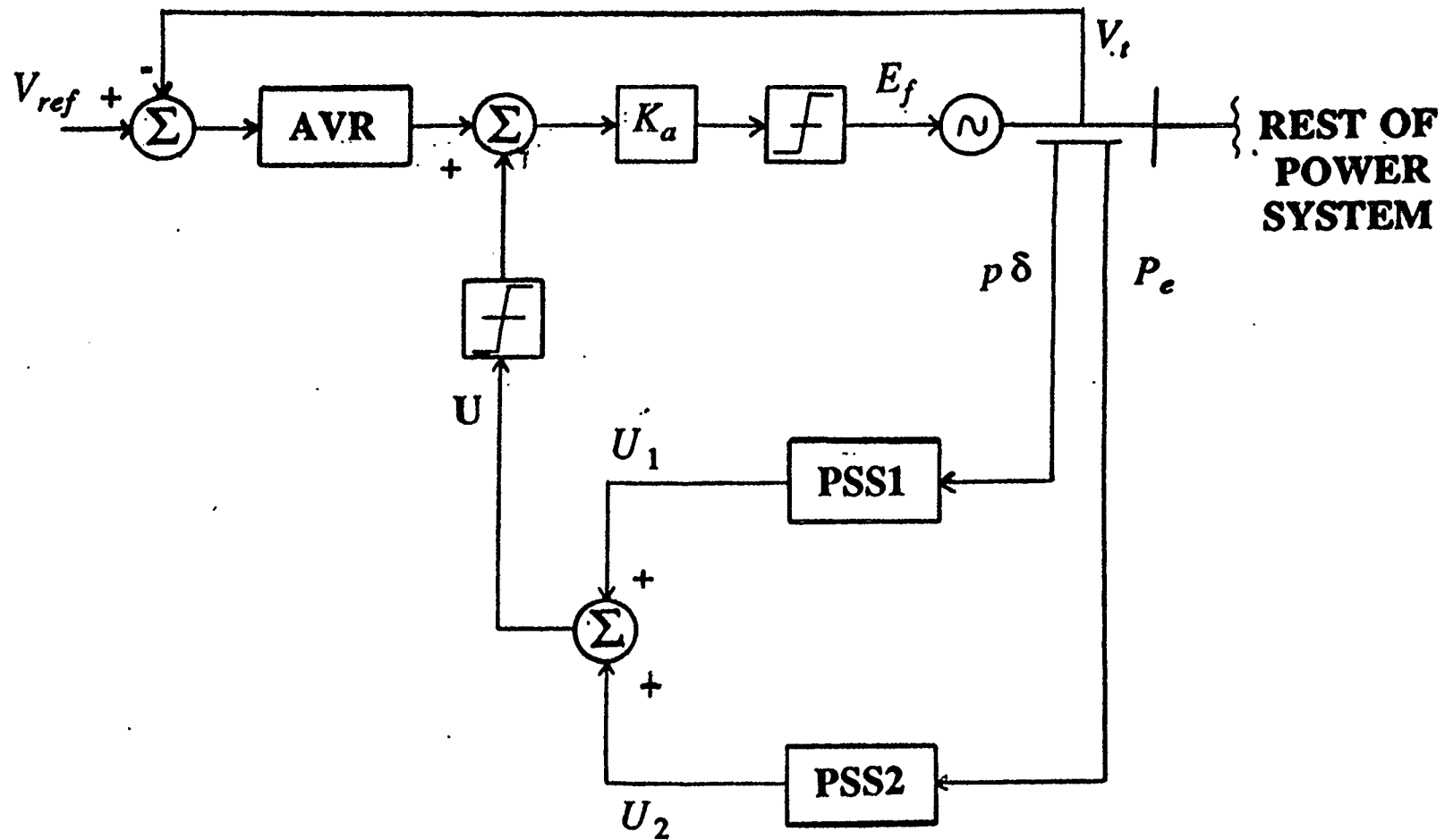


Fig. 2.4 Block diagram of a multi-input multi-channel controller

to remove any dc superimposed on the electric power signal.

This scheme has an advantage over the single input multi-channel controller. It uses input signals that characterize the modes of oscillation to which they have been assigned. The interarea modes of oscillation are low frequencies associated with the mechanical part of the system, and hence are best controlled by a signal derived from a mechanical quantity i.e $p\delta$. The local modes of oscillation are slightly higher frequencies associated with the electrical part of the system, and hence are more sensitive to a control signal derived from an electrical quantity such as P_e . Since each mode of oscillation is more sensitive to its own input signal, no filtering is required. This eliminates any problems associated with the filters.

There is one problem associated with incorporating this scheme. This problem is due to the power transfer between machines which causes the controls to interact. However this is not a serious problem and can easily be avoided. *This problem is discussed in more detail in chapter 4.*

2.5. Summary

This chapter introduces the concept of stability and the use of a supplementary control signal to improve the system stability. The basic principles of a PSS are introduced, and limitations of the conventional means of stabilization are discussed. The use of a multi-channel controller to overcome these limitations and the principles behind the multi-channel controller are also introduced.

CHAPTER 3

MULTI-MACHINE POWER SYSTEM MODEL

In this chapter the power system model used for computer simulation of the multi-modes of oscillation is introduced. This special power system oscillation problem has been given a great deal of attention in recent years. The problem can be seen in multi-machine power systems in which the machine's rotors, behaving as rigid bodies, oscillate with respect to one another using the electrical transmission path between them to exchange energy [25]. For a multi-machine power system, in which the interconnected generating units are weakly connected and have quite different inertia constants, multi-mode oscillation occurs. These modes of oscillation can be divided into three categories; local mode, interarea mode, and intraplant mode. This chapter describes a five machine power system model used for simulation. Two modes of oscillation (of the three different modes of oscillation possible) are observed in the five machine model.

3.1. Multi-machine power system model

In order to simulate the multi-modes of oscillation, a multi-machine power system must be developed which contains them. A three machine power system model developed by Shi-jie Cheng [6] based on the system used in [25] is

extended in this thesis into a five machine power system model, and is discussed in this section.

The five machine power system that is used for simulation purposes is shown in Fig. 3.1. Five generating units are connected through the transmission network. In this system a 1000 MVA generating unit (G #1) is connected to an area with a capacity of 10 GVA represented by G #2 [6]. Two other power systems are connected to this area. G #3 has a 10 GVA capacity and is connected to this area through a long transmission line. G #5 has a 1000 MVA capacity and is connected to this area through a medium length transmission line. G #4 has a 10 GVA capacity and is connected to the area served by G #3 through a long transmission line. Each area normally serves its own load and is almost fully loaded with a small load flow over the tieline. An infinite bus is not included.

3.2. System modes of oscillation

The oscillation of a multi-machine power system is quite complicated in nature, however the range of frequencies of concern to stability can be identified [6]. The frequency range of interest occurs from 0.2 to 2.5 Hz. This frequency range is further subdivided into the three categories, local mode, interarea mode, and intraplant mode.

The experiences of E. V. Larsen and D. A. Swann show that "local mode oscillation occurs when remote generating units are connected to a relatively large power system through weak, essentially radial transmission lines. Its natural

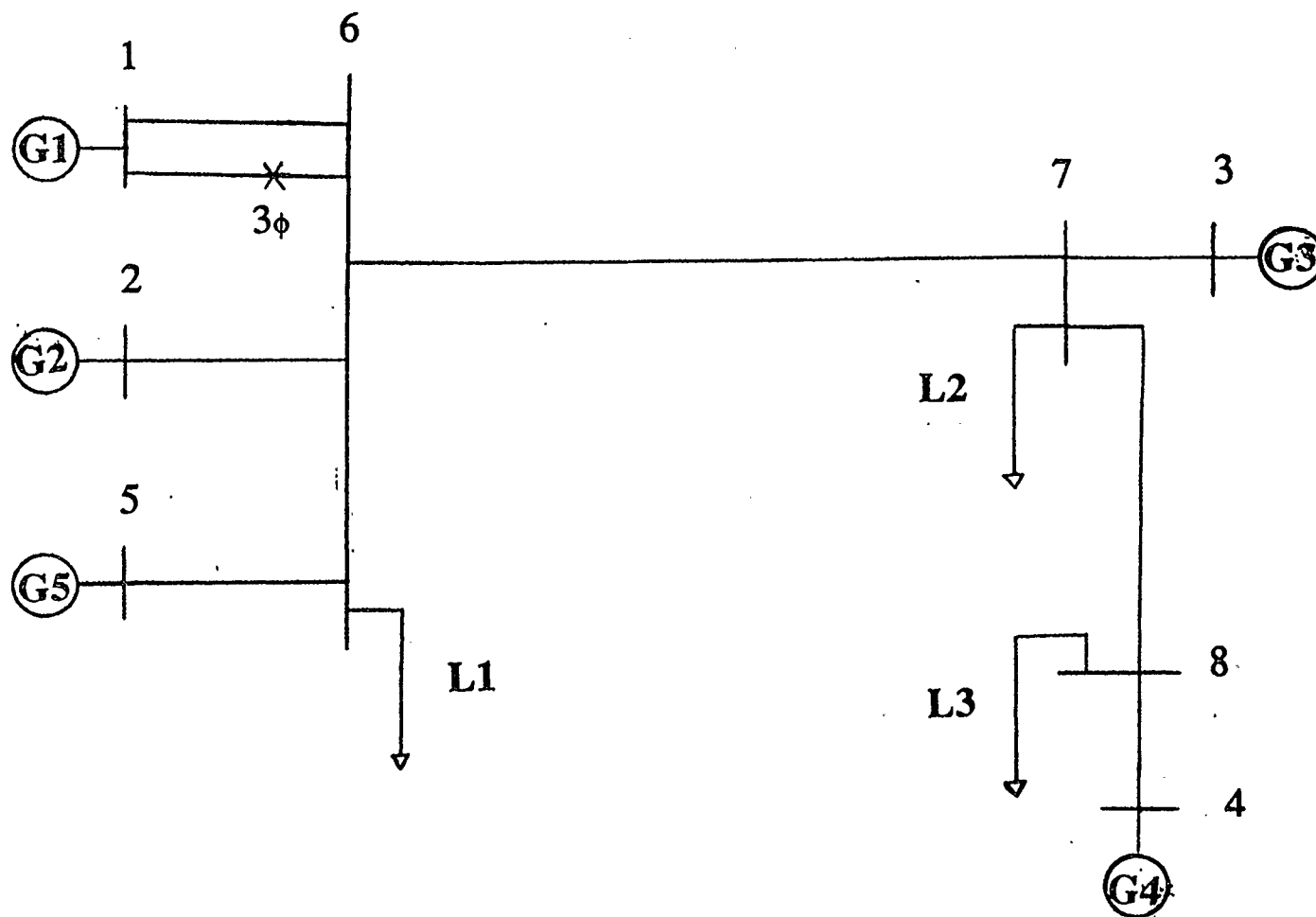


Fig. 3.1 Five machine power system used in simulation

frequency is typically in the range of 0.8 to 1.8 Hz" [25].

Interarea mode oscillation occurs when the aggregate of units at one end of the intertie oscillate against the aggregate of units at the other end [22,25,28,29]. Its natural frequency is typically in the range of 0.2 to 0.5 Hz.

The third kind of oscillation mode is the intraplant mode. These oscillations occur between units in the same plant, and are a consequence of their controls interacting rather than power transfer stability limits. It is generally undesirable for a stabilizer to respond to these intraplant oscillations, typically ranging in frequency from 1.5 to 2.5 Hz, as this detracts from its ability to enhance transfer limits from the power plant [25,30]. Since it is undesirable to control intraplant modes of oscillation, they are not taken into account when designing power system stabilizers.

For the five machine model, two modes of oscillation (local and interarea) have been observed. The local mode of oscillation frequency was measured to be in the 1.1 Hz range. The interarea mode of oscillation frequency was measured to be in the 0.3 Hz range. The frequency of oscillation is dependent on the type of disturbance applied.

To illustrate the multi-modes of oscillation, the system response to a large disturbance is shown. As can be seen from Figs. 3.2 to 3.7, multi-modes of oscillation exists in the five machine power system. Fig. 3.2 shows the local area speed oscillations between G #1 and G #2. Since both these generators are in the same area, they exhibit local mode of oscillation. The length of the transmission

line between G #1 and G #2 is relatively weak, and accounts for the local mode of oscillation being close to the lower limit (0.8 Hz). Fig. 3.3 shows the modes of oscillation between G #1 and G #3. This contains both interarea and local mode of oscillation, although the local mode of oscillation dominates. Both modes of oscillation are observed because G #1 is dominant mainly in local mode, while G #3 is mainly dominant in interarea mode of oscillation. Fig. 3.4 shows the local and interarea mode of oscillation between G #2 and G #3. G #2 contains both modes of oscillation, and since G #3 is a remote generating unit, interarea mode of oscillation is exhibited. This is also true for other combinations of generating units. Figs. 3.5 to 3.7 show the local and interarea modes of oscillation that are observed between the other machines. It can be seen from these figures that although both modes are present, the interarea mode of oscillation dominates. This is expected since the large generators are positioned to contribute interarea mode of oscillation to the system.

3.3. Simulation procedure

Each generating unit is modelled by five first order differential equations given below [6] :

$$\dot{\delta} = v$$

$$\dot{v} = \frac{(T_m + g - T_e)\omega_o}{2.H}$$

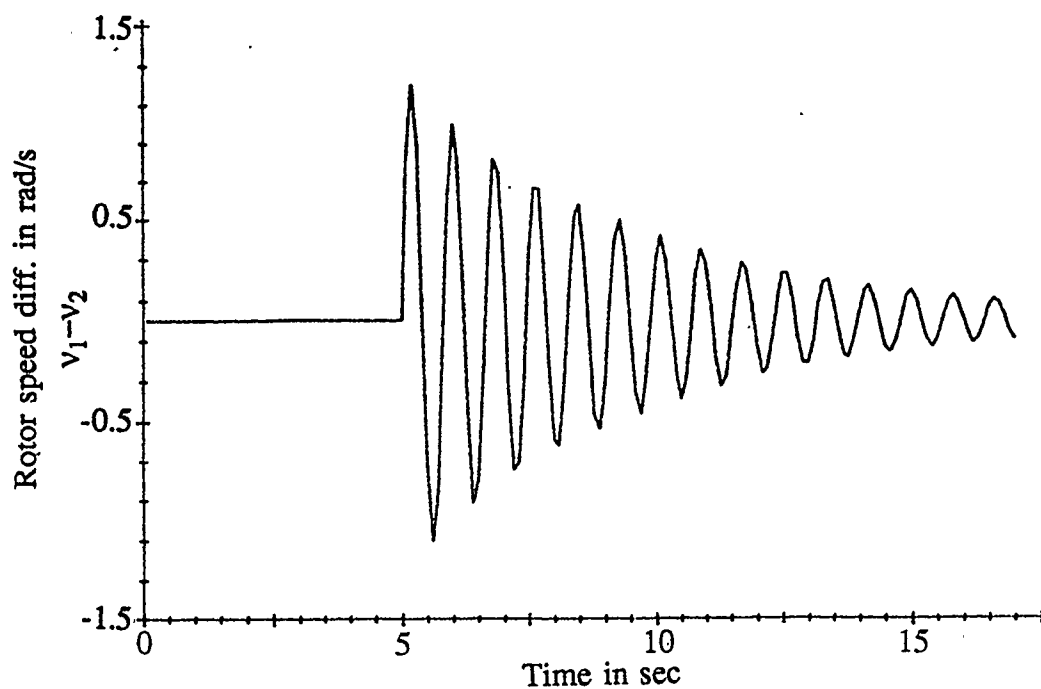


Fig. 3.2 Local mode oscillation between G #1 and G #2

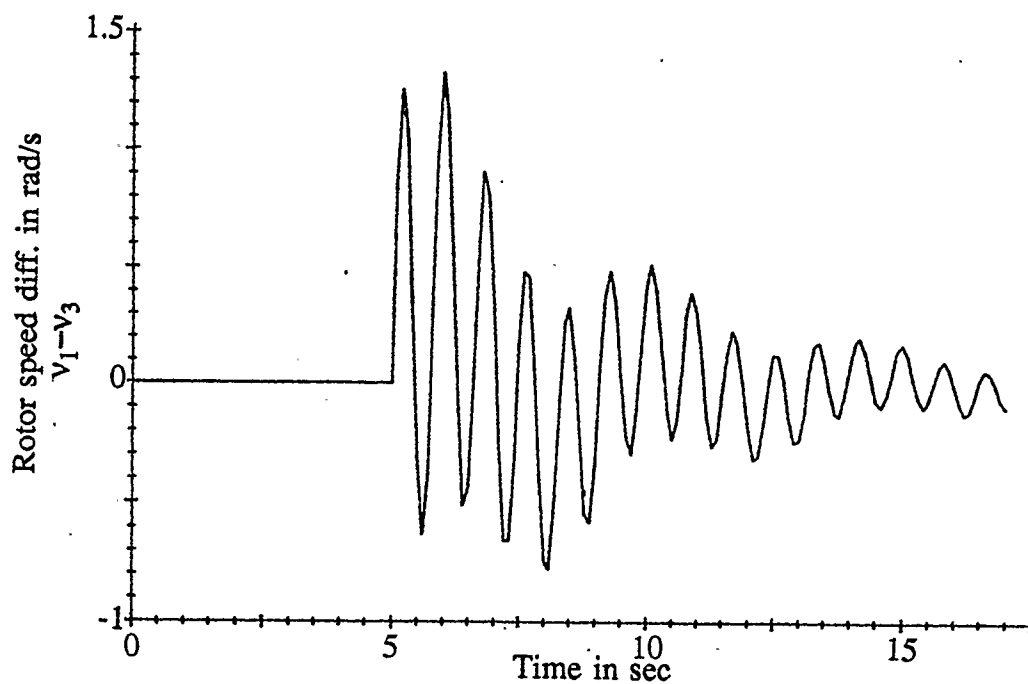


Fig. 3.3 Local (dominant) and interarea mode oscillation between G #1 and G #3

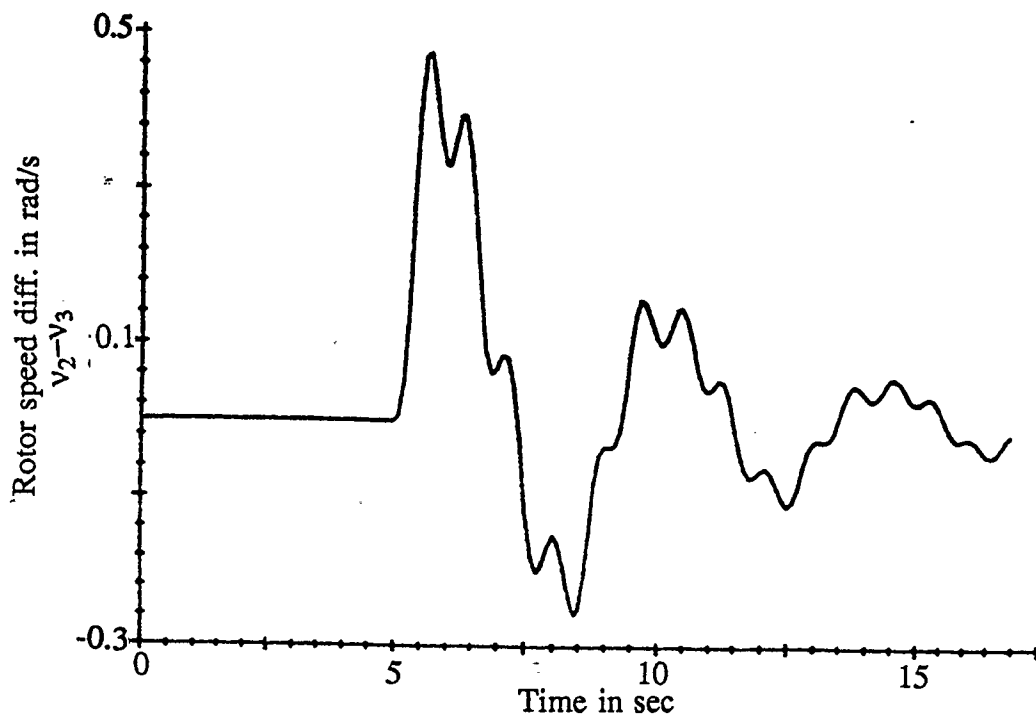


Fig. 3.4 Local and interarea (dominant) mode oscillation between G #2 and G #3

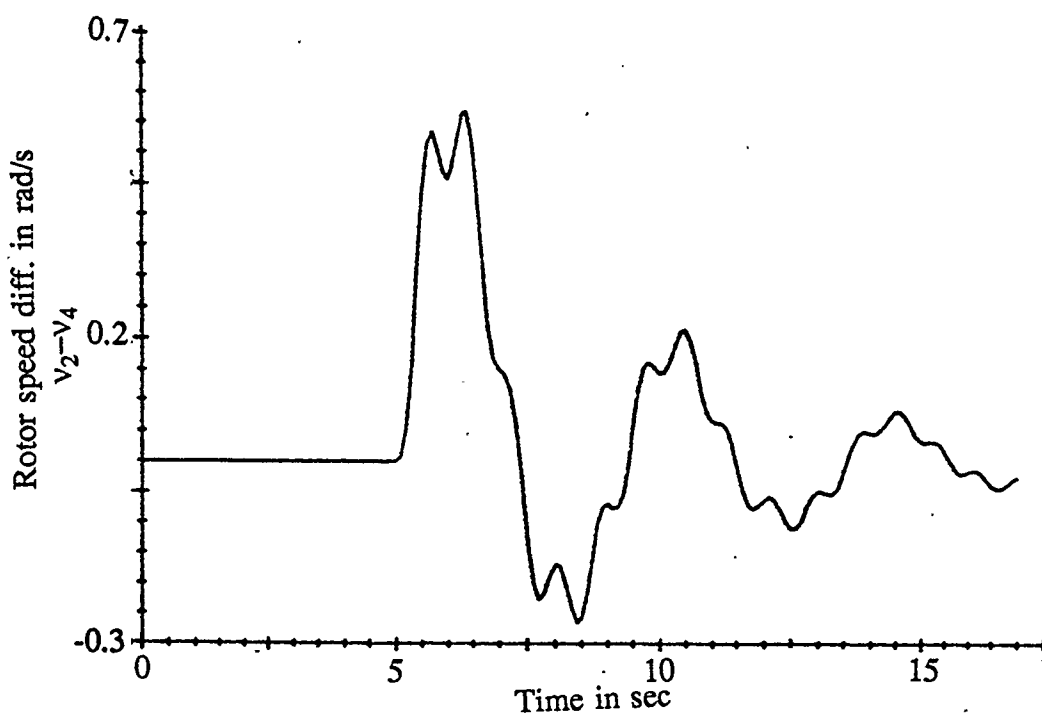


Fig. 3.5 Local and interarea (dominant) mode oscillation between G #2 and G #4

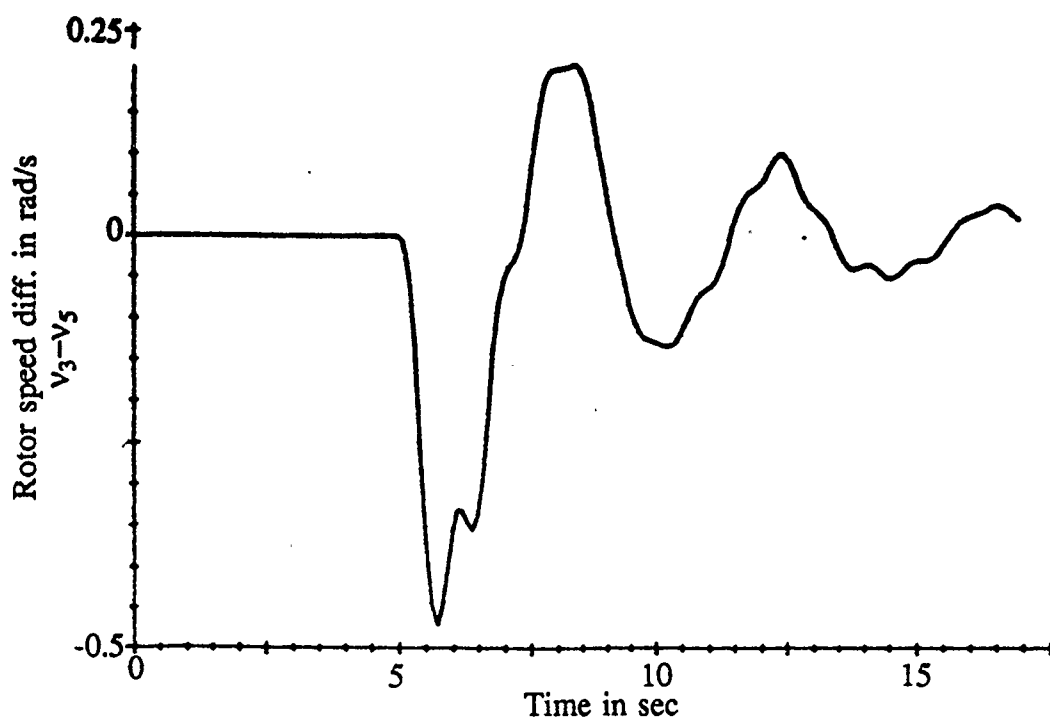


Fig. 3.6 Interarea mode oscillation between G #3 and G #5

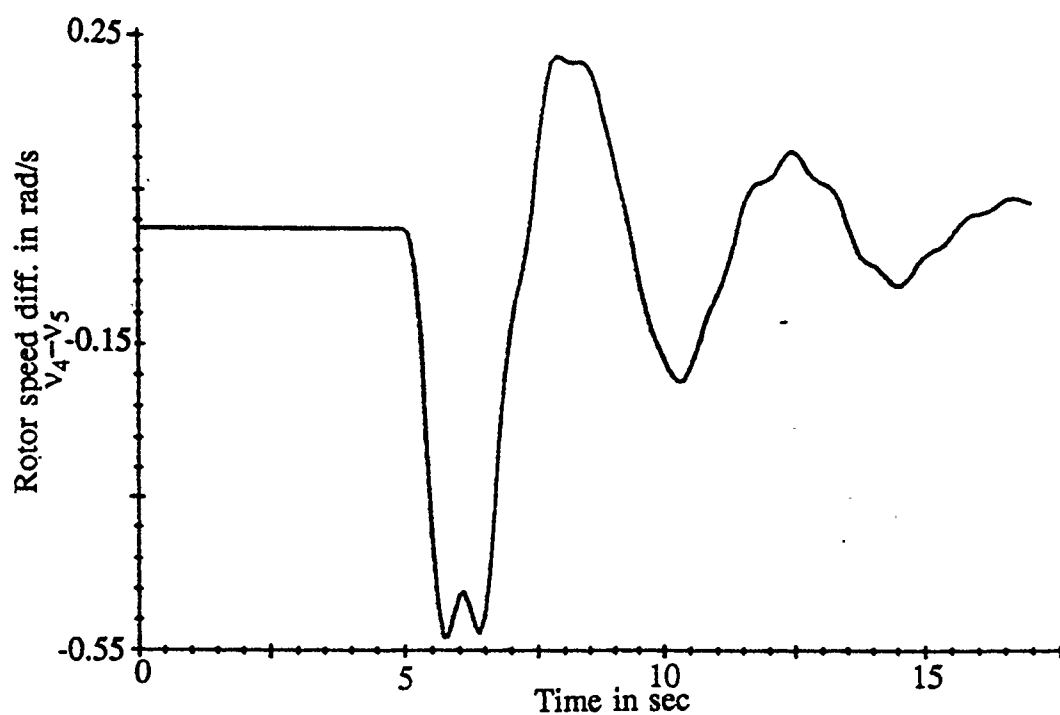


Fig. 3.7 Interarea mode oscillation between G #4 and G #5

$$\dot{e}_q' = \frac{e_f - e_q' + i_d(x_d - x_d')}{T_{d0}'} \quad 3.1$$

$$\dot{e}_q'' = \frac{-e_q'' - i_d(x_d' - x_d'') + e_q' + T_{d0}'' + \dot{e}_q'}{T_{d0}''}$$

$$\dot{e}_d'' = -\frac{e_d'' + i_q(x_q - x_q'')}{T_{q0}''}$$

The state variables are e_d'' , e_q'' , e_d' , δ , and v . Taking e_q'' and e_d'' as the state space variables, the generators are represented as voltages e_q'' and e_d'' behind the reactances x_q'' and x_d'' . The simulation procedure as developed by Shi-jie Cheng [6] can be summarized as follows :

- (1) form the original admittance matrix
- (2) form the reduced network admittance matrix
- (3) obtain the reduced network impedance matrix from the above
- (4) select the initial terminal voltages, and solve for the terminal currents by using the network admittance matrix
- (5) calculate the terminal variables in d-q frame for each generating unit from the x-y frame variables, as shown in Fig. 3.8 for reference
- (6) solve the five differential equations using the fourth order Runge-Kutta integration method ($\Delta t = 0.001$ sec.)
- (7) obtain V_{xi} and V_{yi} from the d-q frame variables e_{di}'' and e_{qi}''

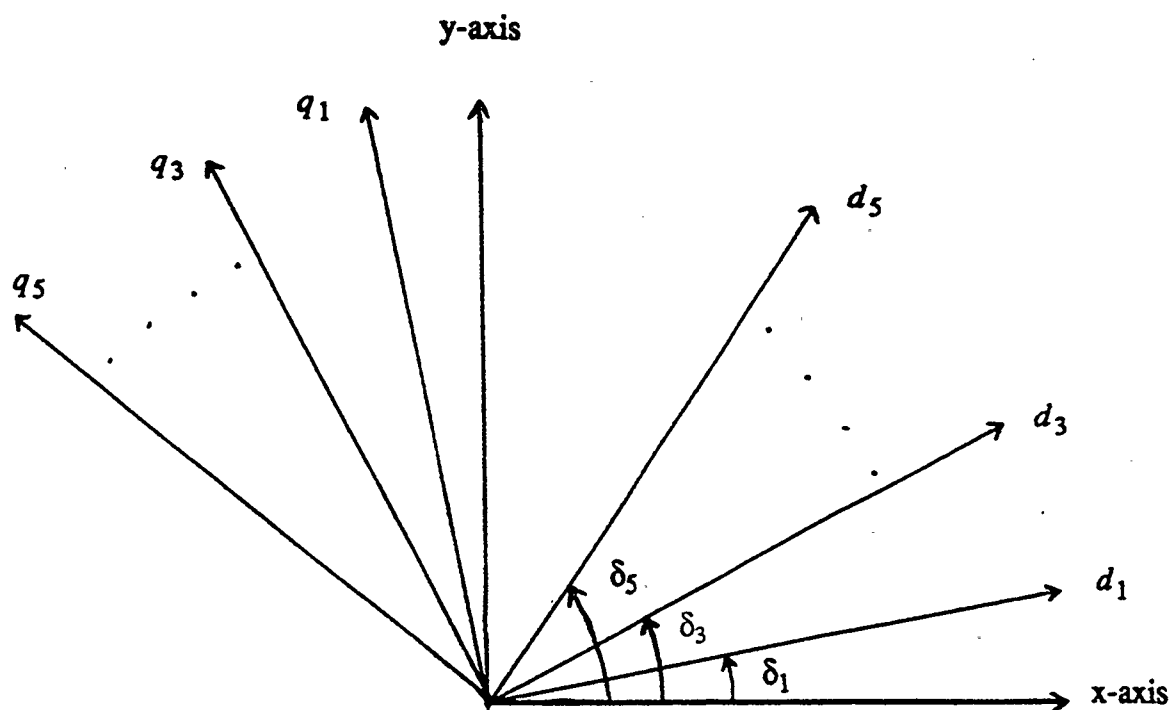


Fig. 3.8 Frame transformation for a multi-machine system.

- (8) change the generator sub-transient reactances into equivalent reactances in the x-y frame and combine with the network impedance matrix to obtain the combined network impedance matrix
- (9) solve for I_x and I_y and then for V_x and V_y using the combined admittance and impedance matrices
- (10) obtain the d-q frame variables I_d , I_q , V_d , and V_q from the x-y frame variables I_x , I_y , V_x , and V_y
- (11) repeat steps (6) to (10) using the d-q frame variables

The above procedure is repeated until the required time of simulation has been achieved.

3.4. Summary

This chapter deals with the five machine model used for simulation. The power system configuration is presented, with a description of the different modes of oscillation that exist. An example of the multi-modes of oscillation present in the five machine model is also presented. A brief description of the simulation procedure of the five machines is also introduced.

CHAPTER 4

SIMULATION RESULTS FOR MULTI-CHANNEL CONTROLLER

In this chapter the results of simulation studies using the five machine model described in chapter 3 with various disturbances applied ranging from small to large are shown. Comparisons between the multi-channel controller, described in chapter 2, and conventional means of stabilization have been conducted. This chapter introduces some problems associated with the SIMC controller and the improvements that can be achieved with a MIMC controller.

4.1. Simulation Studies

Various studies have been performed using both the SIMC and the MIMC controller. Two simulations were done for the SIMC controller simply to illustrate the problems associated with this structure. Studies for the MIMC controller were conducted to show how it controls multi-modes of oscillation.

For tests on the SIMC controller the same disturbance was applied in both cases. However the operating condition was changed. This changed the local mode of oscillation frequency from 1.1 Hz. to 0.9 Hz. and introduced a problem because the phase compensation required at each frequency is different. This problem is associated with the filters used in the SIMC structure and is discussed in *section*

4.3. The following studies were conducted on the five machine power system using the SIMC controller.

SIMC case (1)

40% increase in input mechanical torque applied at G #1 with the SIMC controller on all five machines.

SIMC case (2)

40% increase in input mechanical torque applied at G #1 with the SIMC controller on all five machines, with new initial operating conditions. The terminal voltages of G #1, G #4, and G #5 are reduced from 1.3, 1.25, 1.3 p.u. respectively to 1.1 p.u.

The following tests were performed on the five machine power system for the MIMC controller

MIMC case (1)

Three phase short circuit of 0.1 seconds duration applied at G #1 with the proposed MIMC controller on G #1 and conventional controllers on G #2, G #3, G #4, and G #5.

MIMC case (2)

Three phase short circuit of 0.1 seconds duration applied at G #1 with the MIMC controller on all five machines.

MIMC case (3)

10% decrease in the load connected to area 1 (G #1 and G #2), with MIMC controllers on all five machines.

MIMC case (4)

5% increase in reference voltage of G #1 with MIMC controllers on all five machines.

MIMC case (5)

5% increase in reference voltage of G #1 with MIMC controllers on all five machines, with new initial operating conditions. The terminal voltages of G #1, G #4, and G #5 are reduced from 1.3, 1.25, 1.3 p.u. respectively to 1.1 p.u.

To illustrate the problem associated with the MIMC controller the following additional tests were performed :

MIMC case (6)

40% increase in torque on generator #1, with MIMC controller on generator #2 only. The gain is set equal to the gain of the MIMC controller used on generator #1.

MIMC case (7)

40% increase in torque on generator #1, with MIMC controller on generator #2 only. The gain is set to one tenth of the gain of the MIMC controller used on generator #1.

These simulations give different types of disturbances, ranging from small perturbations to large sudden impact. Also, simulations in which the initial operating condition have been changed were performed.

4.2. Simulation Results

The same simulation studies conducted for the SIMC controller were repeated with no controllers on any of the five machines. This is simply for comparative purposes to show the effect of the SIMC controller on the multi-modes of oscillation. Figs. 4.1 and 4.2 show the comparative results for tests SIMC case (1) and SIMC case (2) respectively. It should be noted that these results are not as good as results obtained using a conventional controller. This is due to the time delay and phase contribution of the filters used in the SIMC structure. This is discussed in more detail in *section 4.3*.

In Fig 4.1 (a), the speed difference between G #1 and G #2 displays local mode of oscillation. The SIMC is tuned reasonably close to the oscillation frequency and provides good damping. From Fig. 4.1 (a) it can be seen that the first cycle to cycle and a half exhibits little or no damping, and the following

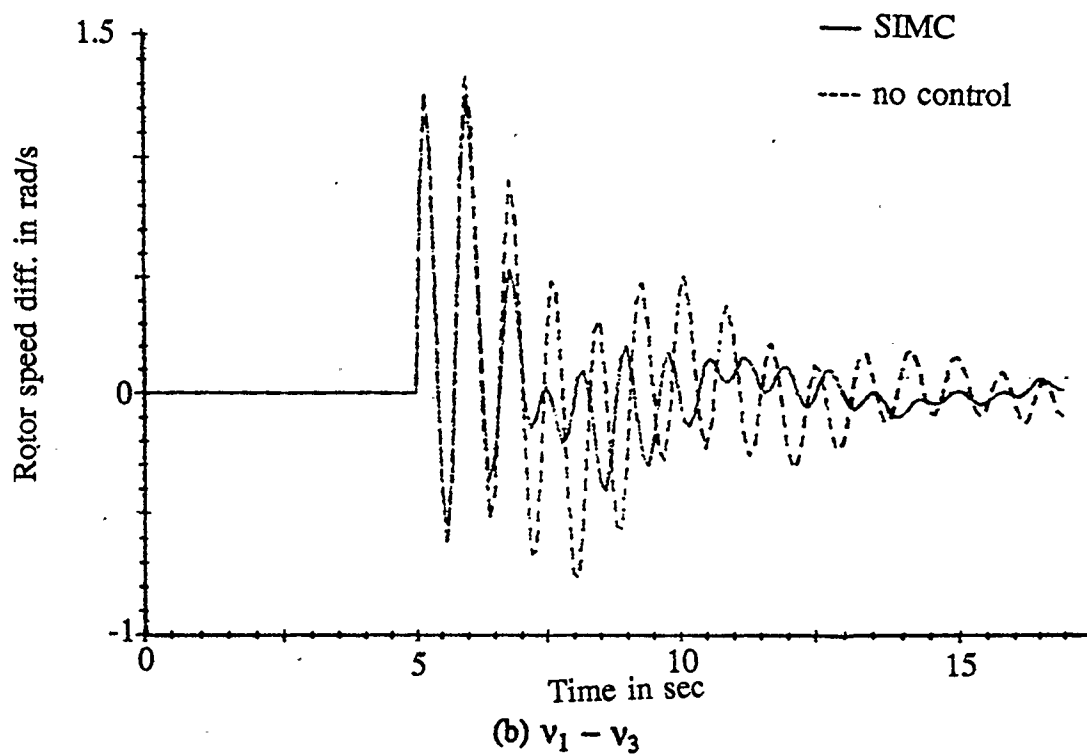
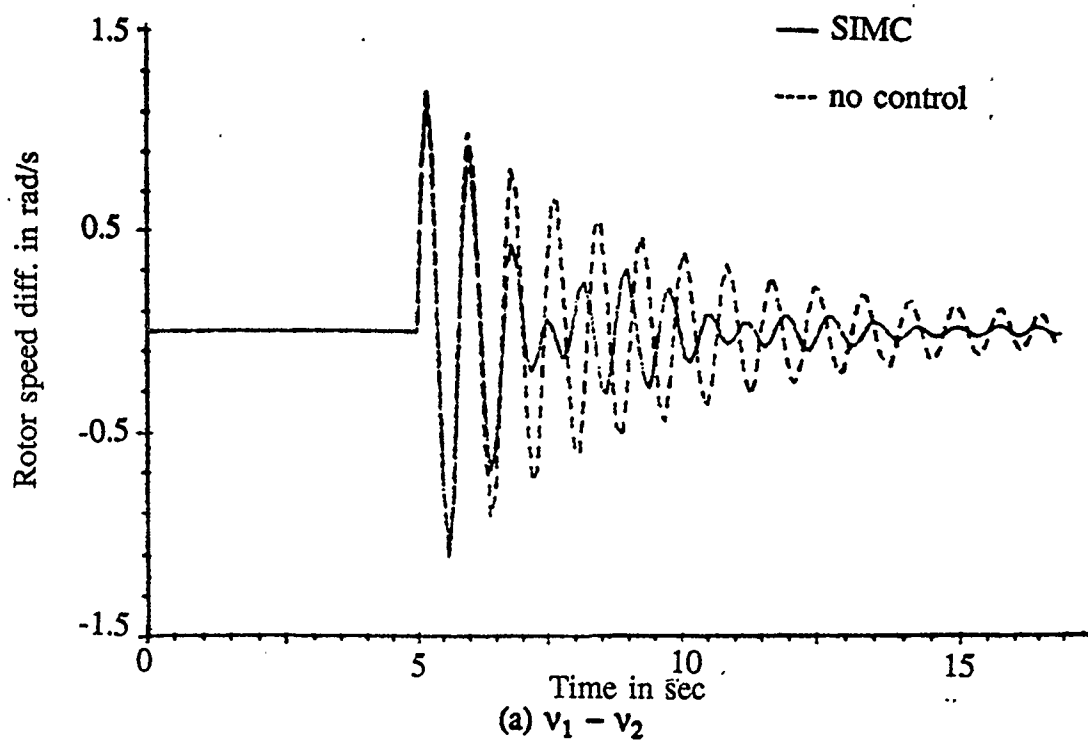


Fig. 4.1 SIMC case (1)

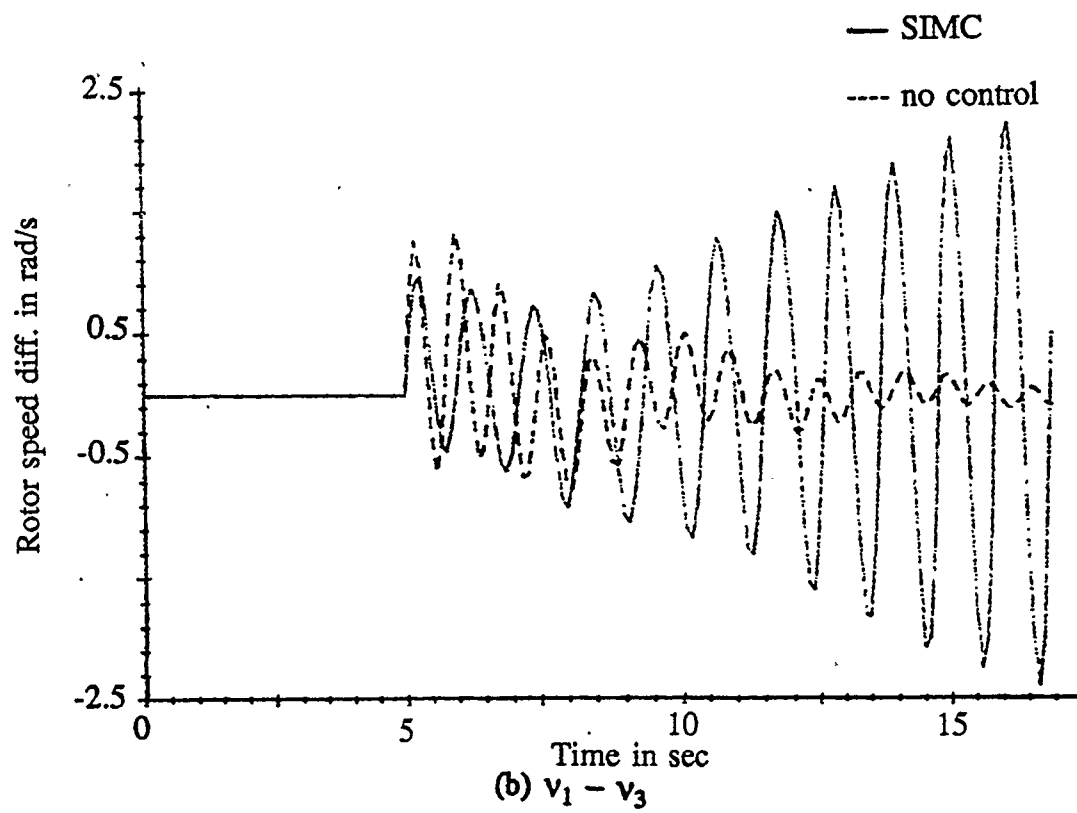
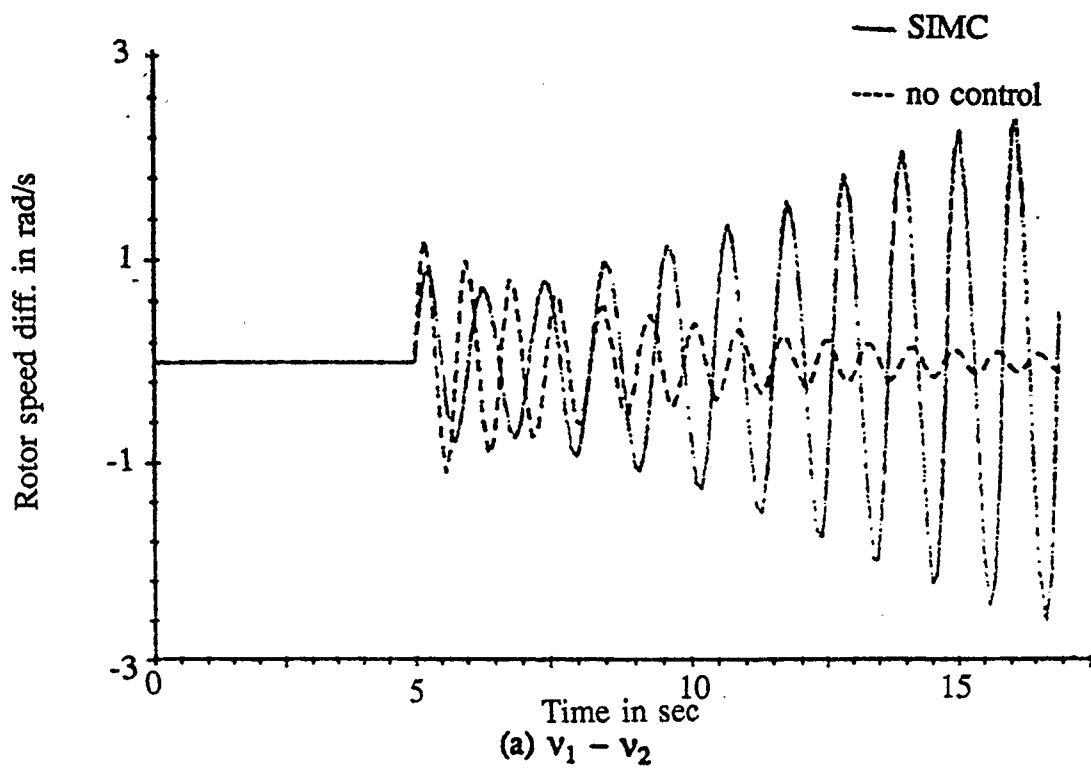


Fig. 4.2 SIMC case (2)

cycles exhibit good but erratic damping. This is due to the time delays associated with the filters. Fig. 4.1 (b) shows the speed difference between G #1 and G #3 which displays both local and interarea modes of oscillation. The SIMC is reasonably effective in damping the local mode of oscillation and provides some damping to the interarea mode of oscillation. However, note that there still is a problem due to the time delay associated with the filters.

Fig. 4.2 shows the results for SIMC case (2). As can be seen from Figs. 4.2 (a) and (b), the speed difference between $v_1 - v_2$ and $v_1 - v_3$ exhibit unstable characteristics. Changing the operating condition in SIMC case (2) produces change in the local mode of oscillation frequency and little or no change in the interarea mode of oscillation frequency. The result is that the unstable signal oscillates in local mode of oscillation. This is because an incorrect phase compensation is introduced at the new local mode of oscillation frequency, causing the system to become less stable. This problem is associated with the phase characteristics of the filters used.

Simulation studies were also repeated for the MIMC controller cases with conventional controllers on all five machines.

The conventional controller used is that proposed by Ontario Hydro [26] and discussed in chapter 2. The stabilizer is tuned to provide good local mode damping under all operating conditions, and to provide some damping to the interarea mode of oscillation. This is common practice since tuning the PSS is a compromise in the requirement in damping multi-mode of oscillations. The PSSs parameter values

are given in appendix B. Comparative results between MIMC and conventional stabilizers are given in Figs. 4.3 through 4.7 for MIMC test cases (1) to (5) respectively.

Figs. 4.3 and 4.4 show the MIMC case (1) and case(2) tests respectively. These tests give the results of a short circuit test applied at generator #1 for a duration of 0.1 seconds. Since the short circuit test is a sudden impact disturbance, the excitation is driven into saturation during the first half cycle by the AVR. However after the first half cycle the MIMC controller gives excellent damping. This can be seen in Figs. 4.3 and 4.4 (a) through (f). In Fig. 4.3 (a) and (b) it can be seen that the MIMC controller damps out the local mode of oscillations within two and a half cycles (in approximately 2.5 seconds) compared with a conventional stabilizer which damps the oscillations in approximately six cycles (approximately 7.0 seconds). There is also very good damping of the interarea mode of oscillation. This can be seen in Figs. 4.3 (c) to (f). Since the short circuit test results in a system impact that is dominant in local mode of oscillation the main contribution to the damping is due to the P_e channel of the MIMC controller.

The short circuit test produces local mode of oscillation in speed differences involving generator #1. Figs. 4.3 (a) and (b), and 4.4 (a) and (b) show local mode of oscillation between $v_1 - v_2$, and $v_1 - v_3$ respectively. Both local mode and interarea mode of oscillations are observed in the speed differences involving the other generators. Figs. 4.3 and 4.4 (c) to (f) show the speed differences between $v_2 - v_3$, $v_2 - v_4$, $v_3 - v_5$, and $v_4 - v_5$ respectively. As can be seen from these

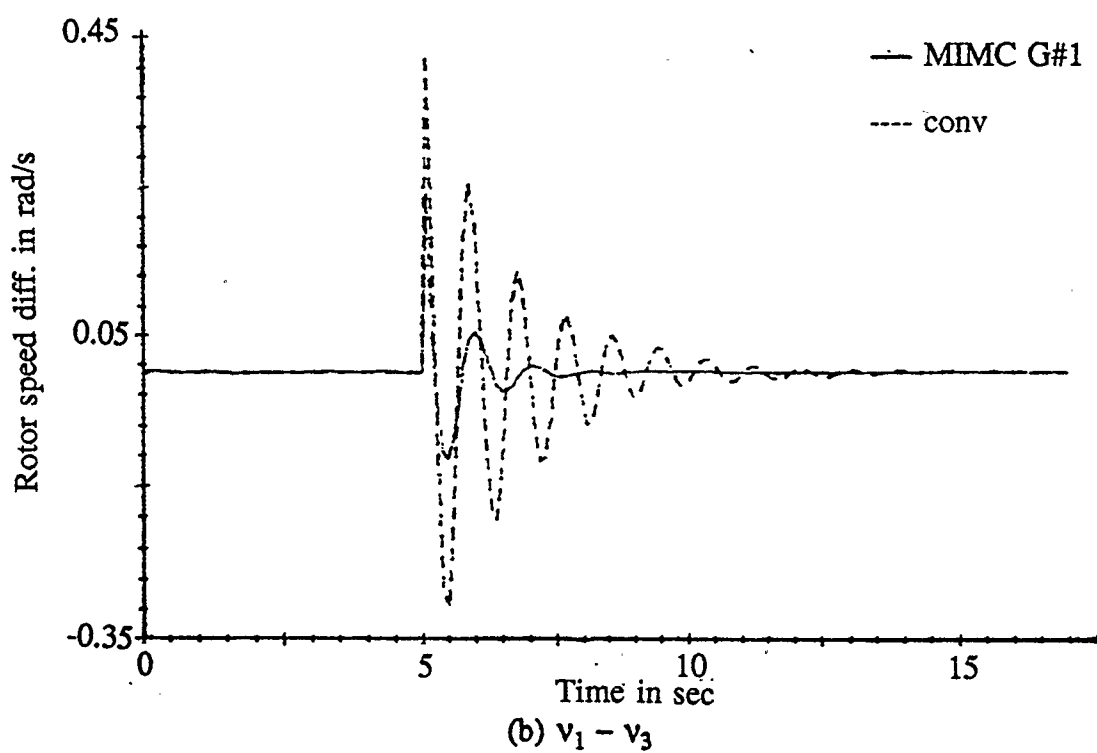
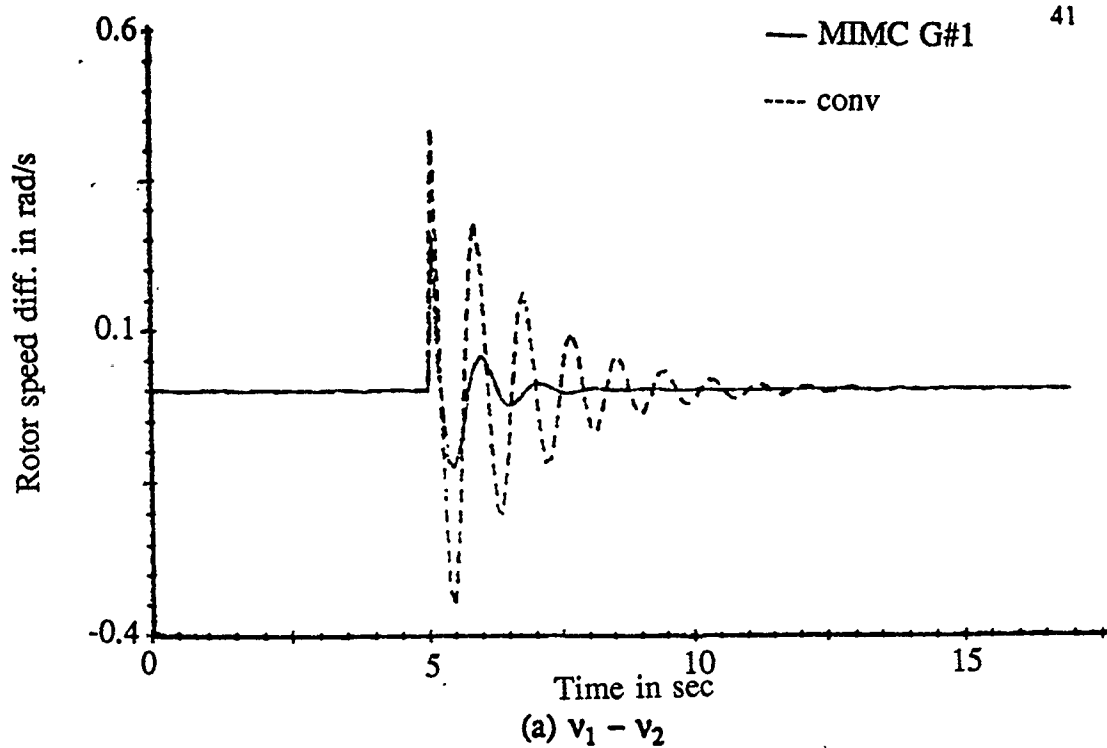


Fig. 4.3 MIMC case (1)

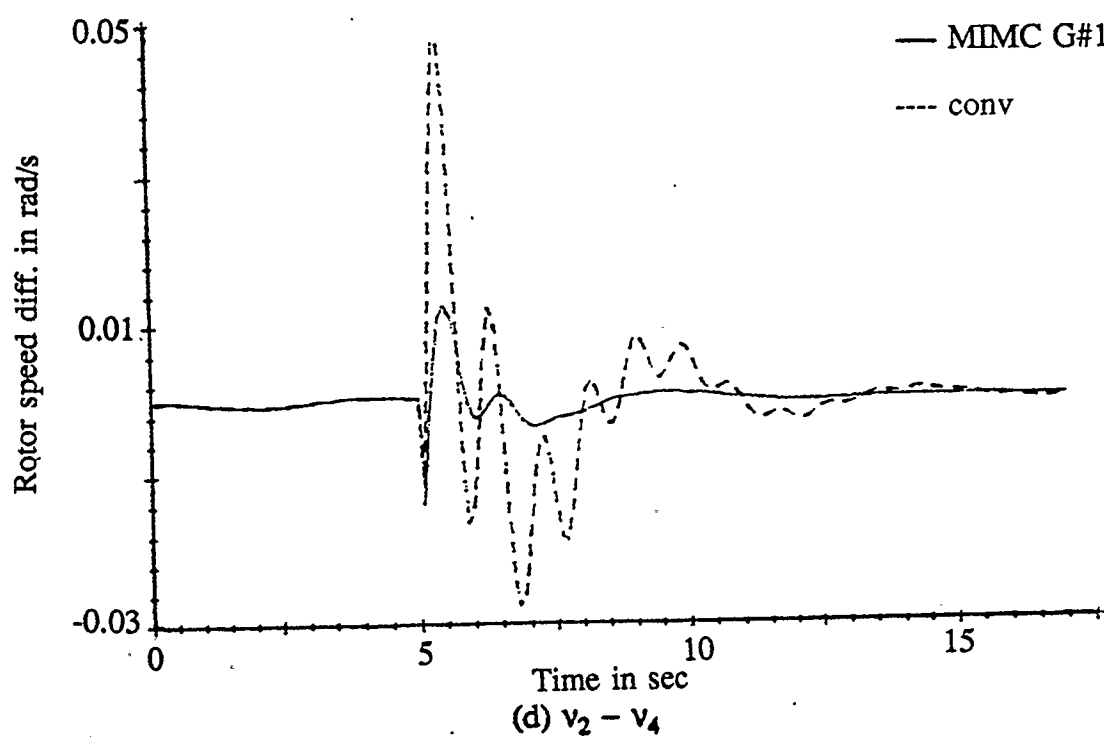
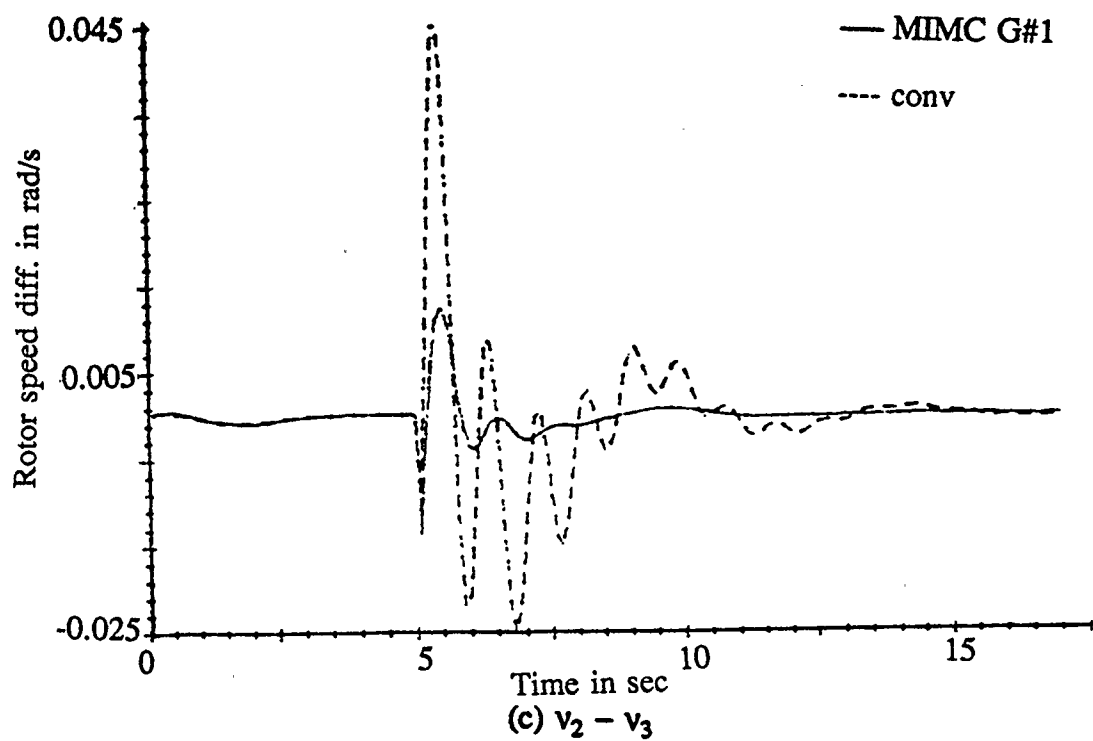


Fig. 4.3 continued

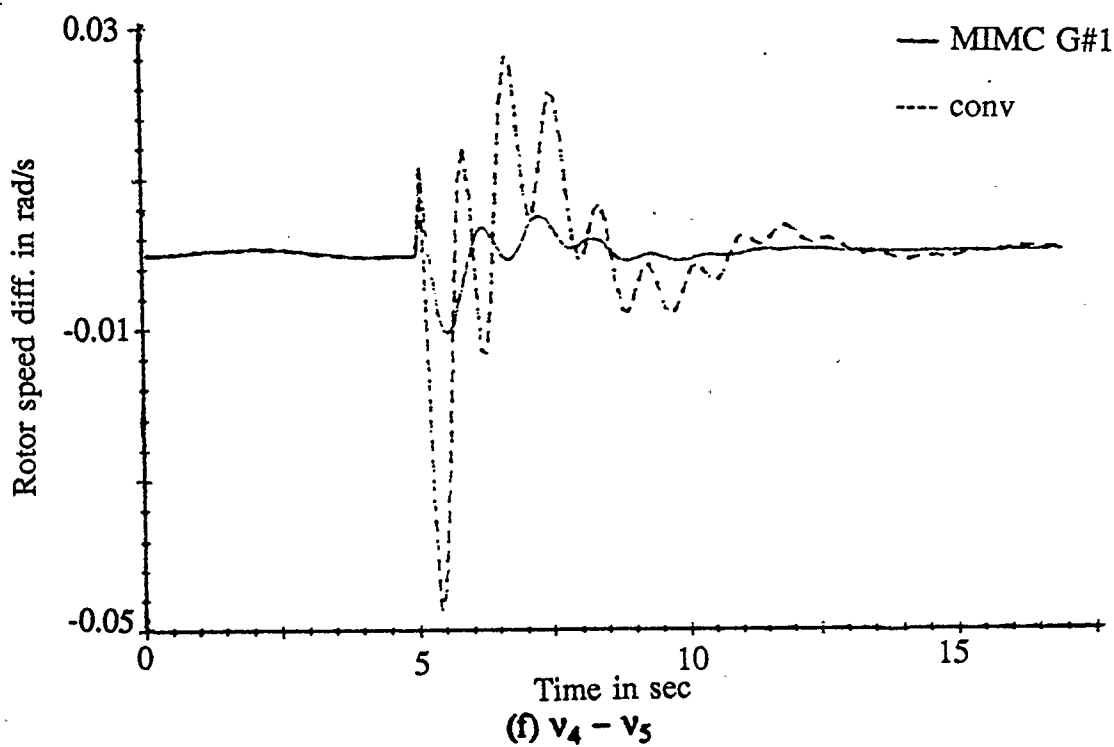
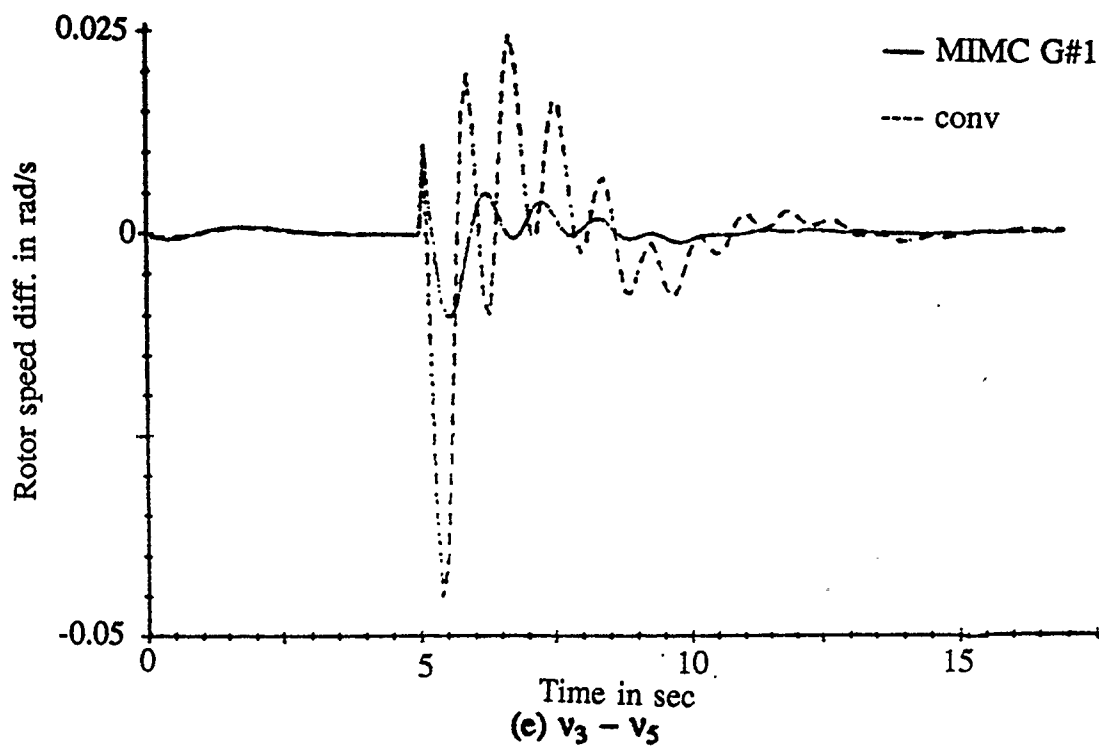


Fig. 4.3 continued

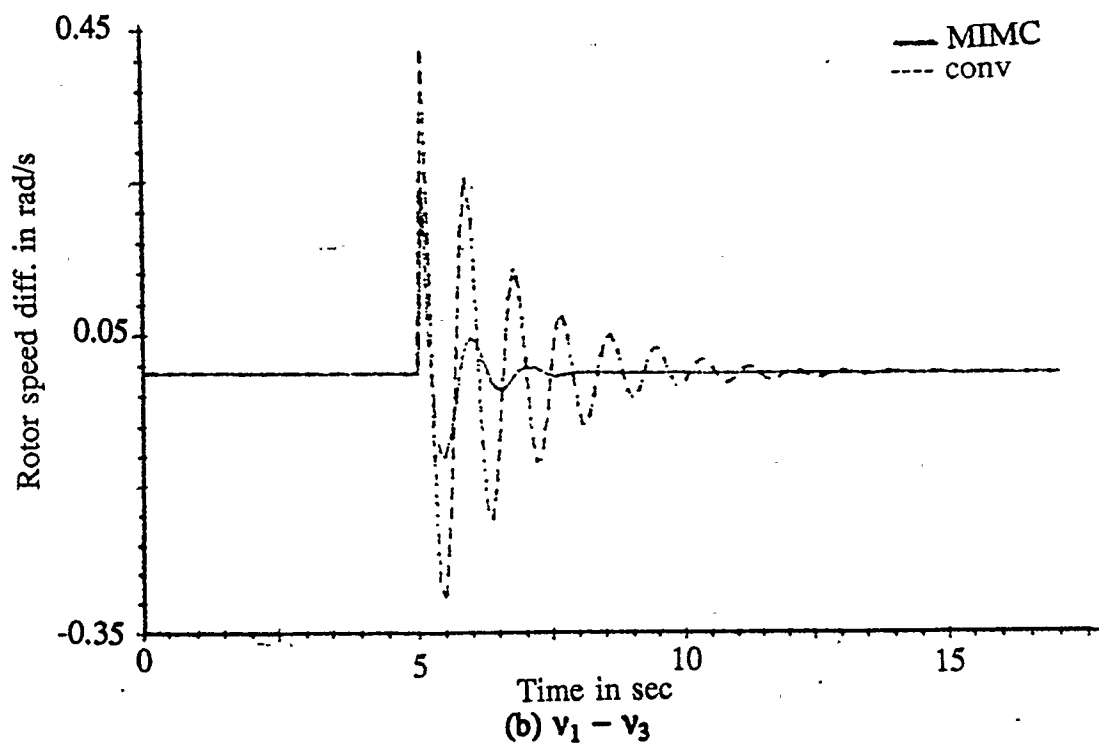
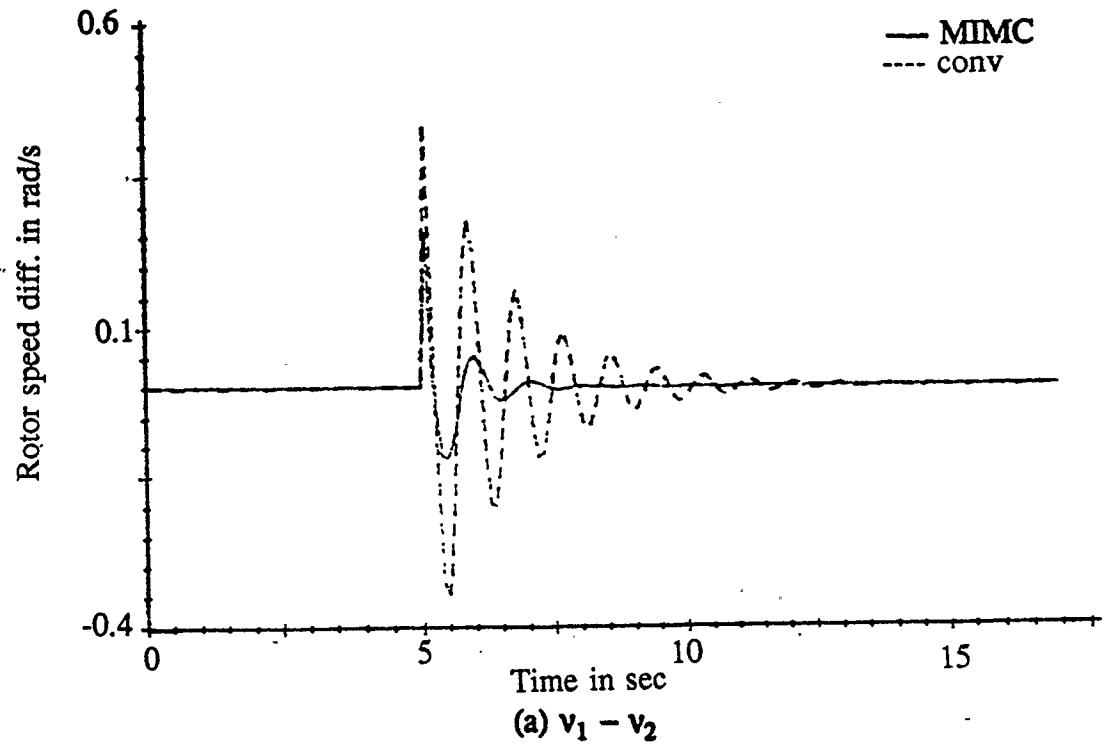


Fig. 4.4 MIMC case (2)

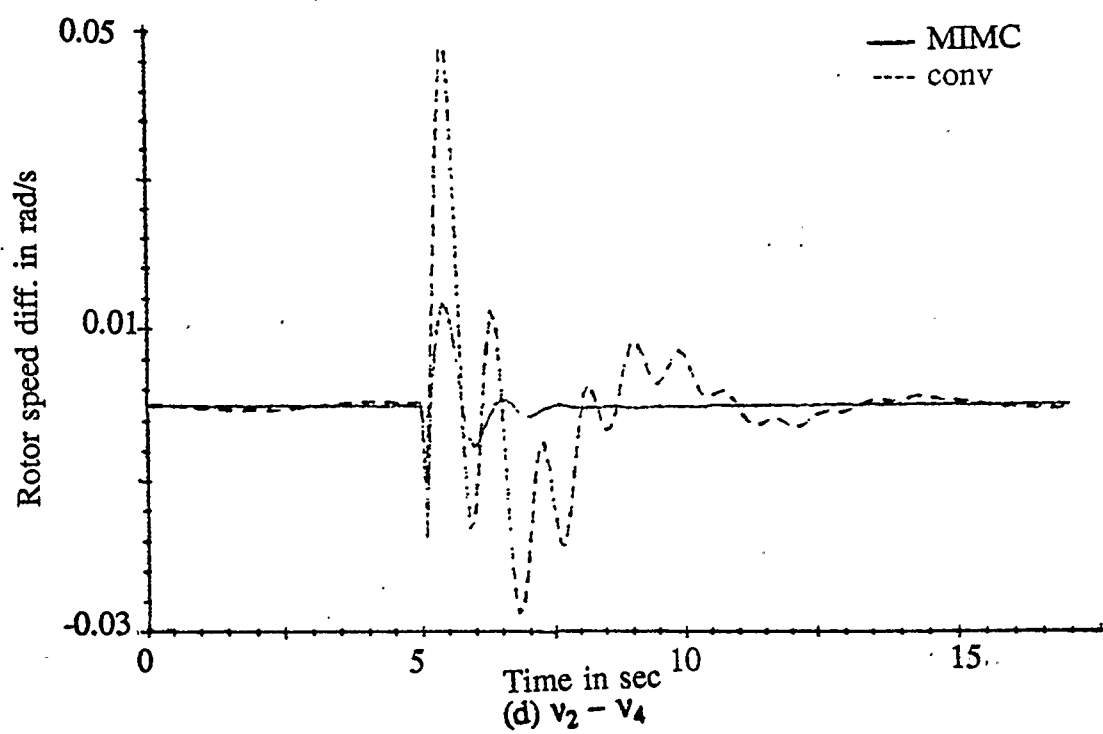
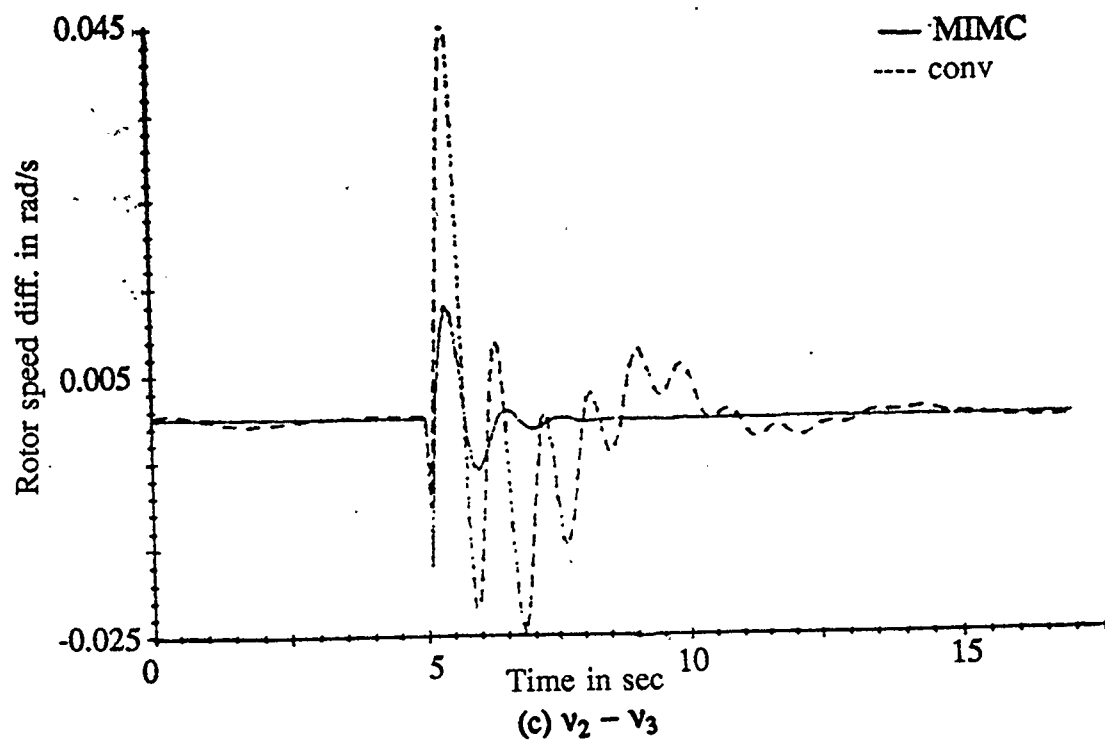


Fig. 4.4 continued

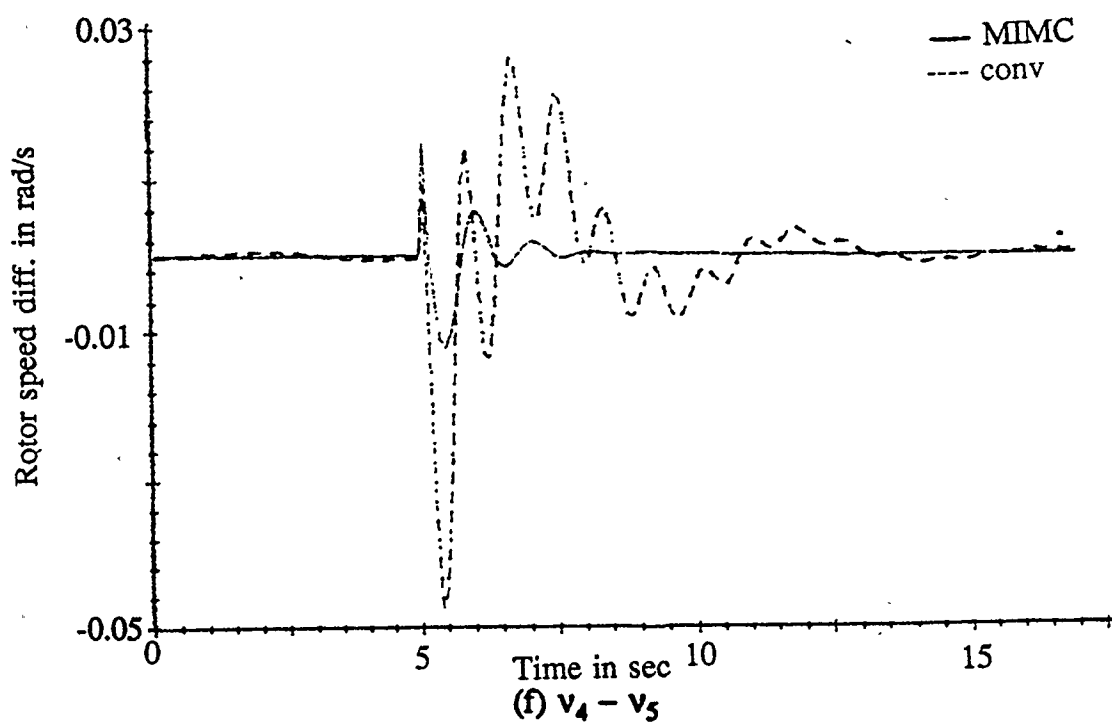
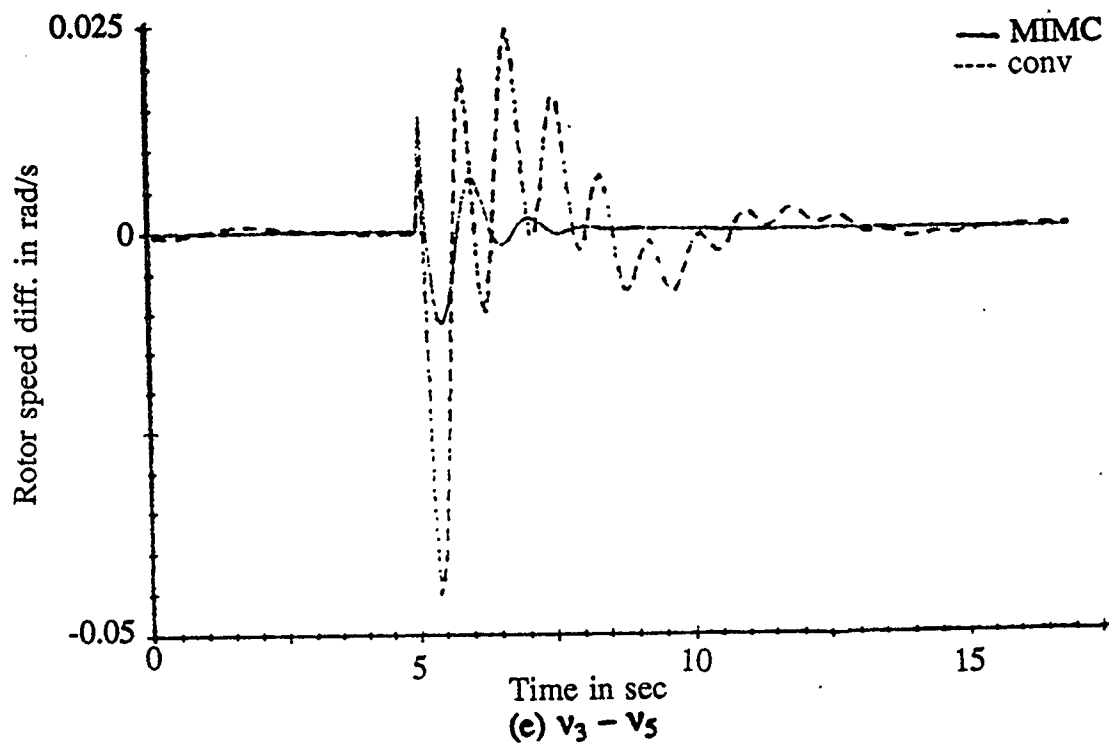


Fig. 4.4 continued

figures both modes of oscillation are present. The local and interarea mode of oscillation frequencies are 1.24 Hz. and 0.24 Hz. respectively.

Fig. 4.5 shows the MIMC case (3) test. This test gives the results of a 10% load change applied at area #1. Again it can be seen in Fig. 4.5 (a) that the MIMC controller damps out the local mode of oscillations in approximately two cycles (approximately 2.0 seconds) compared with a conventional stabilizer which damps the oscillations in approximately six cycles (approximately 6.0 seconds). Fig. 4.5 (b) shows the damping effect of the MIMC controller on interarea mode of oscillations. The MIMC damps the interarea mode of oscillation in approximately 5.0 seconds compared to the conventional stabilizer which damps the oscillation in approximately 10.0 seconds. It can be seen from Figs. 4.5 (b) to (f) that the effect of the MIMC controller is significant. The first half cycle of oscillation is reduced by approximately half, and the next half cycle is almost completely eliminated.

The load change test produces local mode of oscillation in the speed difference between generator #1 and #2 ($v_1 - v_2$) as seen in Fig. 4.5 (a). Figs. 4.5 (b) through (f) show the interarea mode of oscillation observed in the speed differences involving the other generators ($v_1 - v_3$, $v_2 - v_3$, etc.). The load change test results in a system that is dominant in interarea mode of oscillation. The local and interarea mode of oscillation frequencies are 1.2 Hz. and 0.23 Hz. respectively.

MIMC case (4) and case (5) tests are given in Figs. 4.6 and 4.7 respectively. A 5% change in reference voltage is applied at generator #1 in these tests. The

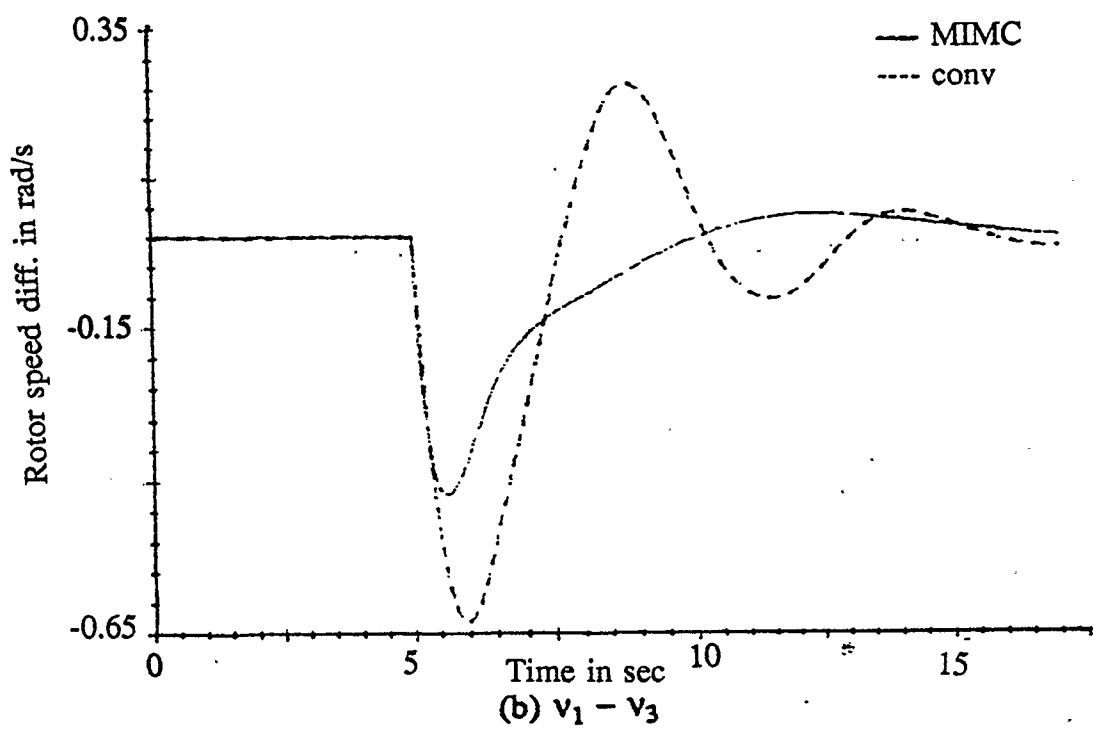
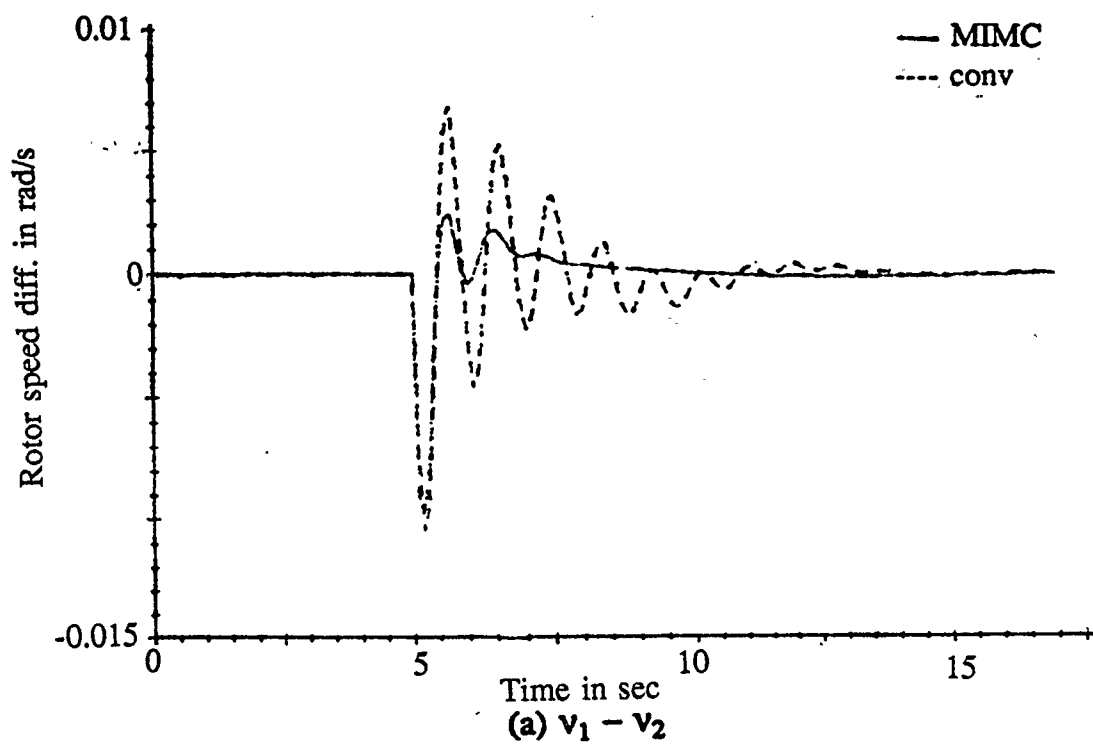


Fig. 4.5 MIMC case (3)

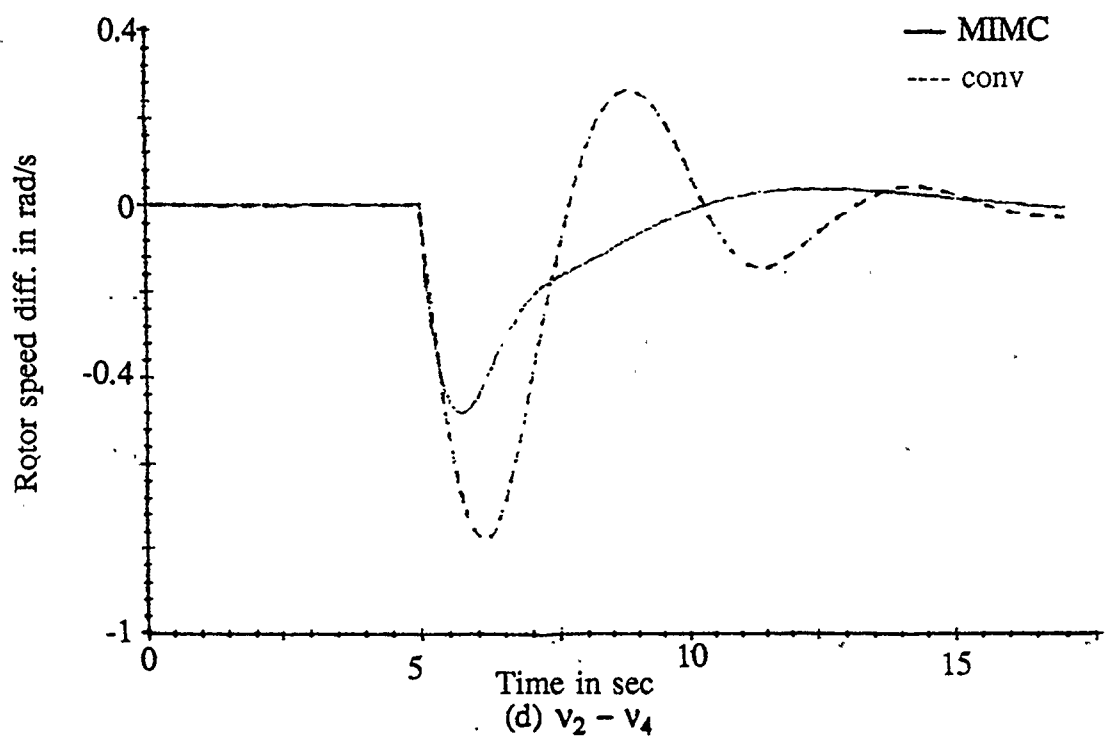
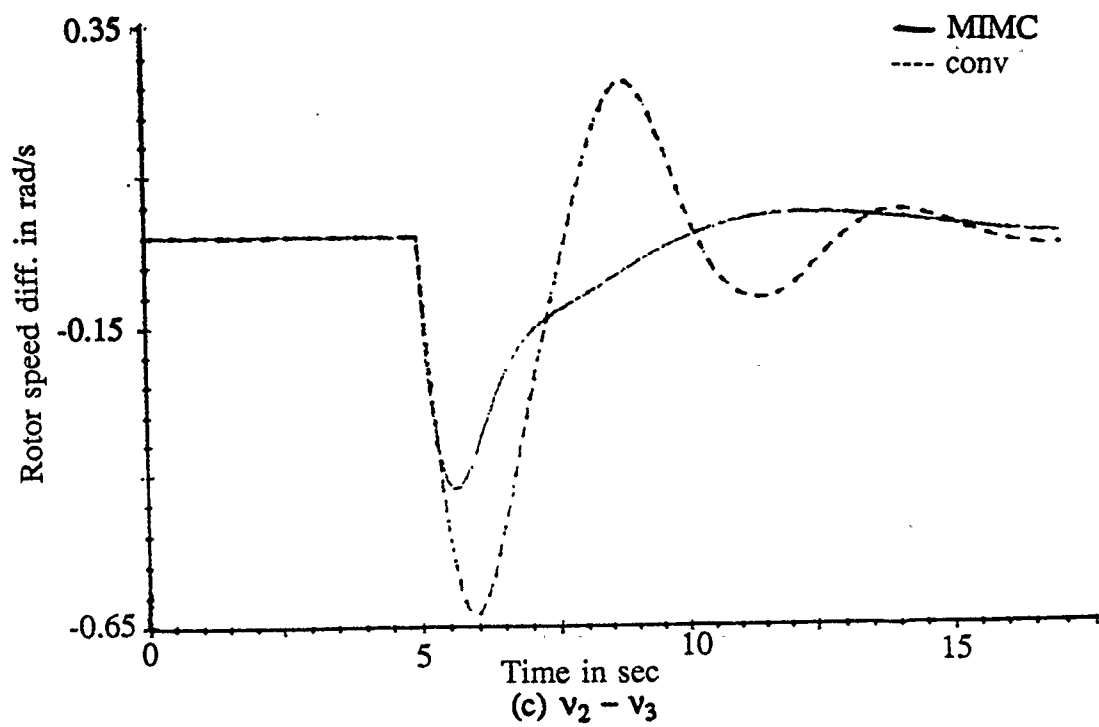


Fig. 4.5 continued

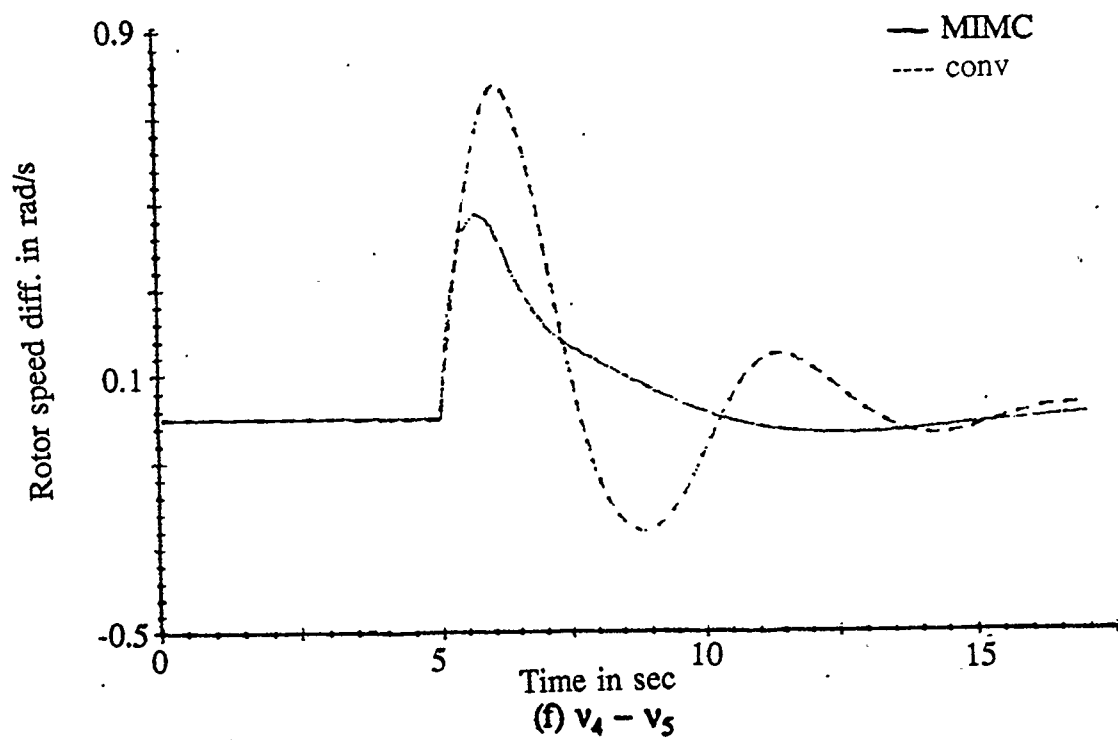
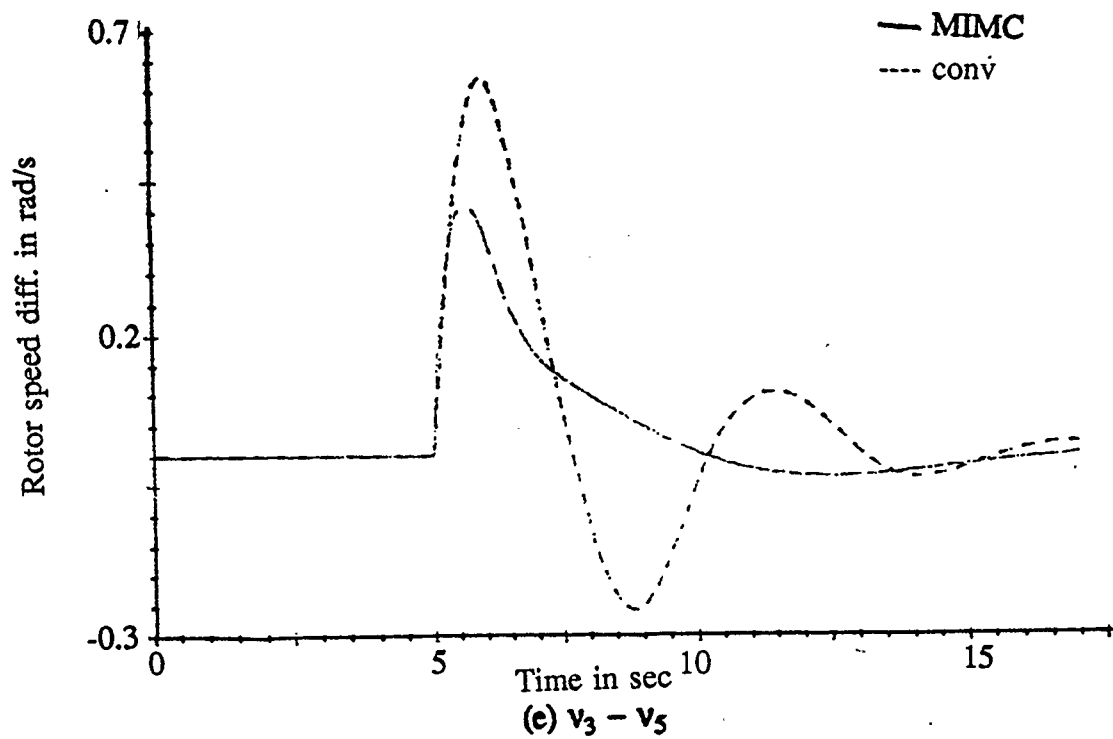


Fig. 4.5 continued

change in reference voltage test produces local mode of oscillation in the speed difference between generator #1 and #2 ($v_1 - v_2$) as seen in Fig. 4.6 and 4.7 (a). Figs. 4.6 and 4.7 (b) through (f) show both interarea and local mode of oscillation observed in the speed differences involving the other generators ($v_1 - v_3$, $v_2 - v_3$, etc.). However, speed differences $v_1 - v_3$ (as shown in Figs. 4.6 and 4.7 (b)), $v_1 - v_4$, and $v_1 - v_5$ are dominant in local mode of oscillation. Whereas the speed differences $v_2 - v_3$, $v_2 - v_4$, etc. are dominant in interarea mode of oscillation, as is shown in Figs. 4.6 and 4.7 (c) through (f). The change in reference voltage test results in a system that is equally dominant in both modes of oscillation. The effectiveness of the MIMC controller is illustrated by the damping action observed on both modes of oscillation, particularly the interarea mode of oscillation. The local and interarea mode of oscillation frequencies observed for MIMC case (4) test are 1.33 Hz. and 0.26 Hz. respectively. The frequencies of oscillation observed for MIMC case (5) test are 0.92 Hz. and 0.21 Hz. respectively for the local and interarea modes of oscillation.

4.3. Some special problems of SIMC

There are two problems associated with the SIMC controller. These problems are due to the filters used to attenuate the other modes of oscillation. These problems are associated with time delay and phase contribution of the filters. Figs. 4.8 and 4.9 show the time delay characteristic and phase response respectively of the 6th order bandpass filter used in channel #1 of the SIMC controller.

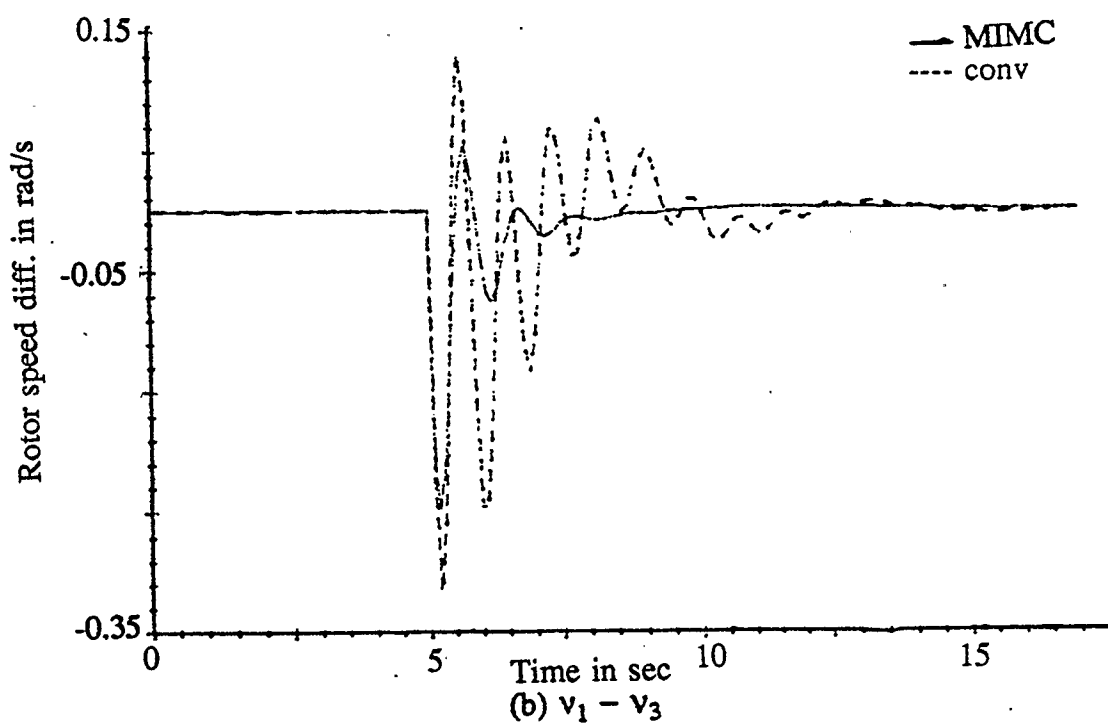
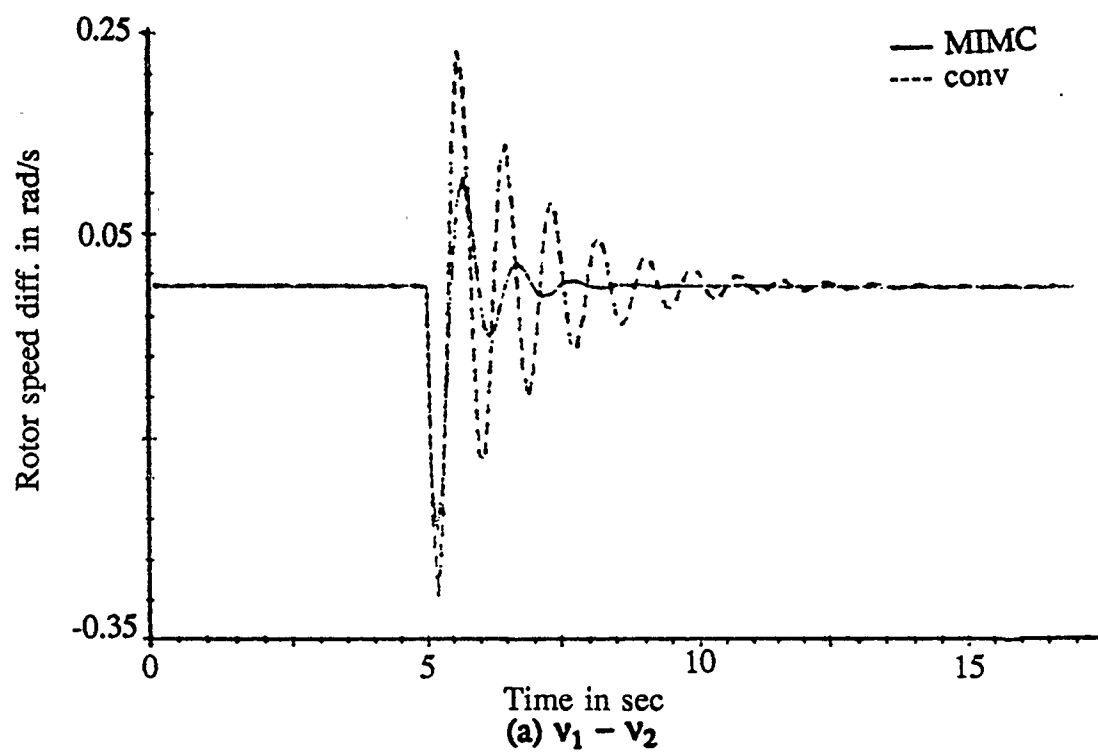


Fig. 4.6 MIMC case (4)

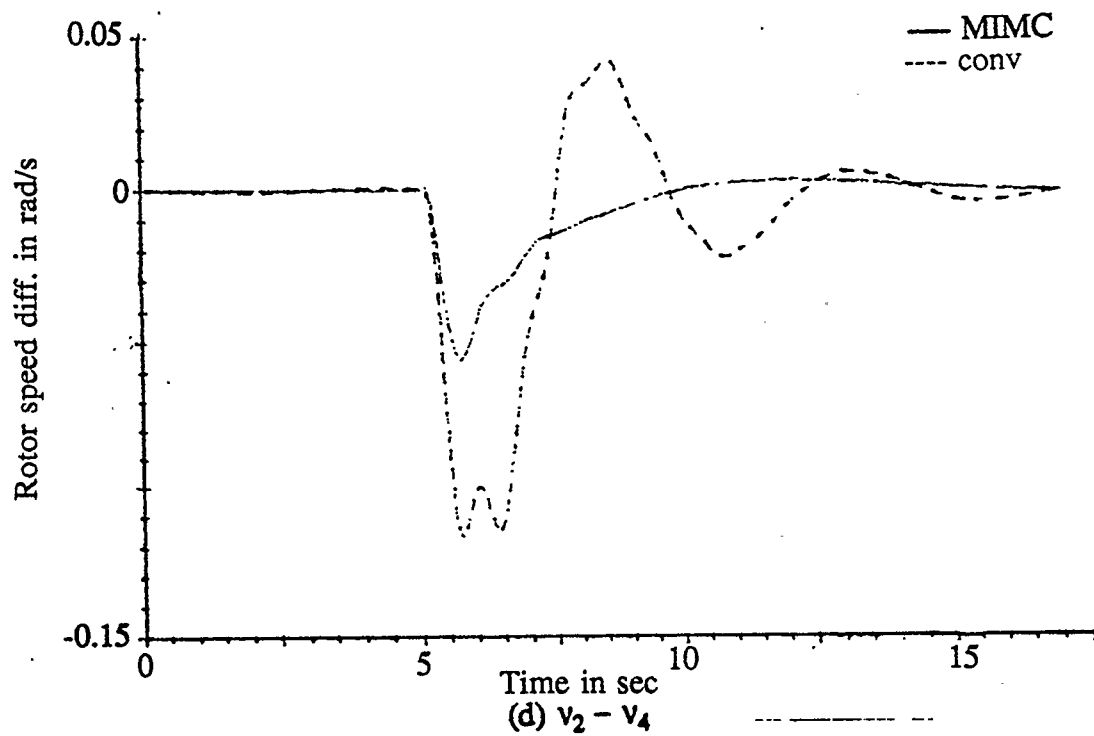
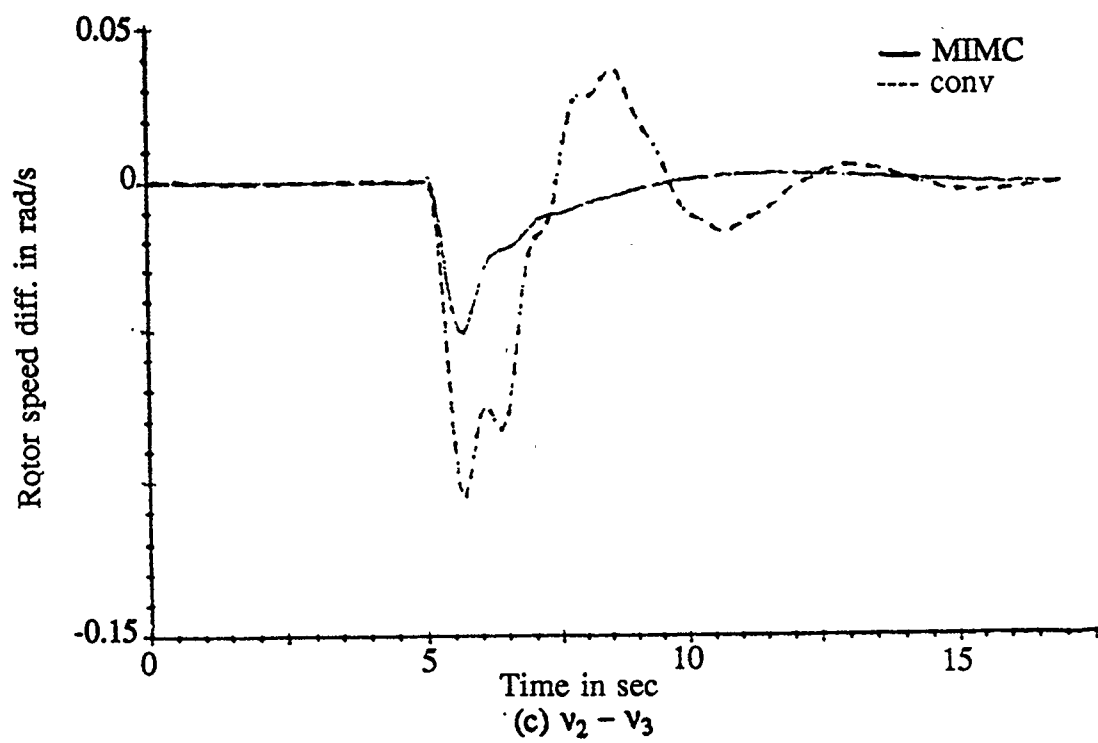


Fig. 4.6 continued

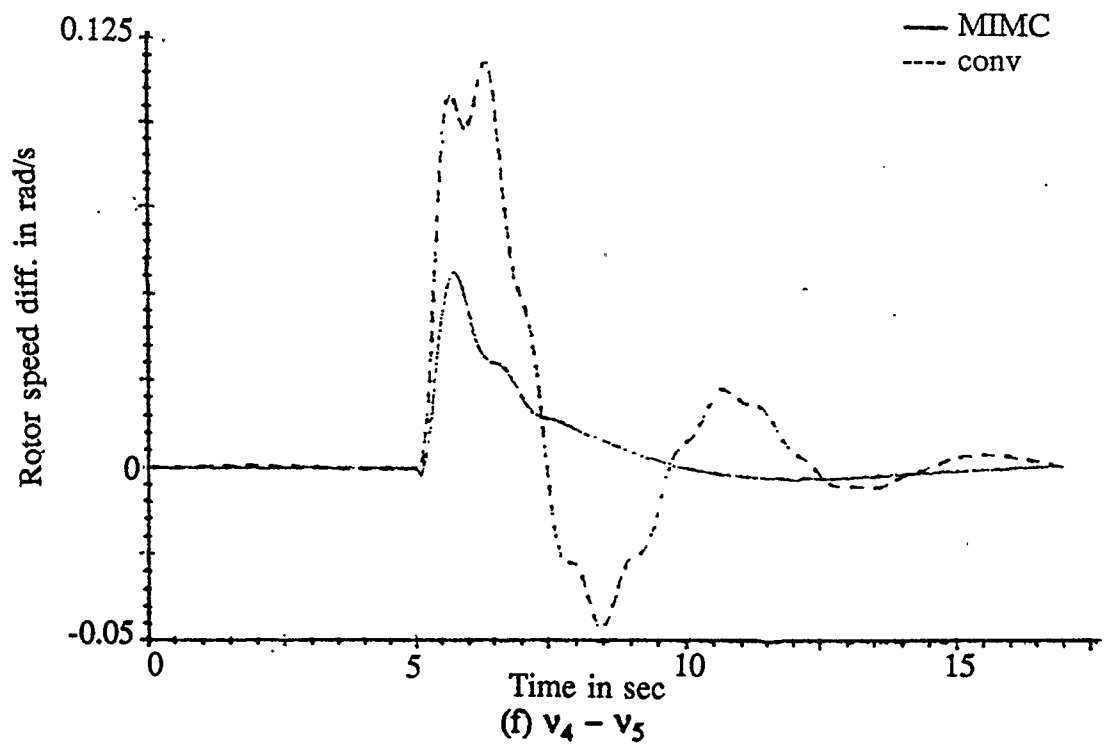
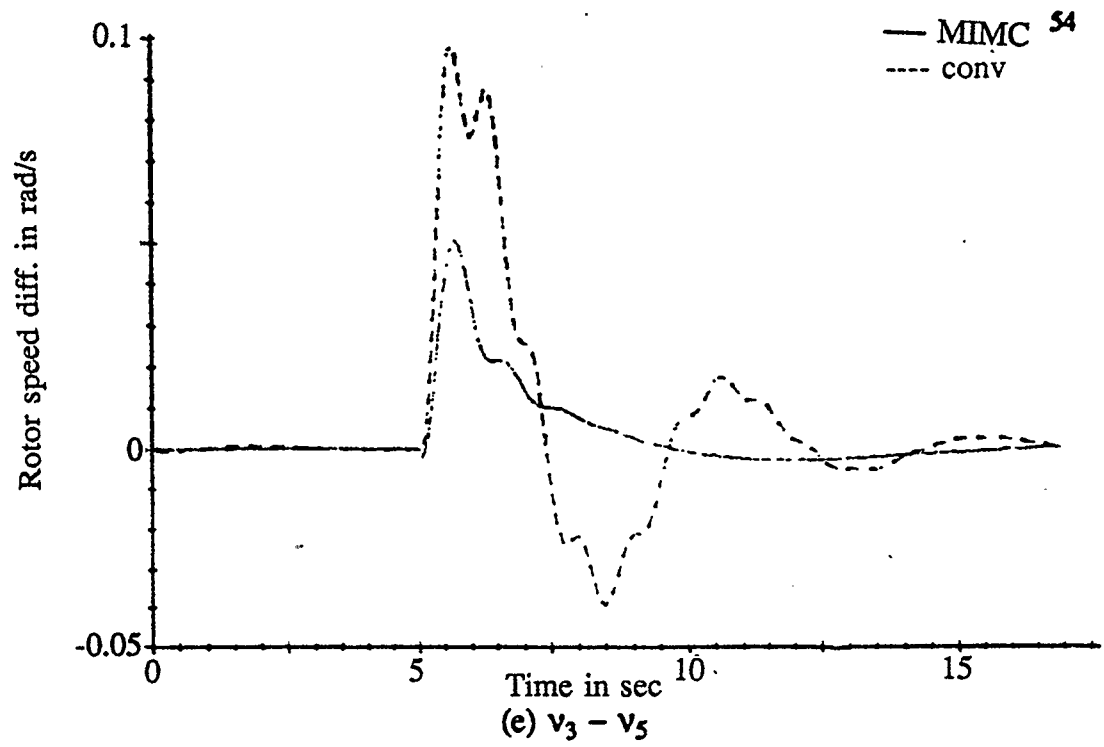


Fig. 4.6 continued

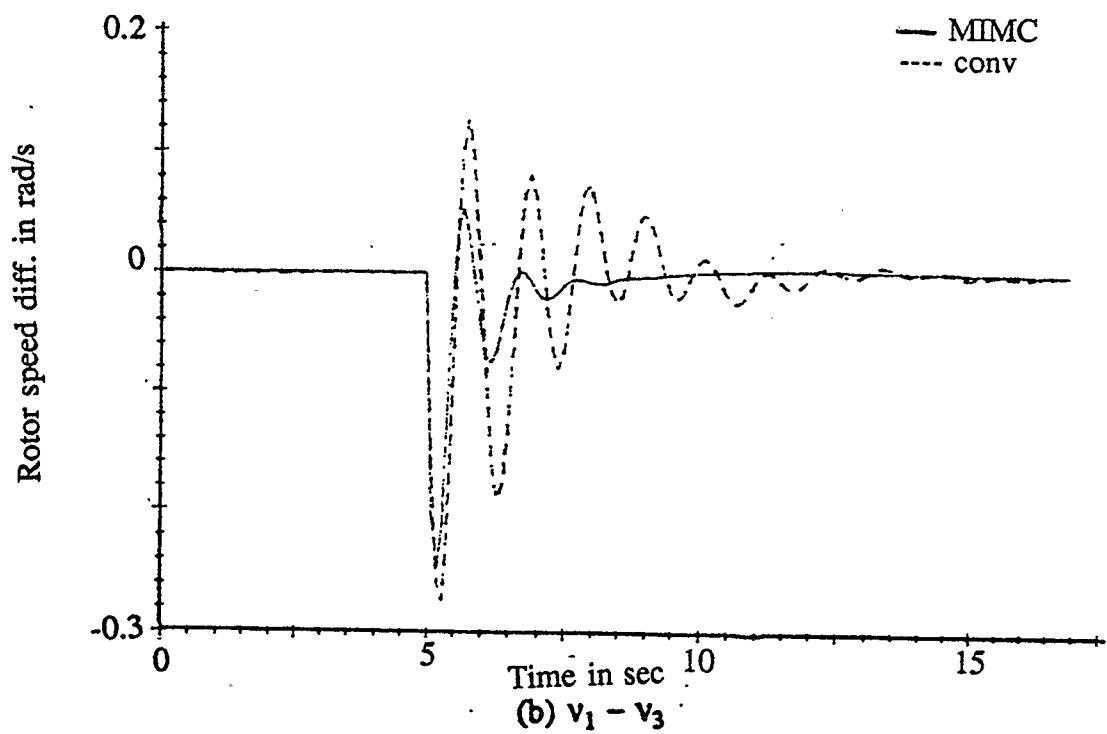
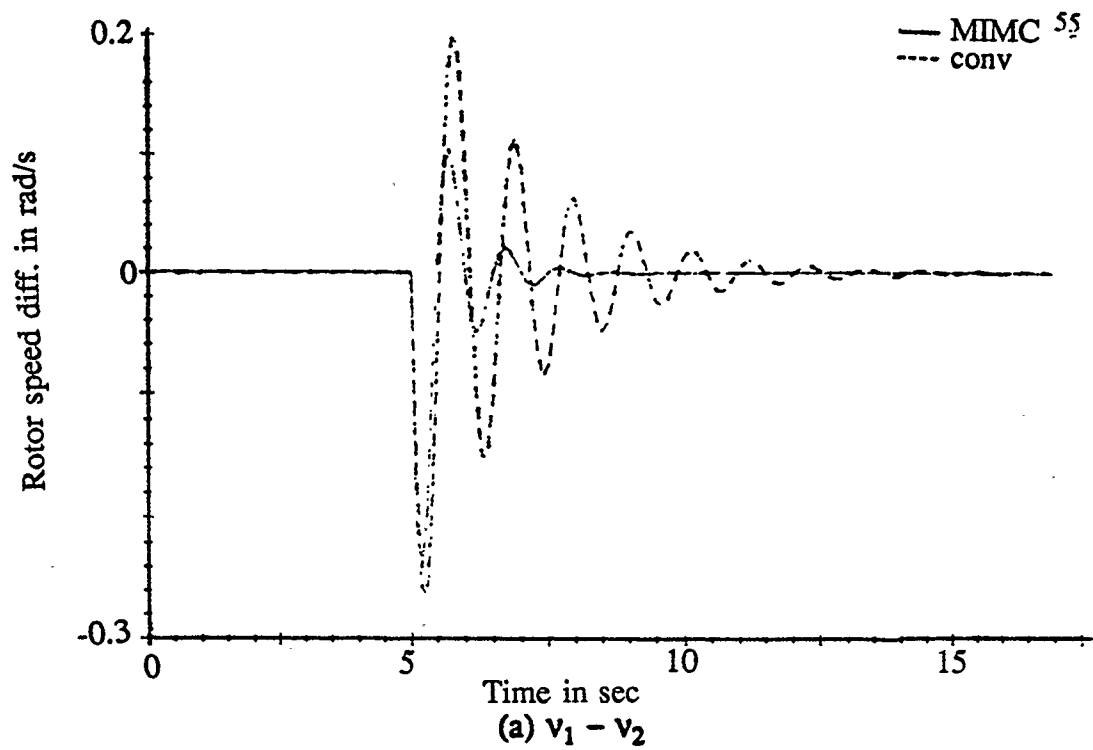


Fig. 4.7 MIMC case (5)

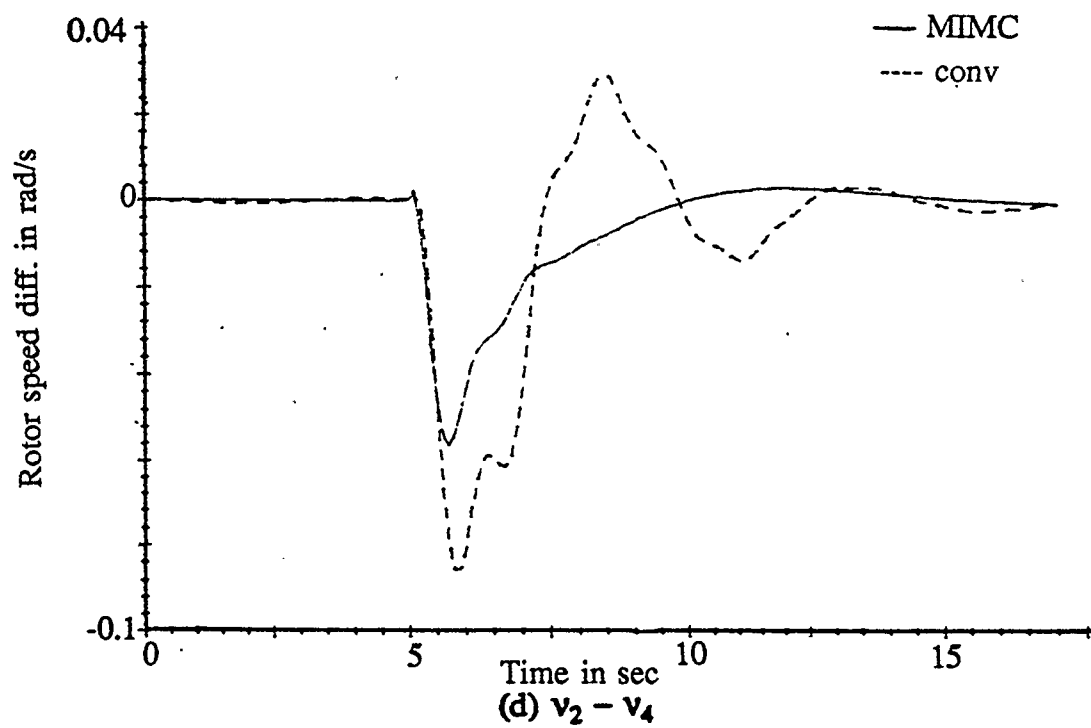
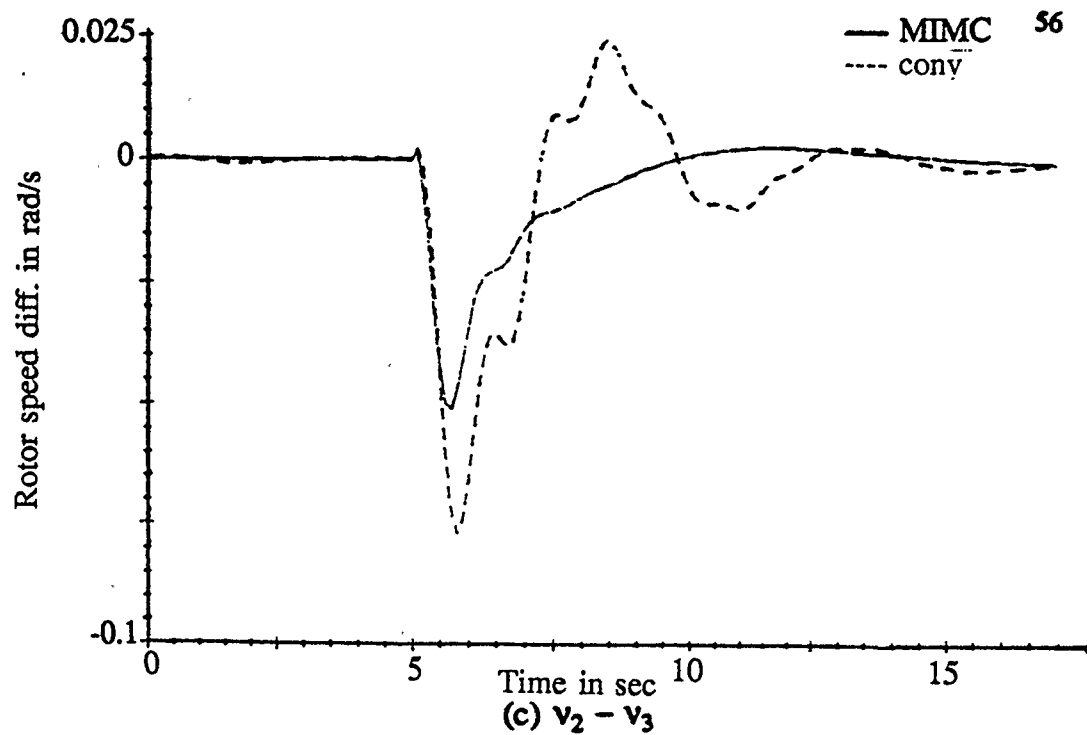


Fig. 4.7 continued

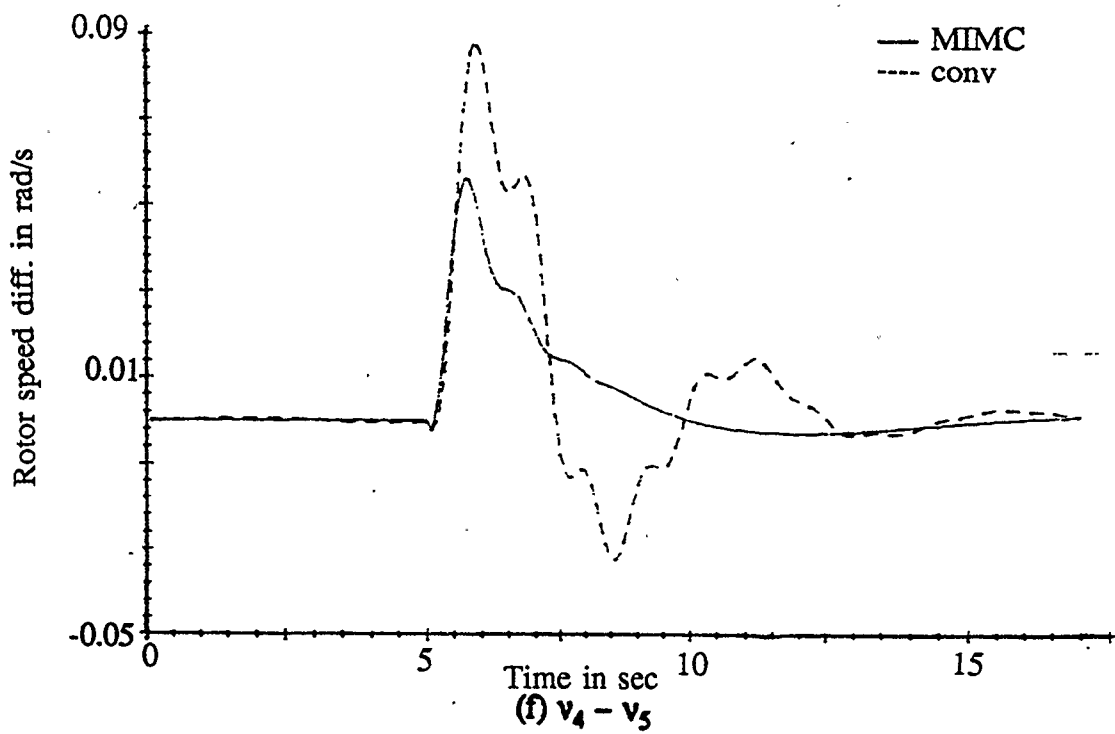
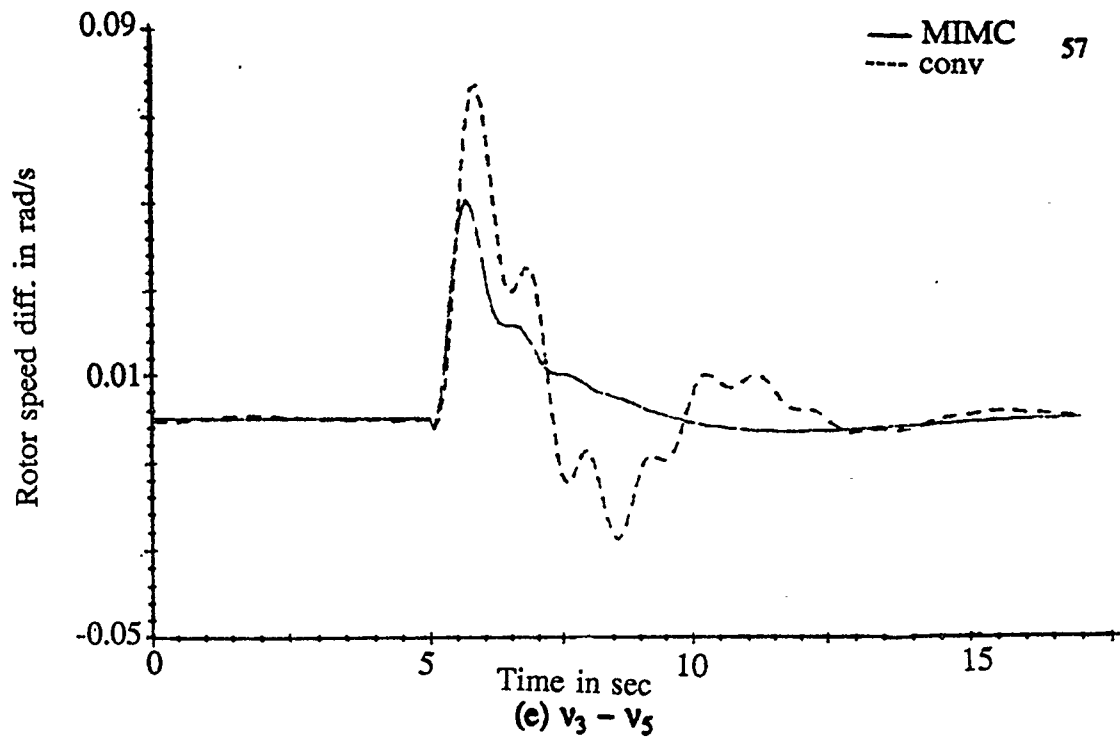


Fig. 4.7 continued

As can be seen from Fig. 4.8, the time delay at the local mode of oscillation frequency of 1.2 Hz. is approximately 1.45 seconds. This means that the control signal provided is delayed by more than 1.45 seconds, and hence is an incorrect control signal. Therefore less than expected damping is applied to the local mode of oscillation. This can be seen in a comparison between Fig. 4.1 and Figs. 4.3 to 4.7.

The problem of instability observed in Fig. 4.2 is due to the phase contribution of the filter. As discussed in Chapter 2, the function of the PSS is to provide adequate phase and gain compensation to the system to increase its stability limits.

The filter contributes to the overall phase of the signal fed to the controller. From Fig. 4.9 it can be observed that the phase characteristic of the filter in the passband region is non-linear and sloping. If the PSS is tuned for a given frequency, say 1.2 Hz., then this would imply that the overall phase compensation provided to the system takes into account the phase contribution of the filter at 1.2 Hz. When the operating condition of the system changes to 1.0 Hz., the phase contribution by the filter changes. The overall phase compensation to the system is totally incorrect, and in fact tends to reduce the stability limits of the power system and cause the system to go unstable. This can be observed in Fig. 4.2. It should be noted that this problem could be reduced by using lower order filters. However it does not completely eliminate the problem.

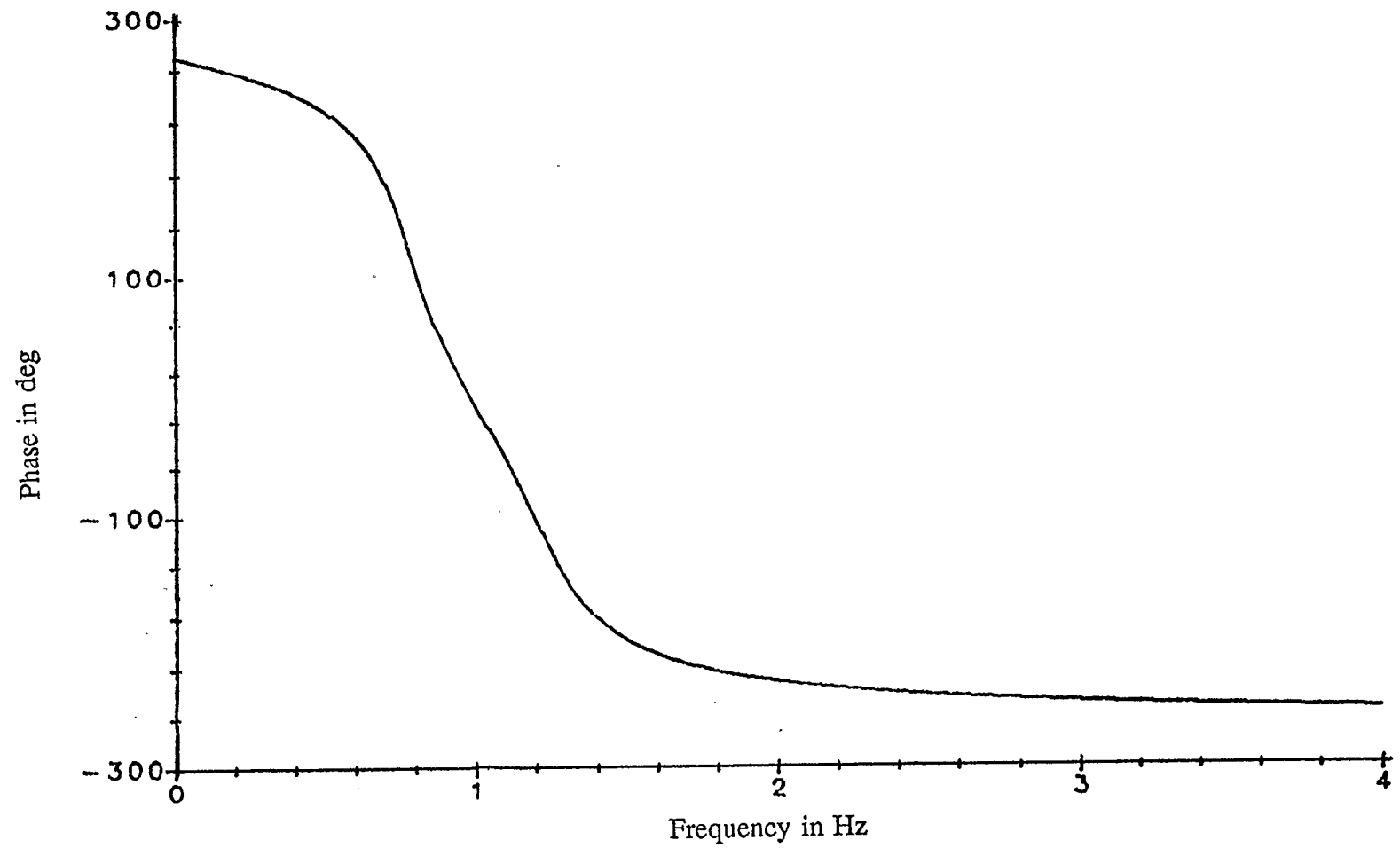


Fig. 4.8 Phase characteristics for 6th order bandpass filter

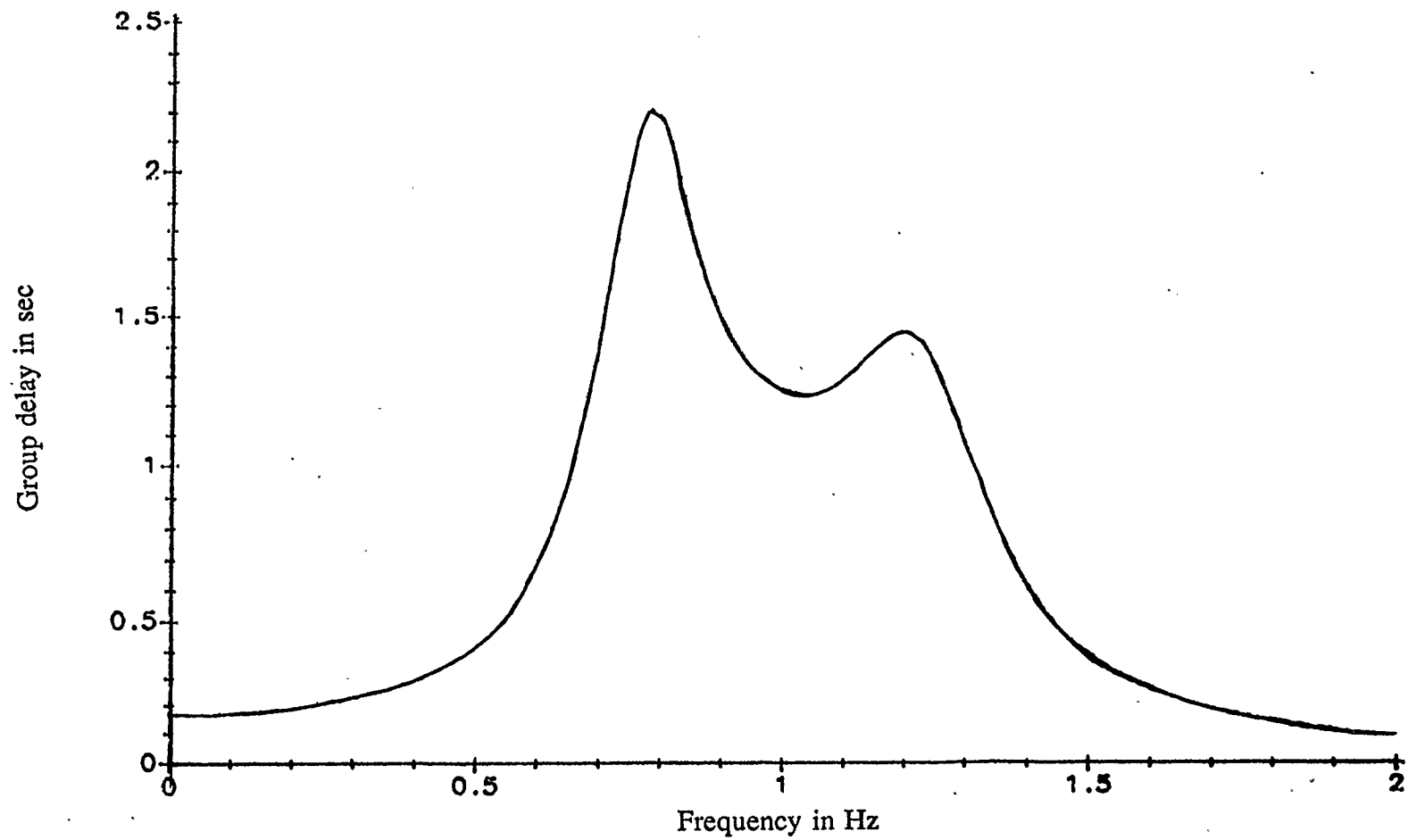


Fig. 4.9 Time delay characteristics for 6th order bandpass filter

4.4. Some special problems of MIMC

There is a problem associated with the MIMC controller. It is a very minor problem which does not reflect in the ability of the MIMC controller to damp the multi-modes of oscillation. The problem is associated with the gain settings in the P_e channel. Since there is electrical power transfer between machines, the entire system is sensitive to any control which incorporates an electrical signal as its input. Intraplant modes of oscillation are introduced. *This oscillation is caused by the controllers of the generators interacting with one another.*

Generator #1 oscillates in local mode of oscillation, generator #2 oscillates in both local mode of oscillation and interarea mode of oscillation. However, generator #2 is more dominant in interarea mode of oscillation. *If the same control gain which is applied to generator #1 is applied to generator #2, intraplant mode of oscillation is introduced to the system, as illustrated in Fig. 4.10. This is because generator #2 controls its own local mode oscillations, and attempts to control local mode oscillations on generator #1. This should never be allowed to occur. Each generator should be responsible for controlling its own modes of oscillation, with some transfer of stability limits to the other generators. Allowing individual generators to transfer control to other generators introduces conflict between the controls.* This conflict is evident when the gain of any of the large generators (generator #2, #3, and #4) exceeds a certain value.

Fig. 4.10 shows the intraplant mode of oscillation introduced when the gain of the P_e channel of generator #2 is set equal to that of generator #1, and no

controllers are applied on the other generators. The speed difference between generator #1 and generator #2 ($v_1 - v_2$) exhibits good damping, however it also exhibits intraplant mode of oscillation. Since generator #1 contributes most of the local mode oscillations, any control applied to generator #2 should only produce some damping. However, this is not the case which indicates transfer of control from generator #2 to generator #1.

This problem is rectified by reducing the gains on the generators that produce this problem. Generators #2, #3, and #4 are ten times the size of generators #1 and #5, and as it turns out the gains on generators #2, #3, and #4 are ten times smaller than those of generators #1 and #5. As the gain is reduced, the intraplant oscillations are eliminated, and damping of $v_1 - v_2$ reduces to what should be expected when control is applied to generator #2 only. This can be seen in Fig. 4.11.

4.5. Analysis of MIMC results

As can be seen from Figs. 4.3 to 4.7, the MIMC controller gives excellent damping to both the local mode and the interarea mode of oscillation. The results show that the MIMC controller gives better results than the conventional stabilizers. This is expected since the design technique of conventional stabilizers is a compromise between the conflicting and sometimes contradictory requirements of responding to the different frequencies simultaneously. This approach does not yield best damping to either mode of oscillation. It should be noted that if the P_e

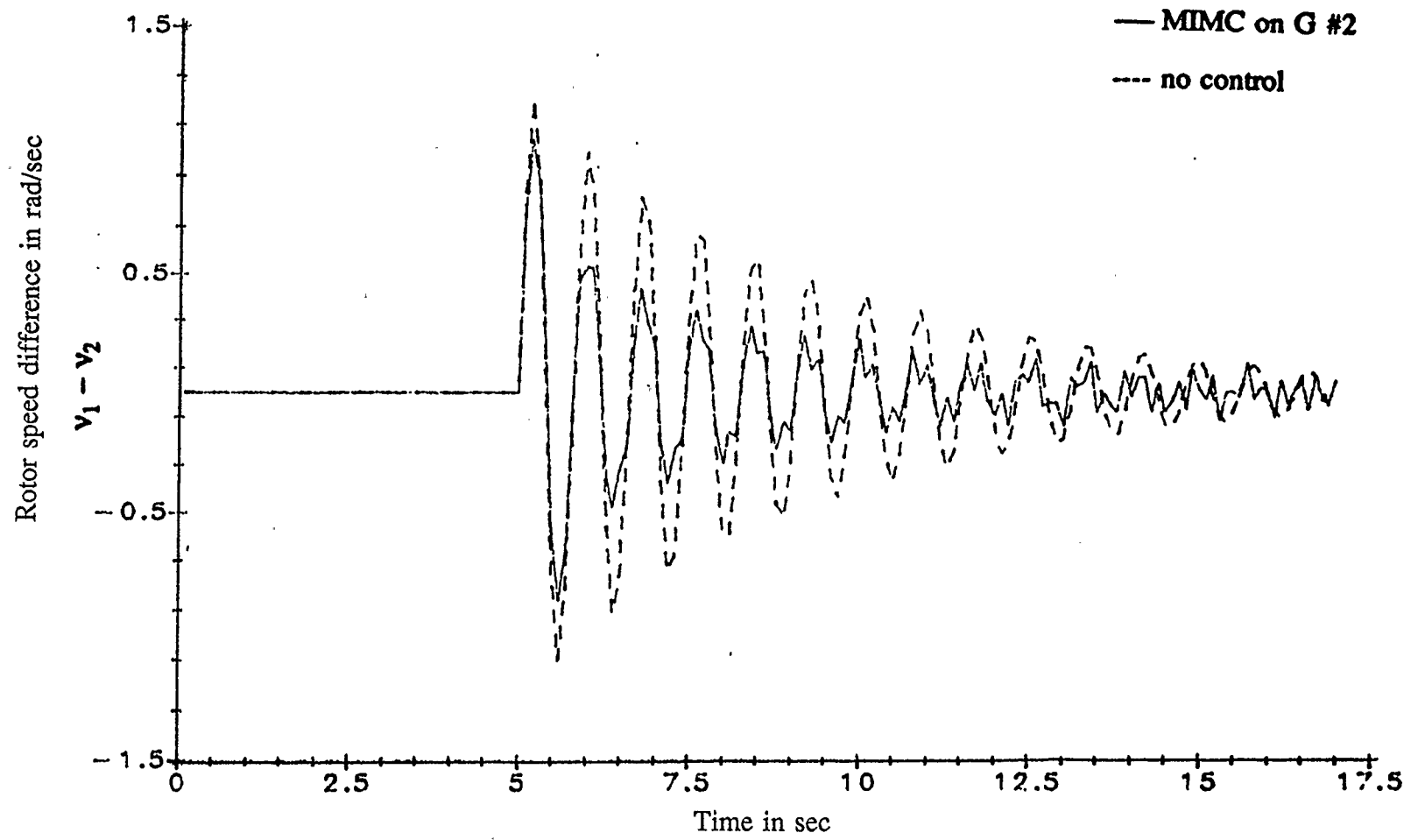


Fig. 4.10 MIMC case (6)

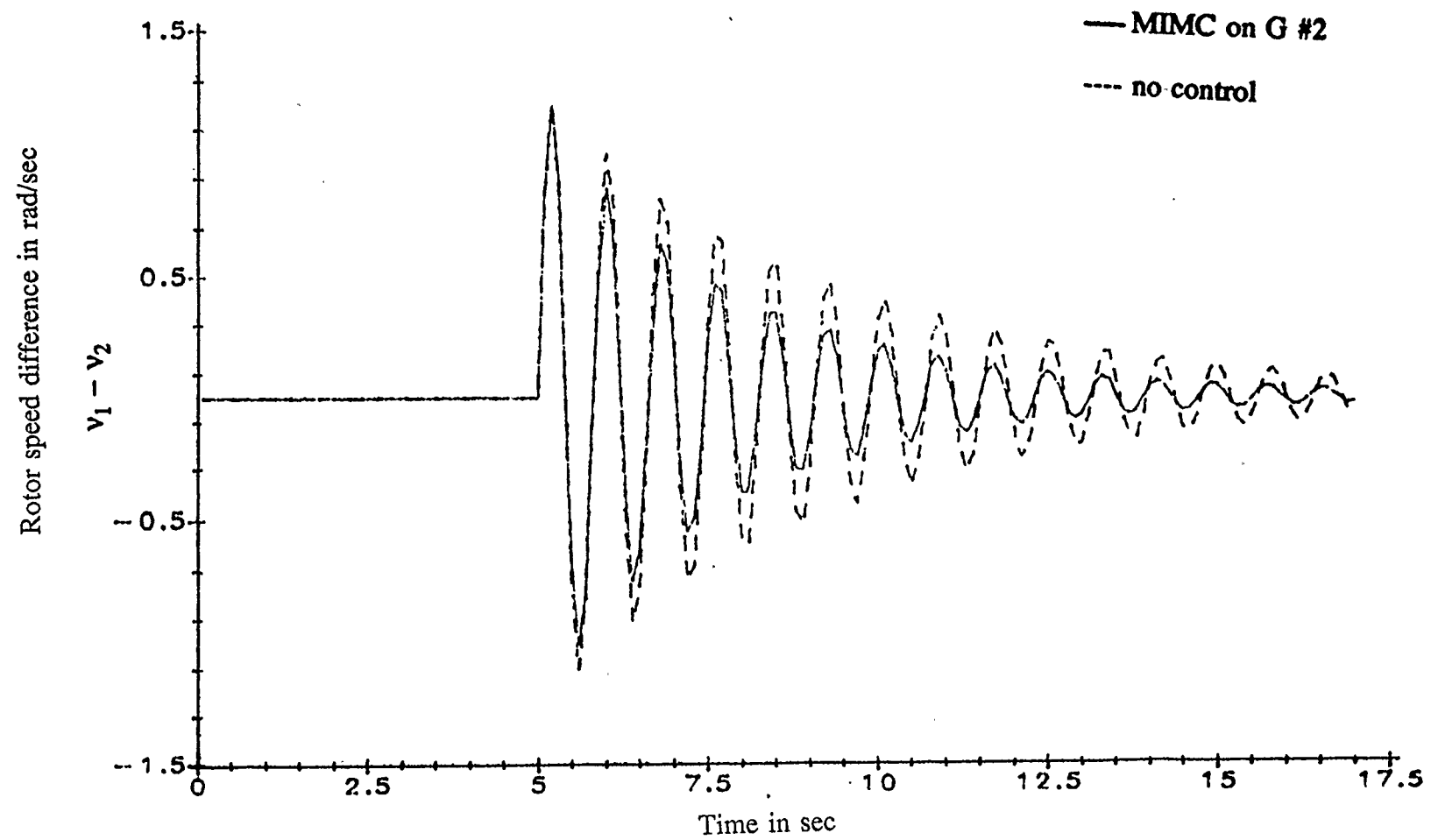


Fig. 4.11 MIMC case (7)

channel alone is used there is excellent damping to the local mode of oscillation, and very little damping to the interarea mode of oscillation. If the $p\delta$ channel is used, there is excellent damping to the interarea mode of oscillation and good damping to the local mode of oscillation. However, neither channel alone damps out both modes of oscillation as effectively as the MIMC controller.

Fig. 4.3 shows the results of applying a MIMC controller on generator #1 only. It can be seen from this figure that the local mode of oscillation between all generators is damped effectively. Since generator #1 and #5 are the main contributors to local mode of oscillation, applying the MIMC controller on generator #1 removes the local mode of oscillation associated with generator #1. It also helps to remove most of the local mode of oscillation associated with generator #5 (since generator #5 is local to generator #1). When a MIMC controller is applied to generator #1 only, it controls the local mode of oscillation associated with generator #1 very effectively. There is some transfer of stability limits to the other generators and hence an improvement in damping to the local mode of oscillation associated with the other generators. However this does not provide the best control action to the other generators. The best control is provided when each generator is equipped with its own controller.

It should also be noted that the interarea mode of oscillation associated with generator #2, #3, and #4 is not affected appreciably. This can be seen by comparing Fig. 4.3 (e) and (f) with Fig. 4.4 (e) and (f). This is partially due to the size of these generators. They are all 10 GVA generators compared to 1 GVA

generation of G #1. It is also partially due the location of these generators (G #3 and G #4 are remote generators). This would have been more apparent if a disturbance, such as MIMC case (3), occurs in which the system is dominant in interarea mode of oscillation, applying a MIMC controller on G #1 only would not damp the interarea mode of oscillation effectively. Therefore MIMC controllers should be applied on all generators to ensure that the best damping action is provided to the generators.

Figs. 4.4 to 4.7 show results for various types of disturbances and operating conditions. The frequency of the local mode of oscillation varies from 0.92 to 1.33 Hz. The frequency of the interarea mode of oscillation varies from 0.21 to 0.26 Hz. However, the performance of the MIMC controller in its ability to control the various frequencies was not hindered. The MIMC controller is capable of handling various operating conditions and damp out the modes of oscillation effectively.

4.6. Summary

Results for both the SIMC and MIMC controllers are given in this chapter. Problems associated with both schemes are introduced, and ways of eliminating these problems are discussed. The results show the effectiveness of the MIMC controller and its ability to damp multi-modes of oscillation in a power system. The results also show that the MIMC controller is more effective than conventional means of control where the PSS is tuned to provide very good damping to one mode of oscillation and some damping to the other mode of oscillation.

CHAPTER 5

IMPLEMENTATION RESULTS

Experimental results using the MIMC controller are presented in this chapter. This chapter gives a description of the experimental power system used for the tests. The setup used to obtain multi-modes of oscillation is discussed. The application of a MIMC controller to the experimental setup and the results obtained for various tests are also introduced. These results support those obtained in the computer simulation.

5.1. Experimental setup

In order to test the MIMC controller on a physical model of a power system, an experimental setup which exhibits multi-modes of oscillation was developed. The three machine power system model developed by Cheng [6] for computer simulation purposes was used as an approximate reference. A power system that resembles the simulation setup was constructed and it gave oscillations that resembled those of local and interarea. The setup is shown in Fig. 5.1.

The remote area was represented by a 50 Hp generator. It serves a load comprised of four induction motors, in which one of the induction motor is running a dc machine that supplies a resistive load. The local area is separated from the

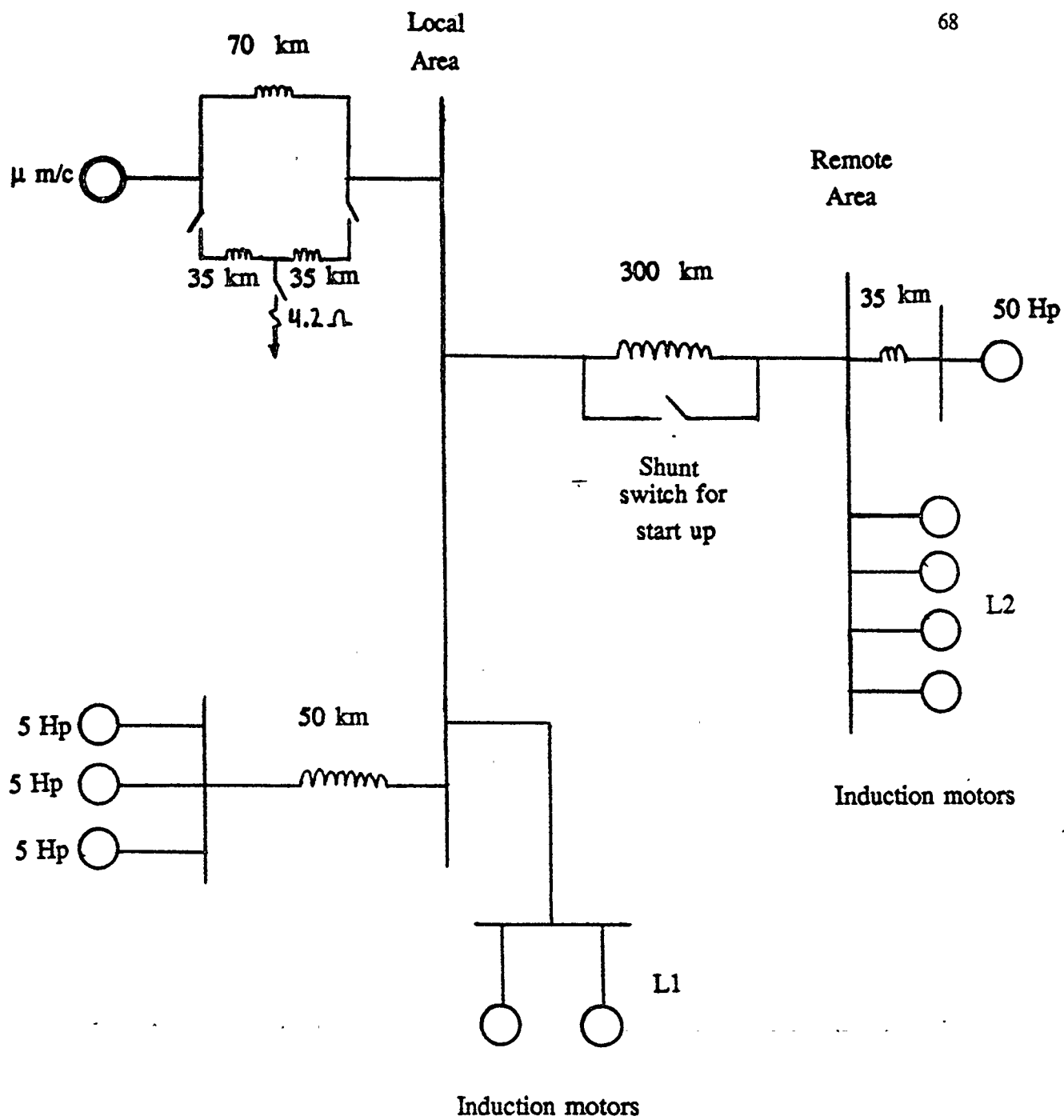


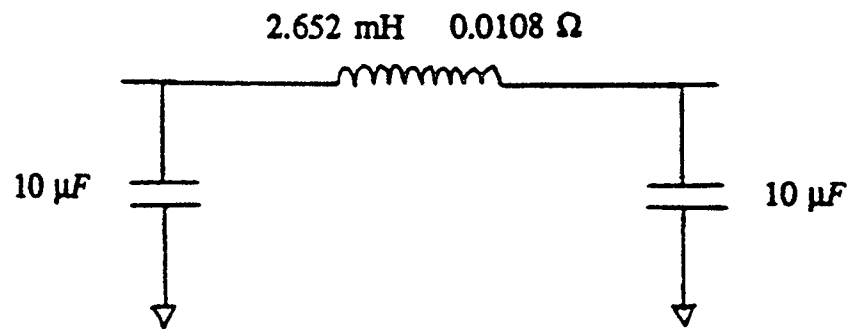
Fig. 5.1 Multi-machine experimental setup

remote area by a long (300 km) transmission line, and is represented by four generators. One of these machines is a 3 KVA synchronous micro-machine connected within the area through a short transmission line. The other three machines are 5 Hp generators connected in parallel to this area also through a short transmission line. The three generators were connected in parallel so as to increase the inertia of the area. The local area supplies a load comprised of two induction motors. Again one of the induction motors supplies a dc machine which is connected to a resistive load.

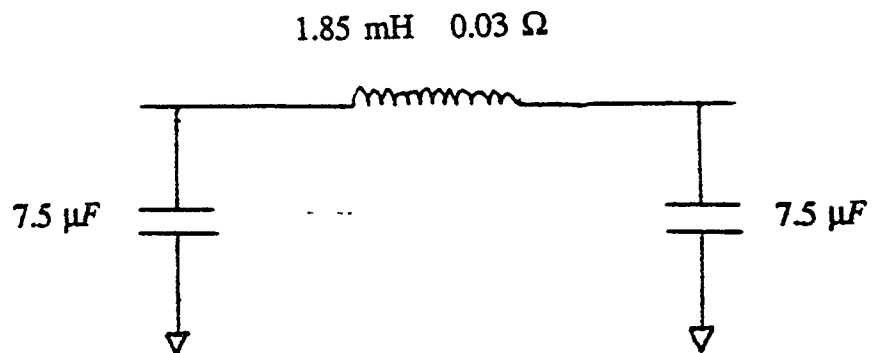
The system has no infinite bus. The idea is to have two areas with equal capacities. Each area is setup to serve its own load with little power transfer across the tie-line.

The 300 km. transmission line is constructed using six 50 km. transmission line sections. Each 50 km. transmission line consists of a LC pi section circuit as shown in Fig. 5.2 (a). The LC circuits representing the 70 km. and 35 km. transmission lines are shown in Figs. 5.2 (b) and 5.2 (c) respectively.

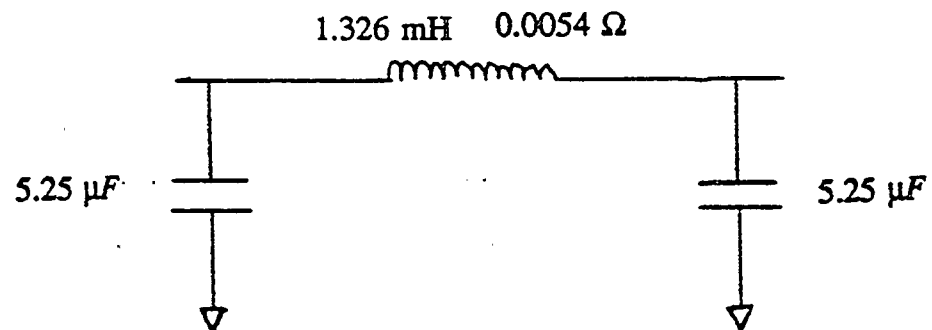
A shunt switch is required across the 300 km. transmission line in the start up procedure. The 50 Hp generator was started and the speed set at 1800 rpm. The 50 Hp generator was then used to start the three 5 Hp generators and bring them to synchronous speed. Without the shunt switch bypass, the voltage at the end of the 300 km transmission line would be insufficient to drive the three generators. Once the three generators were synchronized and operating on their own, the shunt was removed. The micro-machine was started separately, synchronized, and then



(a) 70 km transmission line



(b) 50 km transmission line



(c) 35 km transmission line

Fig. 5.2 Pi section representations of transmission lines

connected to the system.

There are limitations in the modelling capabilities of this experiment. The main limitations are in the equipment used. The 50 Hp generator and the three 5 Hp generators are not equipped with AVRs. Hence, no control can be applied on these generators. However, the 50 Hp generator is equipped with a Hall-effect transducer to observe the electrical power output. The effect of control applied to the micro-machine on the oscillations of the 50 Hp generator was observed using this device.

The micro-machine is equipped with an AVR and exciter. The combined transfer function of the AVR and exciter is :

$$G_e(s) = 100 \frac{s + 1}{10s + 1} \quad 5.1$$

The AVR circuit diagram is given in appendix C.

A time constant regulator (TCR) is used on the micro-machine to simulate the time constant of a large generating unit. The TCR is capable of changing the effective field time constant of the synchronous generator up to 10 seconds [6].

The micro-machine was also equipped with the MIMC controller. Both channels have a washout filter with the transfer function :

$$G_w(s) = \frac{1.47s}{1.47s + 1} \quad 5.2$$

The input signals to the washout stages are P_e and $\Delta\omega$ ($\Delta\omega = \omega - 1800$). The

outputs of the washout stages are ΔP_e and $p\delta$. They are fed into the two channels of the MIMC controller. The transfer function of the PSSs of the two channels are

$$G_{p\delta}(s) = 3.107 \frac{0.207s + 1}{0.122s + 1} p\delta \quad 5.3$$

$$G_{\Delta P_e}(s) = 477.6 \frac{0.137s + 1}{0.0448s + 1} \cdot \frac{0.35s + 1}{3.0s + 1} \Delta P_e \quad 5.4$$

The output of each channel is combined with the AVR signal and is fed into the excitation system. The circuit diagram of the controllers are shown in appendix C. the experimental setup for the micro-machine is shown in Fig. 5.3.

The two frequencies of oscillation observed were approximately 1.0 Hz and 2.0 Hz. The 1.0 Hz oscillation was assigned to the $p\delta$ channel, and the 2.0 Hz oscillation was assigned to the ΔP_e channel.

Since the micro-machine is the only generator equipped with an AVR, any sudden impact disturbance results in a large voltage drop. The voltage dropped to very low levels, and the AVR alone isn't capable of returning the voltage back to its reference. The limits of the control signals were increased to ± 5 volts, so as to assist the AVR in restoring the terminal voltage to its original value.

5.2. Implementation studies

Two cases were studied to test the effectiveness of the MIMC controller using the experimental power system setup. Both cases utilized a short circuit that

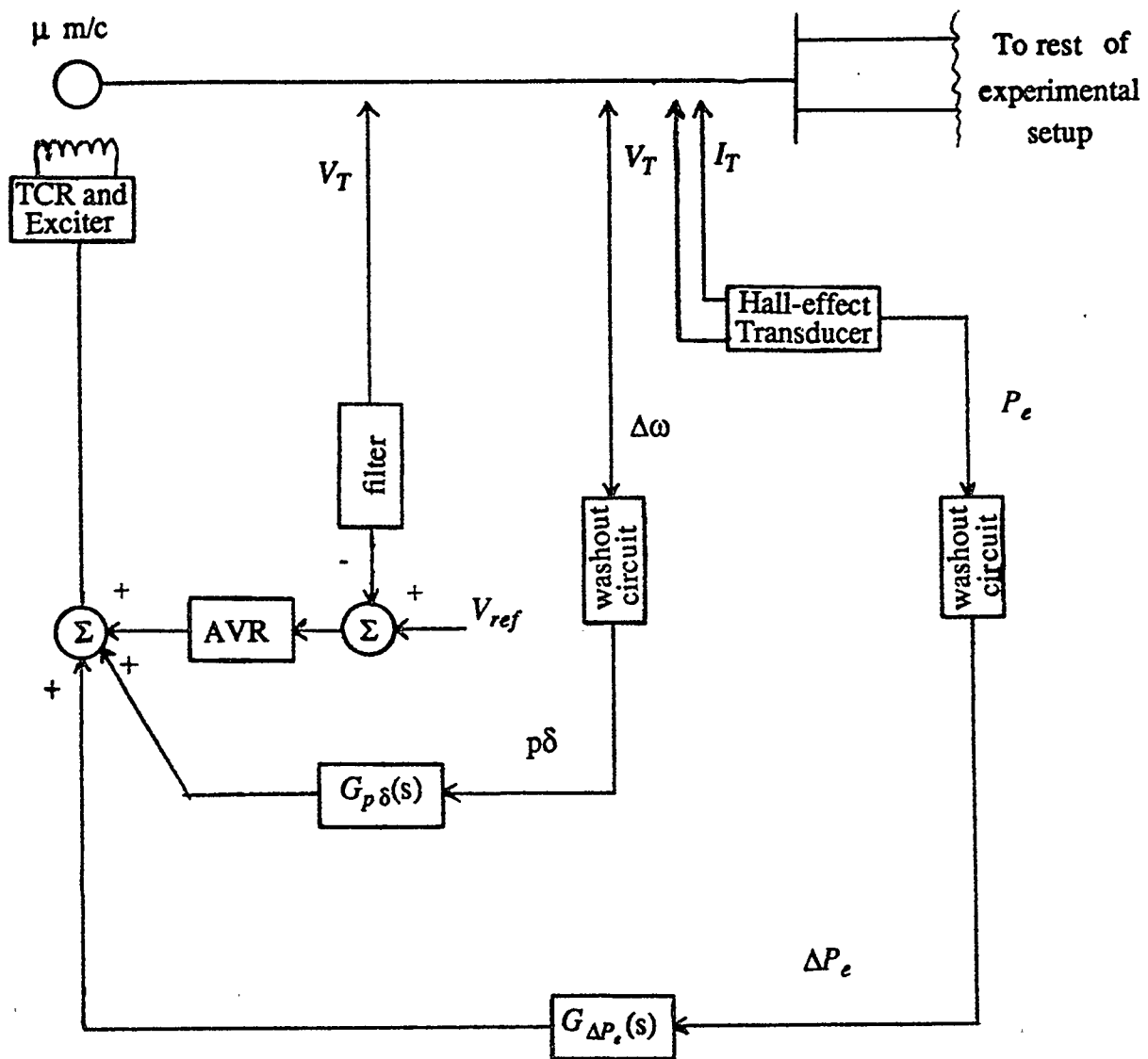


Fig. 5.3 Micro-machine experimental setup

disturbs the system sufficiently to provide multi-modes of oscillation. A short circuit was applied to one of the transmission lines connecting the micro-machine to the system. The short circuit was sustained for approximately 0.1 seconds. The two cases involved two different operating conditions :

(1) 0.8 pf lag, and

(2) 0.9 pf lead.

Other studies were not performed due to time limitations, however the two studies performed do show the effectiveness of using a MIMC controller.

5.3. Implementation results

The two cases were also studied with no controllers, and each channel controller (i.e $p\delta$ and ΔP_e) applied separately. It should be noted that all control was applied to the micro-machine only.

Figs. 5.4 and 5.5 show the results of a short circuit test for case (1). Fig. 5.4 (a) shows the rate of change in the electrical power (ΔP_e) output of the micro-machine with no controller. It can be seen that two different frequencies are present in the signal. This becomes more apparent when the controllers of each channel are applied to the micro-machine.

The $p\delta$ channel is assigned to remove the 1.0 Hz frequency signal. Fig. 5.4 (b) shows the output (ΔP_e) of the micro-machine with the $p\delta$ channel controller

applied. The output (ΔP_e) of the micro-machine now mainly contains the 2.0 Hz signal. Fig. 5.4 (c) shows the output (ΔP_e) of the micro-machine with the ΔP_e channel controller applied. In this case, the ΔP_e channel removes the 2.0 Hz signal component from the output (ΔP_e). It can be seen from Fig. 5.4 (c) that the output (ΔP_e) is mainly dominant in 1.0 Hz oscillations. Fig. 5.4 (d) shows the output (ΔP_e) of the micro-machine with the MIMC controller applied. Comparison between Fig. 5.4 (d) and Fig. 5.4 (a) show that the damping is effective after the first swing. Both modes of oscillation are damped, as is seen by comparing Fig. 5.4 (d) to Figs. 5.4 (b) and 5.4 (c).

Fig. 5.5 (a) shows the electrical power output (ΔP_e) of the 50 Hp generator with no controller applied. Although this signal contains both modes of oscillation, the 2.0 Hz dominates. Fig. 5.5 (b) shows the output (ΔP_e) of the 50 Hp generator with the $p\delta$ channel controller applied. It can be seen in Fig 5.5 (b) that the first peak of the second swing is reduced. This is due to the reduction of the 1.0 Hz component. Fig. 5.4 (c) shows the effect of applying the ΔP_e channel controller. It can be seen that the first peak of the second swing is not damped, however the subsequent oscillations are. This is due to the reduction of the 2.0 Hz component in the output. Fig. 5.5 (d) shows the output (ΔP_e) of the 50 Hp generator with the MIMC controller applied. Comparing Fig. 5.5 (d) with Fig. 5.5 (a), it can be seen that the damping after the first swing has been improved. It can also be seen that there is improvement in Fig. 5.5 (d) over Figs. 5.5 (b) and 5.5 (c).

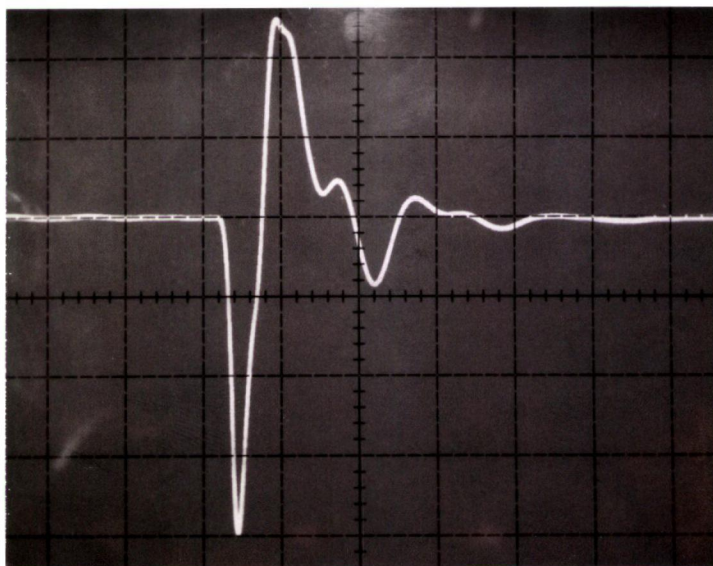
Figs. 5.6 and 5.7 show the results for the short circuit case (2). Figs. 5.6 (a) through (d) show the output (ΔP_e) of the micro-machine with no controllers, $p\delta$ channel only, ΔP_e channel only, and MIMC controller applied, respectively. Similarly, Figs. 5.7 (a) through (d) show the output (ΔP_e) of the micro-machine with no controllers, $p\delta$ channel only, ΔP_e channel only, and MIMC controller applied, respectively. Again, comparisons between the various figures show that the MIMC controller provide better damping than either channel separately. This is apparent in comparing Fig. 5.6 (d) to Figs. 5.6 (b) and (c). The peak after the first swing in Fig 5.6 (b) is shifted downwards when the 1.0 Hz signal is damped out. The peak after the first swing in Fig. 5.6 (c) is shifted upwards when the 2.0 Hz signal is removed. This is because the two signals present in the system are opposite in phase and tend to cancel each other. Removing one of the signals from the output causes the other to become dominant. Using the MIMC controller, both modes are damped causing the overall damping of the output signal to be improved, as seen in Fig. 5.6 (d). The same effect can be seen in the output (ΔP_e) of the 50 Hp generator observed in Figs. 5.7 (a) through (d).

The above tests show the effectiveness of the MIMC controller in damping multi-modes of oscillation in a power system. The MIMC controller was applied for various operating conditions and the MIMC controller is capable of damping the modes of oscillation for either operating condition.

5.4. Summary

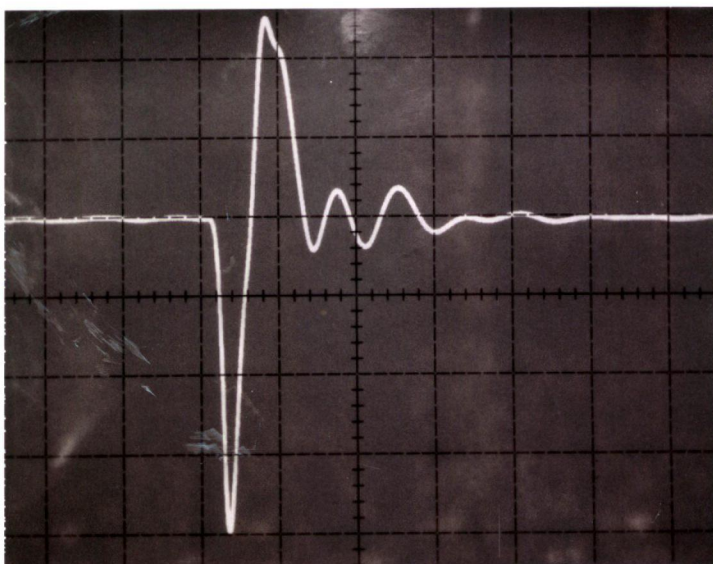
The effectiveness of a MIMC controller in damping multi-modes of oscillation on a experimental power system is demonstrated for two different operating conditions. Short circuit tests were conducted, and comparisons between no controller, $p\delta$ channel controller, ΔP_e channel controller, and MIMC controller applied on the micro-machine were obtained.

2.0 volts/div



(a) no controller

2.0 volts/div

(b) $p\delta$ channel controller

0.5 seconds/div

Fig. 5.4 Short circuit test, 0.8 pf lag, ΔP_e output of micro-machine

0.8 lag
no control

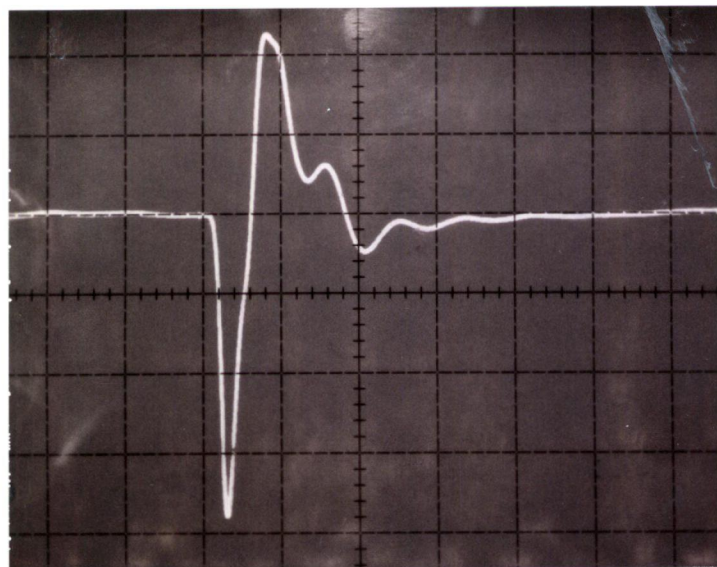
$\mu m/c$

0.8 lag

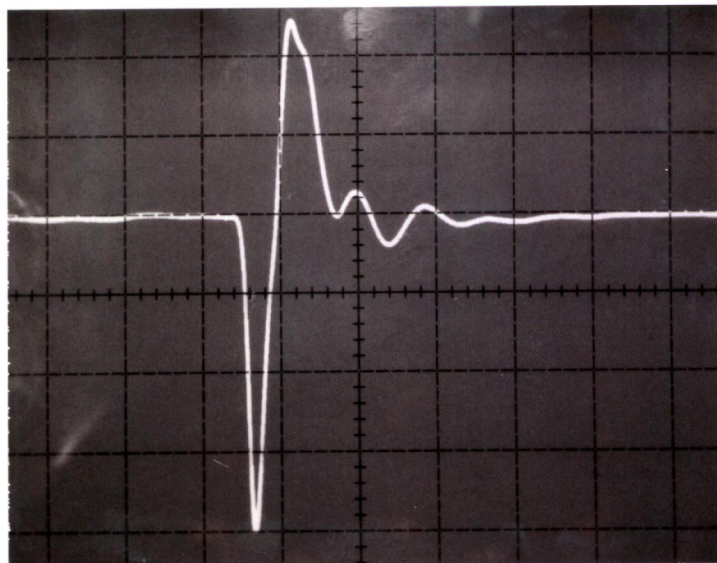
pl

$\mu m/c$

2.0 volts/div

(c) ΔP_e channel controller

2.0 volts/div



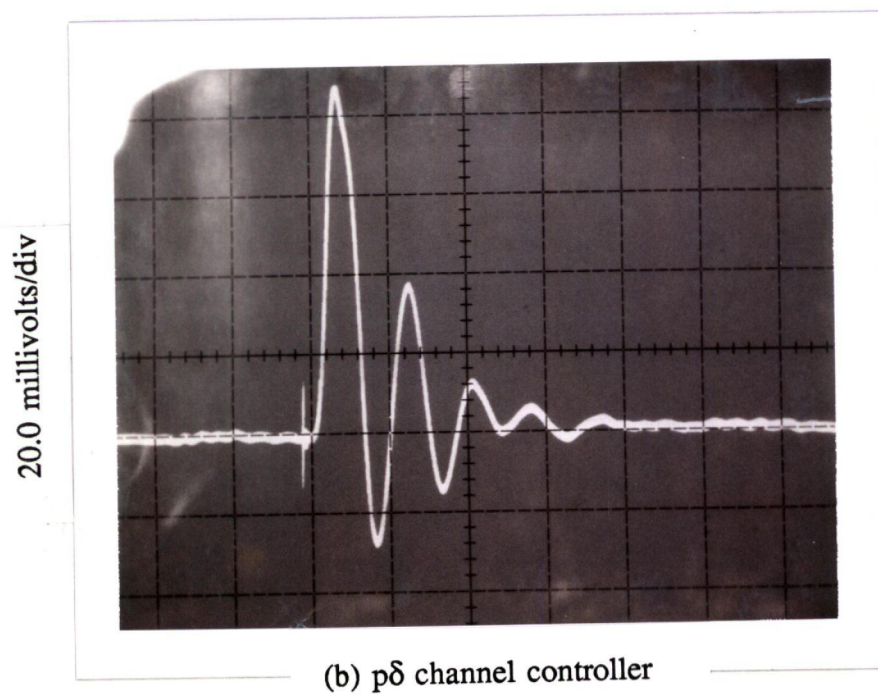
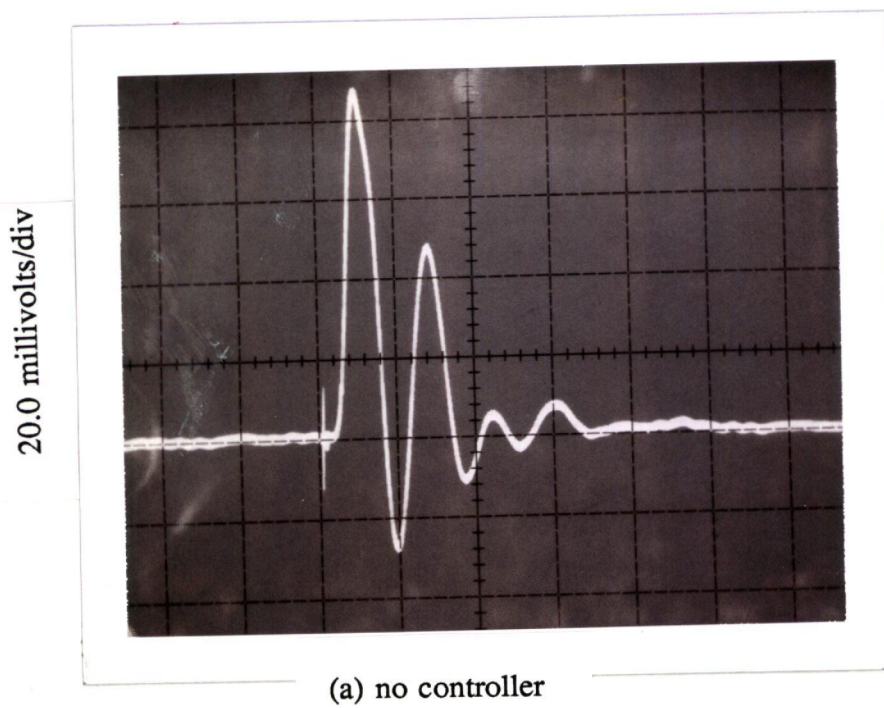
(d) MIMC controller

0.5 seconds/div

Fig. 5.4 (continued)

0.8129
P_E channel
mm/c

0.8129
M_E MC
mm/c



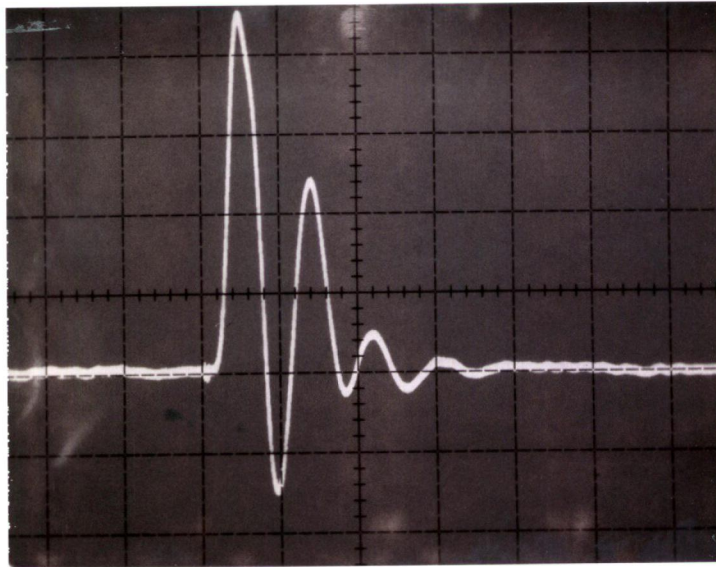
0.5 seconds/div

Fig. 5.5 Short circuit test, 0.8 pf lag, ΔP_e output of 50 Hp generator

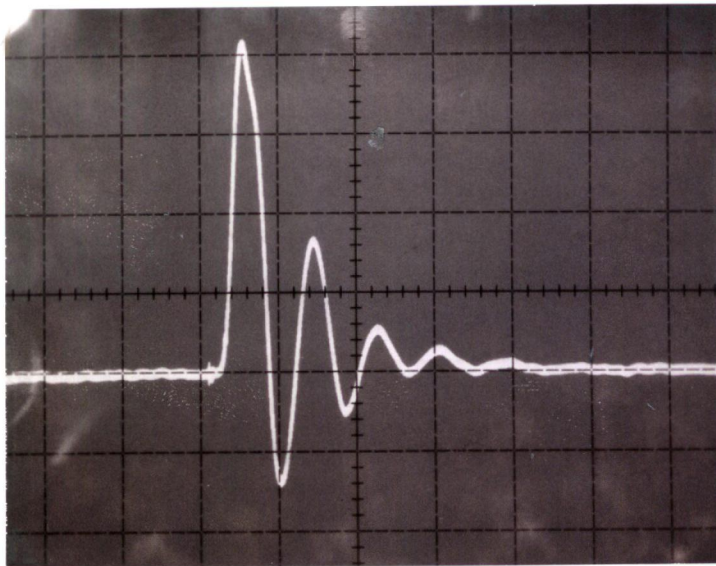
50 Hz
no controller
0.8 lag

PS channel

20.0 millivolts/div

(c) ΔP_e channel controller

20.0 millivolts/div



(d) MIMC controller

0.5 seconds/div

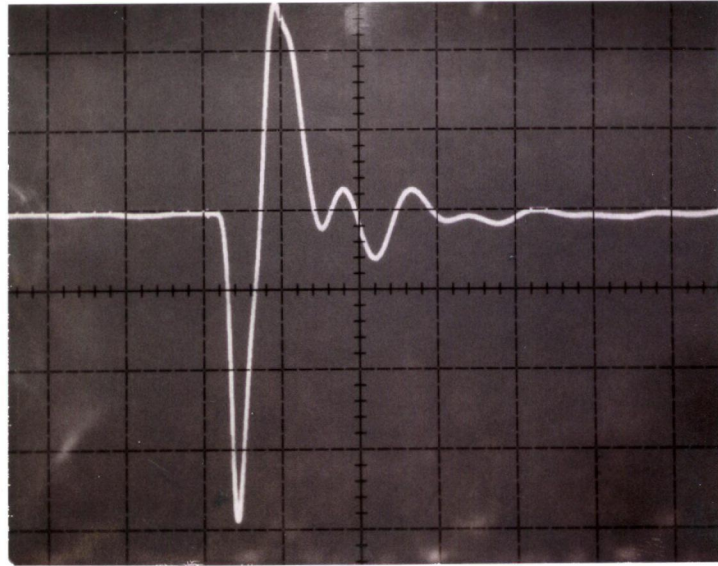
Fig. 5.5 (continued)

50HP
display

2 PE

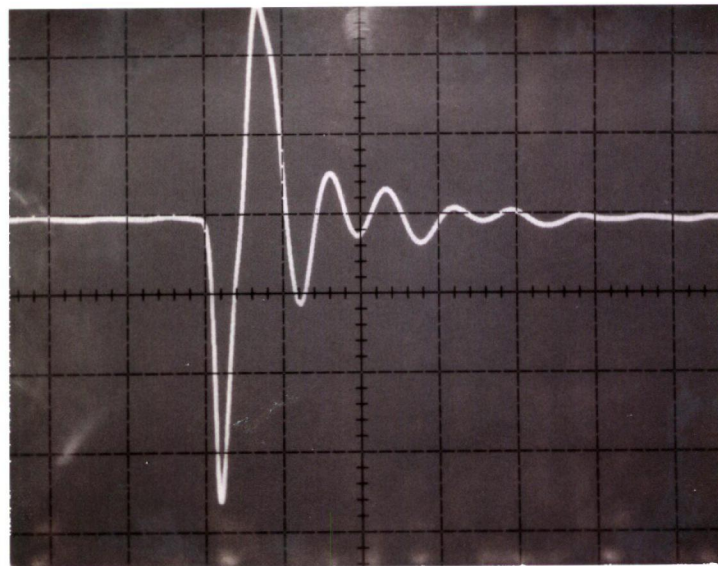
MI MC

2.0 volts/div



(a) no controller

2.0 volts/div

(b) $p\delta$ channel controller

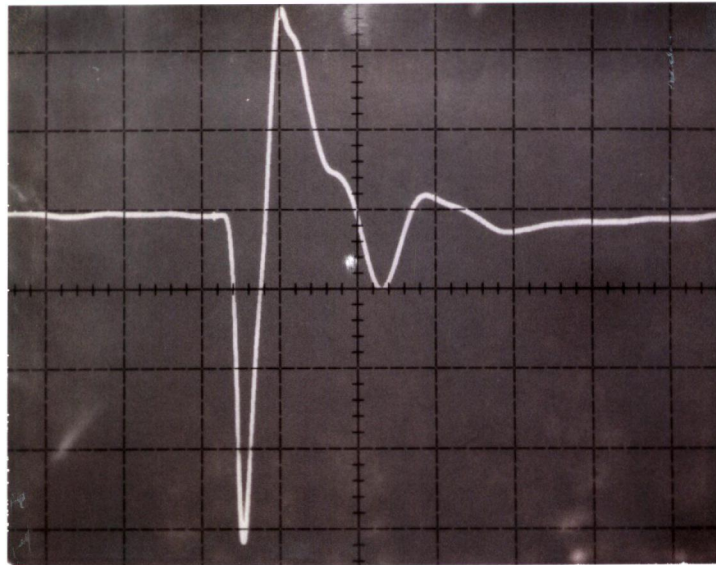
0.5 seconds/div

Fig. 5.6 Short circuit test, 0.9 pf lead, ΔP_e output of micro-machine

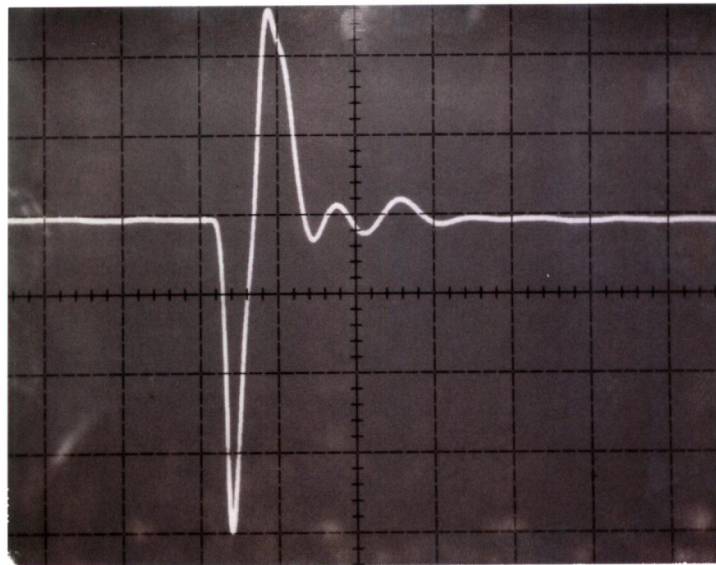
on lead
muc
no cont

96

2.0 volts/div

(c) ΔP_e channel controller

2.0 volts/div



(d) MIMC controller

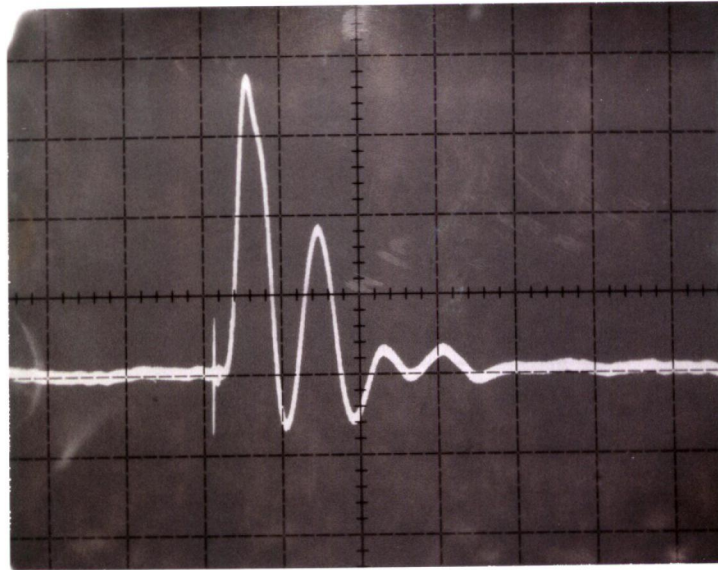
0.5 seconds/div

Fig. 5.6 (continued)

0.9
 ΔPE
 $\mu m/c$

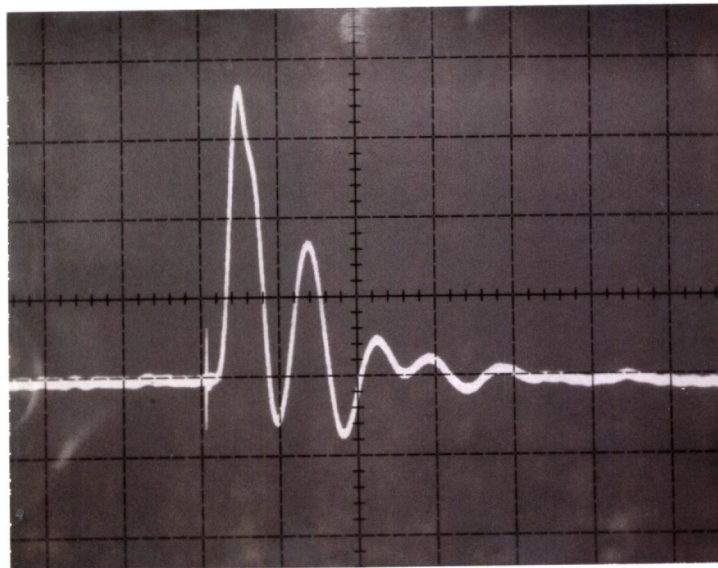
MSIMC

20.0 millivolts/div



(a) no controller

20.0 millivolts/div

(b) $p\delta$ channel controller

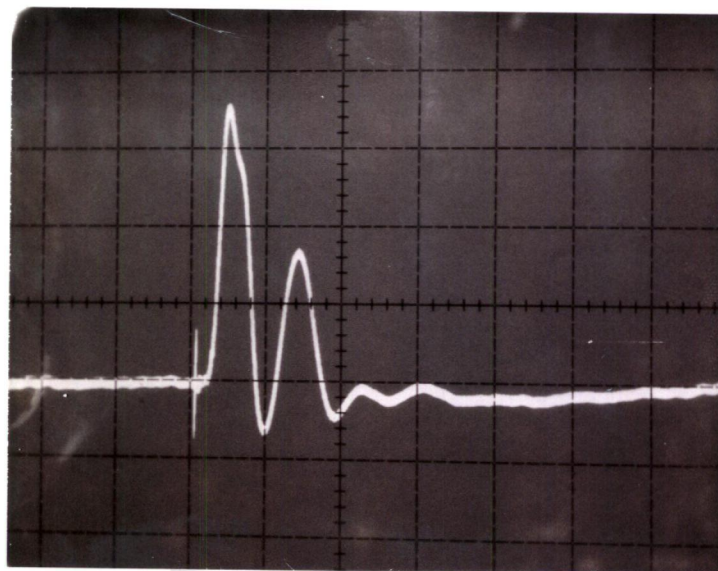
0.5 seconds/div

Fig. 5.7 Short circuit test, 0.9 pf lead, ΔP_e output of 50 Hp generator

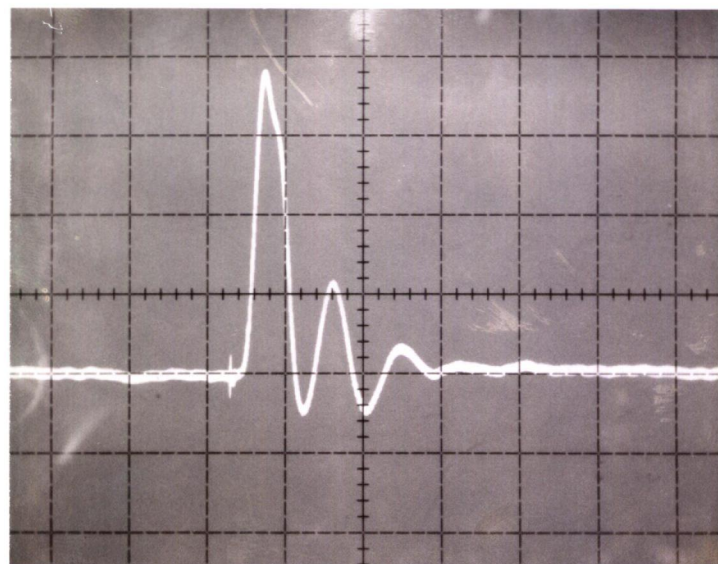
50 HP
0.9 lead
no cont

PS

20.0 millivolts/div

(c) ΔP_e channel controller

20.0 millivolts/div



(d) MIMC controller

0.5 seconds/div

Fig. 5.7 (continued)

0.7 lead
solid
DPE

MIMC

CHAPTER 6

CONCLUSION

Power system stability is an important area of interest to a power system engineer. Modern society requires an increase in the supply of electrical power. To supply this demand complex power systems are designed. These power systems are reduced in stability as more generators and loads are added, making the stability problem a concern to the engineer. Research has been conducted into various control strategies to improve the dynamic stability.

In this chapter conclusions are given on the studies into the development of a MIMC controller and its effectiveness in controlling multi-modal oscillations. Ideas for future work in this area are also presented.

6.1. Conclusions and Thesis contribution

One form of control strategy based on the classical control theory is to use a fixed transfer function controller to provide a supplementary control signal. In this thesis the concepts behind using a PSS to provide a supplementary signal that is fed back to the excitation system are discussed. The PSS is a fixed transfer function controller that is widely used in the power industry, and is easy to tune for one frequency. The problem of contradiction that exists when attempting to

control multi-modal oscillations with a conventional power system stabilizer is presented, and two different structures of multi-channel controllers capable of handling this contradiction are introduced and discussed.

The MIMC controller is introduced. This structure incorporates conventional PSSs. The MIMC controller has two channels, each dedicated to controlling one mode of oscillation (i.e. local mode and interarea mode of oscillation). Each channel is tuned to provide the best damping action of the mode to which it is assigned. This eliminates the contradiction by having each channel provide the best phase and gain margins to each mode of oscillation. Each channel uses an input signal which best characterizes the mode of oscillation it is to damp. The local mode channel has P_e as its input, and the interarea mode channel uses $p\delta$ as input.

The MIMC controller has proven to be very effective in controlling multi-modes of oscillation. Simulation studies performed show comparative results between the MIMC controller and a conventional PSS. The results show that the MIMC controller improves the damping of both the local mode and interarea mode of oscillation. The damping for the local mode of oscillation was improved from 6 cycles for a conventional PSS to 2-2.5 cycles for a MIMC. The damping action of the interarea mode of oscillation is generally reduced from ten seconds using the conventional PSS to about five seconds using the MIMC controller. This is expected since each channel provides the best damping action possible to each mode of oscillation.

Experimental studies conducted using the MIMC controller also show that the MIMC controller is effective in damping multi-modes of oscillation. Results showing comparisons between no controller, $p\delta$ controller, ΔP_e channel controller, and MIMC controller show that the MIMC controller provides better damping than either channel, and damps both modes of oscillation.

The advantages of the a MIMC structure are that it eliminates the contradictory requirement of damping two different modes of oscillations simultaneously and effectively damps multi-modes of oscillation. It is easy to tune and implement and it uses currently accepted and widely used PSSs.

6.2. Future works

Further research can be conducted in this area. An experimental setup which better exhibits multi-modes of oscillation could be developed. More studies using the MIMC controller on an experimental setup could be conducted. This will further support the simulation studies and the use of a MIMC controller.

The use of other inputs such as the accelerating power or the bus frequency as input signals to the MIMC controller, and the use of other fixed transfer functions for PSSs may prove to be more effective.

REFERENCE

- [1] P.M. Anderson and A.A.Fouad "Power System Control and Stability" The Iowa State University Press, Iowa U.S.A, 1977
- [2] Vsevolod I. Astafiev, Yuri M. Gorsky, Dmitrij A. Pospelov "Contradictions in the Control of Large Systems", pp 1-14
- [3] Helena Curtis "Biology" Worth Publishers Inc., 1979, pp 753-770
- [4] M. N. G. Dukes "Meyler's Side Effects of Drugs" Elsevier, 1984, pp 288
- [5] Francis J. Hale "Introduction to Control Systems Analysis and Design" Prentice-Hall Inc., 1973, pp 94-101
- [6] Shi-jie Cheng, "A Self Tuning Power System Stabilizer.", Ph.D. Thesis The University of Calgary, 1986
- [7] N.K. Sinha "Reduction of the Sensitivity of an Optimal Control System to Plant Parameter Variations" IEEE Trans. Vol. AC-15, 1970, pp 589-590
- [8] W. Watson and G. Manchur "Experience with Supplementary Damping Signal for Generator Static Excitation System" IEEE Trans. Vol. PAS-92, 1973, pp 199-211
- [9] P. Kundur, D.C. Lee, and H.M. Zein El-Din "Power System Stabilizers for Thermal Units: Analytical Techniques and On-Site Validation" IEEE Trans. Vol. PAS-100 No. 1, 1981, pp 81-95

- [10] A.D. Gerhart, T. Hillesland, J.F. Luini, and Rockfield Jr. "Power System Stabilizer: Field Testing and Digital Simulation" IEEE Trans. Vol. PAS-90, 1971, pp 2095-2100
- [11] F.P.deMello and T.F.Laskowski "Concepts of Power System Dynamic Stability" IEEE Trans. Vol. PAS-94, 1975, pp 827-833
- [12] E.V. Larsen and D.A. Swann, "Applying Power System Stabilizers Part 1: General Concepts" IEEE Trans. Vol. PAS-100 1981 No. 6, June 1981, pp 3017-3024
- [13] Ferber R. Schleif, Harvey D. Hunkins, Glenn E. Martin, and Ellis E. Hattan "Excitation Control to Improve Powerline Stability" IEEE Trans. Vol. PAS-87 No. 6, June 1968, pp 1426-1434
- [14] F.P.deMello and D.N.Ewart "Stability of Synchronous Machine as Affected by Excitation Systems, Machine System Parameters" Proc. Am. Power Conf. Vol. 26, 1965, pp 1150-1159
- [15] F.P.deMello and C.Concordia "Concepts of Synchronous Machine Stability as Affected by Excitation Control" IEEE Trans. Vol. PAS-88 No. 4, 1968, pp 316-329
- [16] O.P.Malik, G.S.Hope and D.W.Huber "Design and Test Results of a Software Based Digital AVR" IEEE Trans. Vol. PAS-95, 1976, pp 634-642
- [17] R.Doraiswami, A.M.Sharaf and J.C.Castro "A Novel Excitation Control Design for Multimachine Power System" IEEE Trans. Vol. PAS-103 No. 5,

1984, pp 1052-1058

- [18] R.T.Byerly, F.W.Keay and J.W.Skooglund "Damping of Power Oscillations in Salient Pole Machines with Static Exciters" IEEE Trans. Vol. PAS-89 No. 6, 1970, pp 1009-1021
- [19] Jack L. Dineley, Anthony J. Morris and Clive Preece "Optimal Transient Stability from Excitation Control of Synchronous Generators" IEEE Trans. Vol. PAS-87 No. 8, August 1968, pp 1696-1705
- [20] P.O.Bobo, J.W.Skooglund and C.L.Wagner "Performance of Excitation System under Abnormal Conditions" IEEE Trans. Vol. PAS-87 No. 2, February 1968, pp 547-553
- [21] P.G.Brown, F.P.deMello, E.H.Lenfest and R.J.Mills "Effects of Excitation, Turbine Energy Control, and Transmission on Transient Stability" IEEE Trans. Vol. PAS-89 No. 6, 1970, pp 1247-1252
- [22] Oscar W. Hanson, C.J.Goodwin and Paul L. Dandeno "Influence of Excitation and Speed Control Parameters in Stability Inter-system Oscillation" IEEE Trans. Vol. PAS-87 No. 5, May 1968, pp 1306-1313
- [23] S.N.Iyer and B.J.Cory "Optimal Control of a Turbo-generator Including an Excitation and Governor" IEEE Trans. Vol. PAS-90, 1971, pp 2142-2148
- [24] D.C.Lee and J.R.R.Service "A Power System Stabilizer using Speed and Electrical Power Inputs- Design and Field Experience" IEEE Trans. Vol. PAS-100 No. 9, 1981, pp 4151-4157

- [25] E.V. Larsen and D.A. Swann, "Applying Power System Stabilizers Part 2: Performance Objectives and Tuning Concepts" IEEE Trans. Vol. PAS-100 No. 6, June 1981, pp 3025-3033
- [26] Dandens, P.L., "Practical Application of Eigenvalue Techniques in the Analysis of Power System Dynamic Stability Problems" Can. Elec. Eng. Journal Vol. 1 No. 1, 1976, pp 35-46
- [27] P.L.Dandeno, A.N.Karas, K.R.McClymont and W.Watson "Effect of High-speed Rectifier Excitation System on Generator Stability Limits" IEEE Trans. Vol. PAS-87 No. 1, January 1968, pp 190-200
- [28] D.L.Bauer, W.D.Buhr, S.S.Cogswell, D.B.Cory, G.B.Ostroski and D.A.Swanson "Simulation of Low Frequency Undamped Oscillations in Large Power Systems" IEEE Trans. Vol. PAS-94, 1975, pp 207-213
- [29] K.E.Bollinger, R.Winsor and A.Cambell "Frequency Response Methods for Tuning Stabilizers to Damp Out Tie-line Power Oscillations: Theory and Field-test Results" IEEE Trans. Vol. PAS-98, 1979, pp 1509-1515
- [30] F.R.Schleir, R.K.Feeley, W.H.Phillips and R.W.Torluemke "A Power System Stabilizer Application with Local Model Cancellation" IEEE Trans. Vol. PAS-98, 1979, pp 1054-1060

APPENDIX A

FILTER DESIGN FOR THE SIMC STRUCTURE

The following specifications and transfer functions are used in the filter design:

For Lowpass filter design:

Assign filter specifications:

$$A_p = 1 \text{ dB}, f_p = 0.4 \text{ Hz}$$

$$A_a = 20 \text{ dB}, f_a = 0.9 \text{ Hz}$$

$$f_s = 100 \text{ Hz}$$

Obtain order of filter:

$$K_o = \frac{\tan(\Omega_p \frac{\pi}{\omega_s})}{\tan(\Omega_a \frac{\pi}{\omega_s})}$$

where

$$\Omega_p = 2\pi f_p$$

$$\Omega_a = 2\pi f_a$$

$$K_o = 0.44435$$

For a lowpass filter :

$$K = K_o$$

$$D = \frac{(10^{0.1A_s} - 1)}{(10^{0.1A_p} - 1)}$$

$$D = 382.35$$

$$n \geq \frac{\log(D)}{2\log(\frac{1}{K})} \geq 3.66$$

$$n = 4$$

$$\omega_p = (10^{0.1A_p} - 1)^{\frac{1}{2n}}$$

$$\omega_p = 0.84459$$

$$\lambda = \frac{\omega_p T}{2 \tan(\frac{\Omega_p T}{2})}$$

$$\lambda = 0.33603$$

Calculate the poles for $n = 4$:

$$s_k = \cos \frac{(2k-1)\pi}{8} + j \sin \frac{(2k-1)\pi}{8}$$

$$p_1 = -0.92388 + j0.38268$$

$$p_2 = -0.38268 + j0.92388$$

$$p_3 = -0.92388 - j0.38268$$

$$p_4 = -0.38268 - j0.92388$$

The normalized transfer function is :

$$H_N(s) = \frac{1}{(s + p_1)(s + p_2)(s + p_3)(s + p_4)}$$

$$H_N(s) = \frac{1}{s^4 + 2.61313s^3 + 3.41421s^2 + 2.61313s + 1}$$

To obtain actual filter parameters, substitute

$$s = \lambda s$$

into the normalized transfer function $H_N(s)$:

$$H_{LP}(s) = \frac{78.4266}{s^4 + 7.7764s^3 + 30.2359s^2 + 68.8665s + 78.4266}$$

For Bandpass filter design:

Assign filter specifications:

$$A_p = 1 \text{ dB}, A_a = 20 \text{ dB}$$

$$f_{p1} = 0.8 \text{ Hz}, f_{p2} = 1.2 \text{ Hz}$$

$$f_{a1} = 0.3 \text{ Hz}, f_{a2} = 1.7 \text{ Hz}$$

$$f_s = 100 \text{ Hz}$$

Obtain order of filter:

$$K_A = \tan\left(\frac{\Omega_{p2}T}{2}\right) - \tan\left(\frac{\Omega_{p1}T}{2}\right) = 0.012579$$

$$K_B = \tan\left(\frac{\Omega_{p1}T}{2}\right)\tan\left(\frac{\Omega_{p2}T}{2}\right) = 0.00094813$$

$$K_C = \tan\left(\frac{\Omega_{a1}T}{2}\right)\tan\left(\frac{\Omega_{a2}T}{2}\right) = 0.00050384$$

$$K_1 = \frac{K_A \tan\left(\frac{\Omega_{a1}T}{2}\right)}{K_B - \tan^2\left(\frac{\Omega_{a1}T}{2}\right)} = 0.13797$$

$$K_2 = \frac{K_A \tan\left(\frac{\Omega_{a2}T}{2}\right)}{\tan^2\left(\frac{\Omega_{a2}T}{2}\right) - K_B} = 0.35213$$

where

$$\Omega_{p1} = 2\pi f_{p1}$$

$$\Omega_{p2} = 2\pi f_{p2}$$

$$\Omega_{a1} = 2\pi f_{a1}$$

$$\Omega_{a2} = 2\pi f_{a2}$$

Since $K_C < K_B$:

$$K = K_2$$

$$D = \frac{(10^{0.1A_s} - 1)}{(10^{0.1A_p} - 1)}$$

$$D = 382.35$$

$$n \geq \frac{\log(D)}{2\log(\frac{1}{K})} \geq 2.85$$

$$n = 3$$

$$\omega_p = (10^{0.1A_p} - 1)^{\frac{1}{2n}}$$

$$\omega_p = 0.798354$$

$$\omega_o = \frac{2\sqrt{K_B}}{T}$$

$$\omega_o = 6.1583439$$

$$B = \frac{2K_A}{T\omega_p}$$

$$B = 3.151218$$

The normalized transfer function is :

$$H_N(s) = \frac{1}{s^3 + 2s^2 + 2s + 1}$$

To obtain actual filter parameters, substitute

$$s = \frac{1}{B} \left(\frac{s^2 + \omega_o^2}{s} \right)$$

into the normalized transfer function $H_N(s)$:

$$H_{BP}(s) = \frac{31.2922s^3}{s^6 + 6.3024s^5 + 133.636s^4 + 509.33s^3 + 5068.17s^2 + 9064.93s + 54548.6}$$

APPENDIX B

MULTI-MACHINE MODEL PARAMETERS

The transfer functions and parameter values used in simulation are as follows:

AVR and Exciter

$$v_A = \frac{K_A}{sT_A + 1} \cdot (v_{ref} - v_t)$$

where K_A is the exciter gain

AVR and Exciter parameters

<u>parameter</u>	<u>G #1</u>	<u>G #2</u>	<u>G #3</u>	<u>G #4</u>	<u>G #5</u>
K_A	200.00	200.00	200.00	200.00	200.00
T_A	0.01	0.01	0.01	0.01	0.01

Governor

$$g = (A + \frac{B}{sT_g + 1}) \cdot p \delta$$

Governor parameters

<i>parameter</i>	<i>G #1</i>	<i>G #2</i>	<i>G #3</i>	<i>G #4</i>	<i>G #5</i>
A	-0.001326	-0.00015	-0.00015	-0.001326	-0.00015
B	-0.17	-0.015	-0.015	-0.17	-0.015
T_g	0.25	0.25	0.25	0.25	0.25

Parameters of the generators in pu

<i>parameter</i>	<i>G #1</i>	<i>G #2</i>	<i>G #3</i>	<i>G #4</i>	<i>G #5</i>
x_d	1.026	0.1026	0.1026	0.1026	1.026
x_q	0.658	0.0658	0.0658	0.0658	0.658
x'_d	0.339	0.0339	0.0339	0.0339	0.339
x''_d	0.269	0.0269	0.0269	0.0269	0.269
x''_q	0.335	0.0335	0.0335	0.0335	0.355
T'_{do}	0.367	0.367	0.367	0.367	0.367
T''_{do}	0.0314	0.0314	0.0314	0.0314	0.0314
T''_{qo}	0.0623	0.0623	0.0623	0.0623	0.0623
H	2.8	28.0	28.0	28.0	2.80

Transmission line parameters in pu

<u>Bus conn.</u>	<u>Impedence pu</u>	<u>Fault condition pu</u>
1-6	$0.0600 + 0.4000j$	$0.0800 + 0.5667j$
2-6	$0.0060 + 0.0400j$	$0.0060 + 0.0400j$
3-7	$2.3E-4 + 0.0153j$	$2.3E-4 + 0.0153j$
4-8	$0.0060 + 0.0400j$	$0.0060 + 0.0400j$
5-6	$0.0478 + 0.4124j$	$0.0478 + 0.4124j$
6-7	$0.2250 + 1.5000j$	$0.2250 + 1.5000j$
7-8	$0.0715 + 0.5968j$	$0.0715 + 0.5968j$

Loads (admittances) in pu

<u>All tests</u>	<u>Load change test</u>
$L1 = 8.2000 - 6.4000j$	$L1 = 9.1111 - 7.1111j$
$L2 = 9.8000 - 6.8000j$	$L2 = 9.8000 - 6.8000j$
$L3 = 8.6000 - 6.6000j$	$L3 = 8.6000 - 6.6000j$

Operating condition for all tests except MIMC case (5)

<i>Generator</i>	<i>P (pu)</i>	<i>Q (pu)</i>	<i>V (pu)</i>	<i>delta (deg)</i>
#1	0.7055	0.9682	1.30	5.0
#2	7.0836	7.7991	1.25	6.0
#3	9.5380	8.8108	1.10	0.0
#4	7.9677	9.5918	1.25	4.0
#5	0.7091	0.9695	1.30	6.0

New operating condition for MIMC case (5)

<i>Generator</i>	<i>P (pu)</i>	<i>Q (pu)</i>	<i>V (pu)</i>	<i>delta (deg)</i>
#1	0.5132	0.3505	1.10	5.0
#2	7.0349	8.5832	1.25	6.0
#3	9.5098	8.9931	1.10	0.0
#4	6.2142	7.2852	1.10	4.0
#5	0.5325	0.3610	1.10	6.0

Stabilizers

(1) For MIMC

<i>parameter</i>	<i>conv.</i>	<i>local mode</i>	<i>interarea mode</i>
k_{δ}	0.015	0.0005	0.1008
T_q	1.5	0.5	1.5
T_1	0.3	0.25	0.3063
T_2	0.06	0.0255	0.9189
T_3	-----	0.0255	-----

(2) For SIMC

<i>parameter</i>	<i>conv.</i>	<i>local mode</i>	<i>interarea mode</i>
k_{δ}	0.015	0.001857	0.002653
T_q	1.5	1.5	1.5
T_1	0.3	1.5	0.35
T_2	0.06	0.0116	0.0053

Filter parameters for SIMCLowpass

$$a1 = 7.77640 \quad b4 = 78.4266$$

$$a2 = 30.2359$$

$$a3 = 68.8665$$

$$a4 = 78.4266$$

Bandpass

$$a1 = 6.30240 \quad b3 = 31.2922$$

$$a2 = 133.636$$

$$a3 = 509.334$$

$$a4 = 5068.17$$

$$a5 = 9064.93$$

$$a6 = 54548.6$$

APPENDIX C

EXPERIMENTAL SETUP MACHINE PARAMETERS

The operating conditions and values for the machine parameters used in the experimental setup are :

For 0.8 lag operating condition:

(a) micro-machine

$$I_A = 11.8 \text{ Amps}$$

$$V_A = 195 \text{ volts}$$

$$I_f = 3.25 \text{ Amps}$$

$$V_f = 27.0 \text{ volts}$$

$$V_g = 230 \text{ volts}$$

$$I_g = 6.7 \text{ Amps}$$

$$W_1 = 360 \text{ Watts}$$

$$W_2 = 60 \text{ Watts}$$

$$n = 1800 \text{ rpm}$$

(b) 50 Hp

$$V_g = 210 \text{ volts}$$

$$I_g = 40 \text{ Amps}$$

$$I_f = 4.5 \text{ Apms}$$

(c) 5 Hp

generator #1 : $V_g = 212 \text{ volts}$

$$I_g = 10.2 \text{ Amps}$$

generator #2 : $V_g = 214.0 \text{ volts}$

$$I_g = 9.5 \text{ Apms}$$

$$I_f = 1.0 \text{ Amps}$$

generator #3 : $V_g = 214.0 \text{ volts}$

$$I_g = 10.0 \text{ Apms}$$

$$I_f = 1.85 \text{ Amps}$$

For 0.9 lead operating condition:

(a) micro-machine

$$I_A = 11.8 \text{ Amps}$$

$$V_A = 195 \text{ volts}$$

$$I_f = 3.25 \text{ Amps}$$

$$V_f = 27.0 \text{ volts}$$

$$V_g = 210 \text{ volts}$$

$$I_g = 4.5 \text{ Amps}$$

$$W_1 = 210 \text{ Watts}$$

$$W_2 = 210 \text{ Watts}$$

$$n = 1800 \text{ rpm}$$

(b) 50 Hp

$$V_g = 210 \text{ volts}$$

$$I_g = 40 \text{ Amps}$$

$$I_f = 4.5 \text{ Apms}$$

(c) 5 Hp

$$\text{generator \#1 : } V_g = 202 \text{ volts}$$

$$I_g = 11.0 \text{ Amps}$$

$$\text{generator \#2 : } V_g = 204.0 \text{ volts}$$

$$I_g = 9.8 \text{ Apms}$$

$$I_f = 1.0 \text{ Amps}$$

$$\text{generator \#3 : } V_g = 203.0 \text{ volts}$$

$$I_g = 10.8 \text{ Apms}$$

$$I_f = 1.82 \text{ Amps}$$

Machine ratings

(a) micro-machine

3 KVA 220/127 volts 7.9 Amps 3 phase

(b) 50 Hp

45 KVA 208-416 volts 145.0 Amps 3 phase excitation 6.25 Amps

(b) 5 Hp

5 KVA 120/240 volts 24/12 Amps 3 phase 0.8 pf

Loads

0.8 lag

L1 = 1260 Watts

L2 = 1225 Watts

0.9 lead

L1 = 2347 Watts

L2 = 1225 Watts

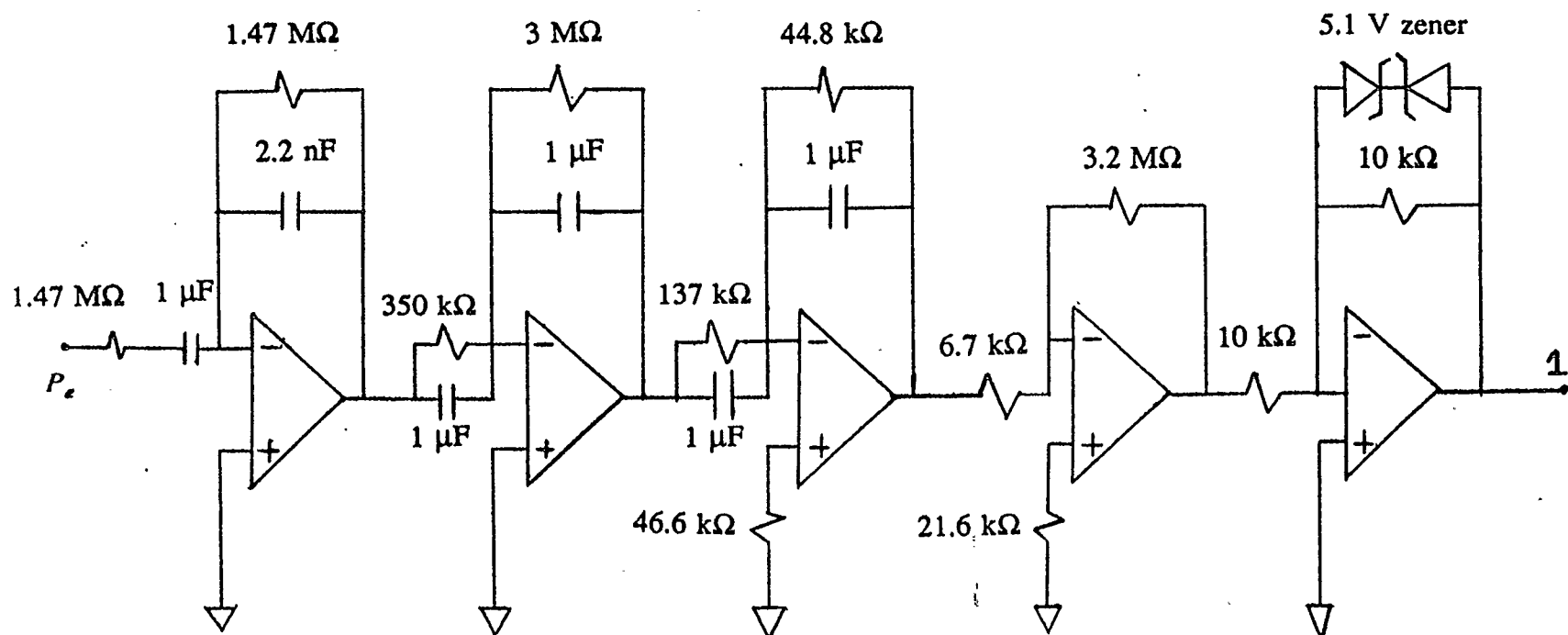


Fig. C.1 ΔP_e channel controller op-amp circuit

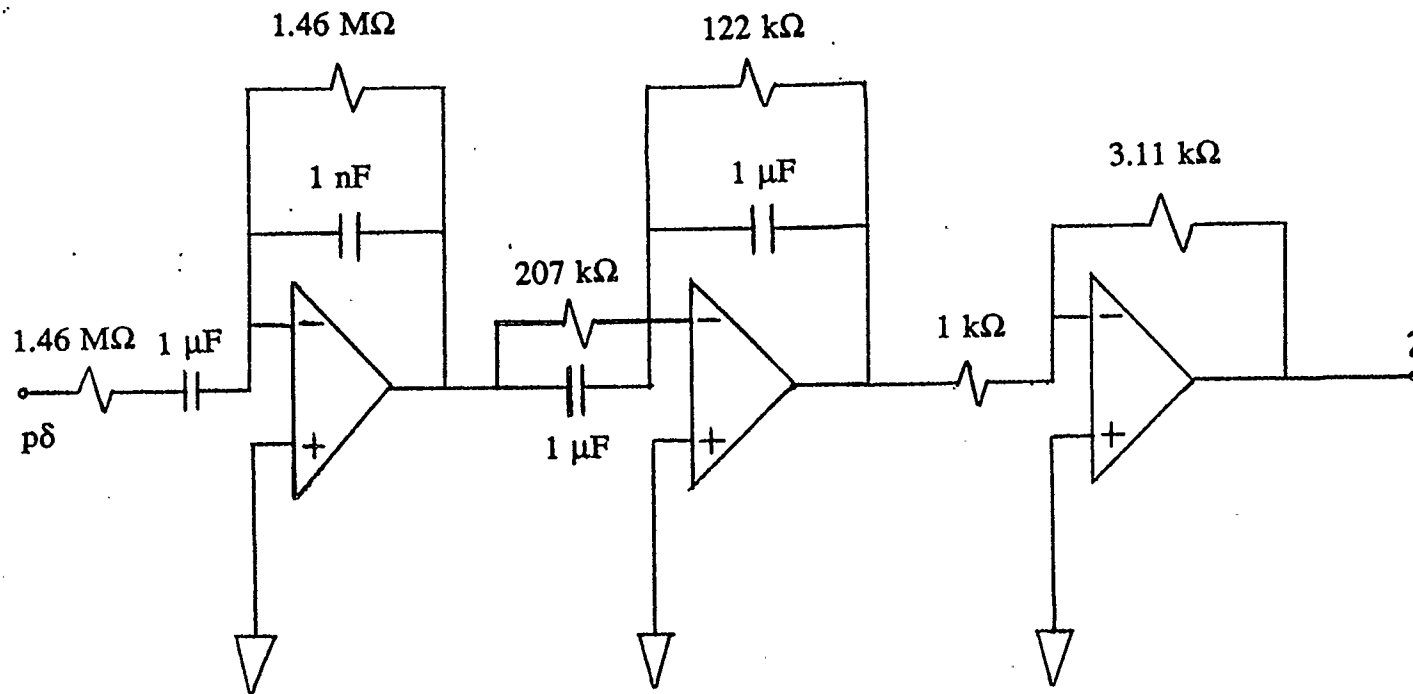


Fig. C.2 $p\delta$ channel controller op-amp circuit